
Theses and Dissertations

Fall 2012

Poly(disulfidediamines) : new biodegradable polymers

Tyler A. Graf
University of Iowa

Copyright 2012 Tyler Anton Graf

This dissertation is available at Iowa Research Online: <http://ir.uiowa.edu/etd/3457>

Recommended Citation

Graf, Tyler A.. "Poly(disulfidediamines) : new biodegradable polymers." PhD (Doctor of Philosophy) thesis, University of Iowa, 2012. <http://ir.uiowa.edu/etd/3457>.

Follow this and additional works at: <http://ir.uiowa.edu/etd>



Part of the [Chemistry Commons](#)

POLY(DISULFIDEDIAMINES) : NEW BIODEGRADABLE POLYMERS

by
Tyler A. Graf

An Abstract

Of a thesis submitted in partial fulfillment
of the requirements for the Doctor of
Philosophy degree in Chemistry
in the Graduate College of
The University of Iowa

December 2012

Thesis Supervisor: Associate Professor Ned B. Bowden

ABSTRACT

The turnovers of a gold(III) chloride catalyst were increased by 3,300% with the addition of several equivalents of (2,2,6,6-tetramethyl-piperidin-1-yl)oxy and catalytic amounts of copper(II) chloride. A three component coupling reaction between piperidine, phenylacetylene, and benzaldehyde yielded a propargylamine in quantitative conversions and isolated yields when gold(III) chloride was added in catalytic amounts, but the gold catalyst decomposed and had little to no reactivity when a second set of piperidine, phenylacetylene, and benzaldehyde were added after the reaction was complete. The addition of (2,2,6,6-tetramethyl-piperidin-1-yl)oxy and copper(II) chloride to reactions with gold(III) chloride maintained the catalytic activity of the gold for up to 33 cycles. This result demonstrates a new way to greatly increase the turnovers of a gold(III) chloride catalyst with the addition of inexpensive, commercially available reagents.

The synthesis and some of the physical properties of the first poly(disulfidediamines) are reported. These polymers were synthesized in high yields and with conversions up to >98% by reactions between secondary diamines and a new disulfide monomer. The disulfide monomer was synthesized in two steps without the need for column chromatography. The polymerizations were robust and completed at room temperature, under ambient atmospheric conditions, and in solvents that were used as purchased. These polymers were stable, but they rapidly decomposed under acidic, aqueous conditions to release hydrogen sulfide. A method for quantifying the hydrogen sulfide released was also developed.

Abstract Approved: _____
Thesis Supervisor

Title and Department

Date

POLY(DISULFIDEDIAMINES) : NEW BIODEGRADABLE POLYMERS

by
Tyler A. Graf

A thesis submitted in partial fulfillment
of the requirements for the Doctor of
Philosophy degree in Chemistry
in the Graduate College of
The University of Iowa

December 2012

Thesis Supervisor: Associate Professor Ned B. Bowden

Graduate College
The University of Iowa
Iowa City, Iowa

CERTIFICATE OF APPROVAL

PH.D. THESIS

This is to certify that the Ph.D. thesis of

Tyler A. Graf

has been approved by the Examining Committee
for the thesis requirement for the Doctor of Philosophy
degree in Chemistry at the December 2012 graduation.

Thesis Committee: _____
Ned B. Bowden, Thesis Supervisor

Louis Messerle

Leonard R. MacGillivray

James B. Gloer

Aliasger K. Salem

TABLE OF CONTENTS

LIST OF TABLES	vi
LIST OF FIGURES	vii
CHAPTER 1 INTRODUCTION	1
Importance of polymers in medicine	1
Drug delivery	4
Polymer-drug conjugates.....	5
Micelles	6
Polymeric nanoparticles	8
Preparation of nanoparticles	8
Surface modification.....	9
Drug loading and release	10
Biodegradable polymer functional groups.....	12
Polyesters	12
Polyanhydrides.....	13
Polyorthoesters.....	14
Polysulfenamides	15
Conclusions.....	18
CHAPTER 2 NEW POLYMERS POSSESSING A DISULFIDE BOND IN A UNIQUE ENVIRONMENT	19
Introduction.....	19
Results and Discussion	23
Synthesis and Stability of Disulfide Monomers.....	23
Synthesis and Stability of Disulfidediamines	25
Synthesis of Poly(disulfidediamines).....	27
Thermal Gravimetric Analysis (TGA)	32
Electrically Conducting Poly(disulfidediamines)	33
Conclusions.....	36
Experimental.....	37
Characterization	37
Materials.....	38
Synthesis of molecule A.....	38
Synthesis of molecule B.....	39
Synthesis of molecule C.....	39
Synthesis of molecule D.....	39
Procedure for Table 2, entry 1.....	40
Procedure for Table 2, entry 2.....	40
Procedure for Table 2, entry 3.....	40
Procedure for Table 2, entry 4.....	41

Procedure for Table 2, entry 5.....	41
Procedure for Table 2, entry 6.....	41
Procedure for Table 2, entry 7.....	42
Stability of disulfidedisuccinimide.....	42
Transamination kinetics/Runge-Kutta integration	42
Stability of disulfidedi(ethylmethylamine)	46
Stability of disulfidedi(ethylmethylamine) in CD ₃ OD:D ₂ O	46
Transamination kinetics	47
Thermal gravimetric analysis	48
Synthesis of the conjugated poly(disulfidediamine)	48
Diode fabrication.....	49
¹ H NMR Spectra.....	50

CHAPTER 3 HYDROGEN SULFIDE GENERATION FROM
DISULFIDEDIAMINES UNDER AQUEOUS CONDITIONS 56

Introduction.....	56
Experimental	60
Materials.....	60
Characterization	61
Synthesis of dimorpholinedisulfide.....	61
Release of H ₂ S from Na ₂ S.....	61
Release of H ₂ S from dimorpholinedisulfide with HCl.....	62
Release of H ₂ S from dimorpholinedisulfide with HOAc.....	62
Results and discussion	62
Conclusion	65

CHAPTER 4 EXTENDED LIFETIMES OF GOLD(III) CHLORIDE
CATALYSTS USING COPPER(II) CHLORIDE AND
(2,2,6,6-TETRAMETHYL-PIPERIDIN-1-YL)OXYL..... 67

Introduction.....	67
Experimental	80
Materials and Methods.....	80
¹ H NMR analysis of three-component coupling reactions.....	80
Procedure for Table 4, Entry 2.....	81
Procedure for Table 4, Entry 3.....	81
Procedure for Table 4, Entry 4.....	82
Procedure for Table 4, Entry 5.....	82
Procedure for Table 4, Entry 6.....	83
Procedure for Table 4, Entry 7.....	84
Procedure for Table 4, Entry 8.....	84
Procedure for Table 4, Entry 9.....	85
Procedure for Table 5, Entry 1.....	85
Procedure for Table 5, Entry 2.....	86
Procedure for Table 5, Entry 3.....	86

Procedure for Table 5, Entry 4	86
Procedure for Table 5, Entry 5	87
Procedure for Table 6, Entry 1	87
Procedure for Table 6, Entry 2	88
Procedure for Table 6, Entry 3	88
Procedure for Table 6, Entry 4	89
Procedure for Table 6, Entry 5	90
Procedure for Table 6, Entry 6	90
Procedure for Table 6, Entry 7	91
Procedure for Table 6, Entry 8	91
Procedure for Table 6, Entry 9	92
Procedure for Table 6, Entry 10	93
Procedure for Table 6, Entry 11	93
Procedure for Table 6, Entry 12	94
Procedure for Table 6, Entry 13	94
¹ H NMR analysis of the hydroarylation reactions	95
Procedure for Figure 51a with AuCl ₃ and CuCl ₂	95
Procedure for Figure 51a in the absence of CuCl ₂	96
Procedure for Figure 51b with AuCl ₃ and CuCl ₂	97
Procedure for Figure 51b the absence of CuCl ₂	97
Procedure for Table 7, Entry 1	98
Procedure for Table 7, Entry 2	98
Procedure for Table 7, Entry 3	99
Procedure for Table 7, Entry 4	99
Procedure for Table 7, Entry 5	99
Procedure for Table 7, Entry 6	100
CHAPTER 5 CONCLUSIONS AND RECOMMENDATIONS FOR FUTURE WORK	101
Conclusions	101
Recommendations for future work	103
APPENDIX SYNTHESIS OF THE FIRST POLY(DIAMINOSULFIDE)S AND AN INVESTIGATION OF THEIR APPLICATIONS AS DRUG DELIVERY VEHICLES	104
Introduction	104
Results and Discussion	108
Synthesis and reactions of sulfur transfer reagents	108
Kinetics of transamination reactions	110
Synthesis of poly(diaminosulfide)s	113
Stability of diaminosulfides in organics and water	115
Fabrication and uptake of poly(diaminosulfide) particles	118
Conclusions	122
Experimental Section	123

Materials.....	123
Characterization	124
Bis(tributyltin) sulfide	125
Bis(succinimide) sulfide.....	125
<i>N,N'</i> -Dithio(bis-ethylmethylanine).....	125
<i>N</i> -Ethylmethylsulfenyl chloride.....	126
Bis(<i>N</i> -ethylmethyl)sulfide.....	126
<i>N,N'</i> -Dithiobis-dimethylamine.....	127
<i>N</i> -Dimethylsulfenyl chloride.....	127
Bis(<i>N,N'</i> -dimethyl) sulfide.....	127
Water-soluble diaminosulfide	128
Entry 1, Table A-2.....	128
Entry 3, Table A-2.....	129
Entry 5, Table A-2.....	129
Reactions of molecule E and <i>N</i> -benzylmethylamine	129
Transamination of molecule F and <i>N</i> -benzylmethylamine	130
Stability of molecule E in organic solvents.....	131
Stability of molecule L in D ₂ O.....	131
Formulation of microparticles.....	132
Determination of particle size and size distribution.....	133
Measurement of surface charge.....	133
Scanning electron microscopy (SEM).....	133
Cell culture	134
Investigation of microparticle uptake by HEK-293 cells.....	134
Evaluation of the cytotoxicity of microparticles	135
REFERENCES	137

LIST OF TABLES

Table 1	The rate constants for the reactions shown in Figure 22.	29
Table 2	The polymerizations were completed as shown in Figure 21.....	30
Table 3	Recovery of generated H ₂ S as PbS.....	65
Table 4	Effect of CuCl ₂ and TEMPO on the lifetimes of AuCl ₃	71
Table 5	Control reactions.....	72
Table 6	Reactions at 1 and 0.1 mol% AuCl ₃	74
Table 7	Effect of AuCl ₃ and CuCl ₂ on the hydroarylation reactions.....	79
Table A-1	Transamination reactions of molecule F and benzylmethylamine.	113
Table A-2	Synthesis of poly(diaminosulfides).	114

LIST OF FIGURES

Figure 1	Cup and ball hip joint.	1
Figure 2	Biodegradable and non-biodegradable polymers used in medicine.	2
Figure 3	Dopamine-mediated heparin coating on a vascular stent.	3
Figure 4	Poly(ϵ -caprolactone fumarate) conduit used for nerve regeneration.	4
Figure 5	Poly(<i>N</i> -(2-hydroxypropyl)methacrylamide) copolymer functionalized with adriamycin via the peptidyl spacer PK1.	5
Figure 6	PEG-p(Asp-Hyd-ADR) block copolymer functionalized with adriamycin via a Schiff base spacer.	7
Figure 7	Schematic of the emulsification-evaporation technique for the synthesis of polymeric nanoparticles.	9
Figure 8	Surface modification of polymeric nanoparticles.	10
Figure 9	SEM micrographs of poly(lactic acid-glycolic acid) copolymer nanoparticle degradation.	11
Figure 10	Common cyclic esters used to form polyesters by ring-opening polymerization.	13
Figure 11	Polyanhydrides are synthesized from diacids using a high-temperature, solvent-free melt condensation polymerization.	14
Figure 12	Acid-catalyzed condensation of diols and diketenes yields polyorthoesters.	15
Figure 13	A mild condensation reaction between diamines and dithiosuccinimides yields polysulfenamides.	16
Figure 14	pH-sensitive microparticle degradation.	16
Figure 15	Uptake of polysulfenamide microparticles (red) into JAWSII (top) and HEK293 (bottom) cells.	17
Figure 16	Sulfenamides, diaminosulfides, and disulfidediamines.	22
Figure 17	A general reaction scheme for the proposed synthesis of poly(disulfidediamines).	23

Figure 18 Disulfur transfer reagent syntheses.	24
Figure 19 The reaction between molecule A and two molar equivalents of molecule E was investigated according to this reaction scheme.....	25
Figure 20 The kinetics of the transamination reaction between molecule A and two molar equivalents of molecule E in C ₆ D ₆	26
Figure 21 How poly(disulfidediamines) were synthesized using molecule D as the disulfide monomer.	28
Figure 22 Comparison of transamination rate constants.....	28
Figure 23 A SEC chromatograph of the polymer from entry 1 of Table 2.....	31
Figure 24 The TGA of the polymer from entry 1 in Table 2.....	33
Figure 25 The structure of polythiazyl.....	33
Figure 26 The synthesis of a conjugated poly(disulfidediamine).....	34
Figure 27 The current-voltage curve for the polymer synthesized as shown in Figure 26.....	36
Figure 28 Runge-Kutta intergration.....	43
Figure 29 Transamination rates.	44
Figure 30 Decomposition of disulfidedi(ethylmethylamine).....	47
Figure 31 Transamination kinetics.....	48
Figure 32 NMR spectra of molecule A.....	50
Figure 33 NMR spectra of molecule B.....	51
Figure 34 NMR spectra of molecule C.....	51
Figure 35 NMR spectra of molecule D.....	52
Figure 36 NMR Spectra of Table 2, entry 1.	52
Figure 37 NMR spectra of Table 2, entry2.....	53
Figure 38 NMR spectra of Table 2, entry 3.	53

Figure 39 NMR spectra of Table 2, entry 5.	54
Figure 40 NMR spectra of Table 2, entry 6.	54
Figure 41 NMR spectra of Table 2, entry 7.	55
Figure 42 Therapeutic targets for hydrogen sulfide (H ₂ S).	57
Figure 43 Diallylpolysulfides are endogenous sources of H ₂ S present in garlic.	58
Figure 44 L-DOPA derivatives with various H ₂ S-releasing functionalities are being investigated for the treatment of Parkinson's.	59
Figure 45 S-diclofenac and GYY4137 were developed for the slow release of H ₂ S.	60
Figure 46 Synthesis of dimorpholinedisulfide.	63
Figure 47 H ₂ S detection method using Pb(OAc) ₂	64
Figure 48 Gold-catalyzed three-component coupling.	69
Figure 49 Lifetime extension of AuCl ₃	70
Figure 50 Mechanism for the increased lifetime of AuCl ₃	76
Figure 51 Additional reactions investigated.	77
Figure A-1 Diaminosulfide synthesis.	106
Figure A-2 The synthesis of two sets of sulfur transfer reagents.	109
Figure A-3 Kinetics of transamination reactions.	111
Figure A-4 A transamination reaction with dimethylamine as the leaving group.	113
Figure A-5 The polymerization of diamines with the sulfur transfer reagent is shown.	113
Figure A-6 The stability of two diaminosulfides at room temperature in organic solvents.	116
Figure A-7 The degradation of molecule L under acidic, neutral, and basic conditions.	117

Figure A-8 SEM micrographs of microparticles fabricated from
the polymer shown in entry 6 of Table A-2. 120

Figure A-9 A laser scanning microscopic image of
cellular uptake of microparticles..... 120

Figure A-10 The cell viabilities of HEK-293 cells incubated
with poly(diaminosulfide) microparticles. 122

CHAPTER 1

INTRODUCTION

Importance of polymers in medicine

Polymers have important and widespread applications in medicine.

Poly(methylmethacrylate), polyacrylamide, silicone polymers, and various carbonate polymers are used to make contact and corrective eyeglass lenses. More recently, polyethylene has been used in total joint replacement because it is less fragile than ceramics and does not have the allergy/toxicity issues associated with metals.¹ Figure 1 shows an artificial hip joint with one of the bearing surfaces composed of polyethylene. Because of the advantages of polyethylene, it has been steadily replacing metals and ceramics in joint replacement.

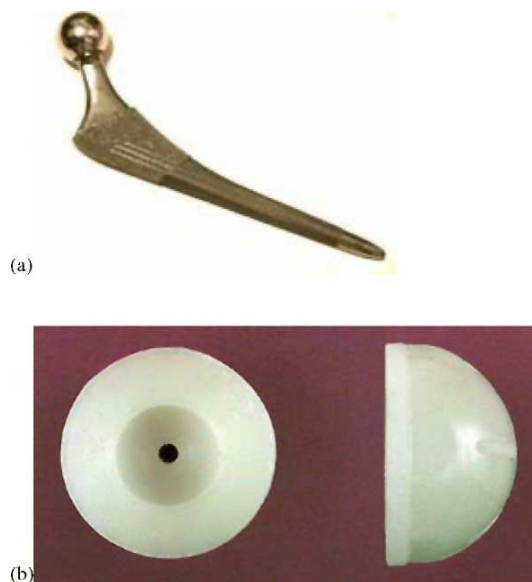


Figure 1 Cup and ball hip joint.
A steel ball (a) and high-density polyethylene cup (b).¹

Biodegradable polymers have also been studied for numerous medical applications. Unlike polyethylene, biodegradable polymers are designed to decompose into small molecules under physiological conditions. It is useful to illustrate this difference by comparing biodegradable poly(lactic acid) (PLA) and chitosan with non-biodegradable polyethylene (Figure 2). The ester bonds in PLA can undergo acid catalyzed hydrolysis and chitosan contains glycosidic linkages which can be cleaved by enzymes. In contrast, polyethylene has no reactive bonds in its backbone, a useful property for long-term treatments such as joint replacement. However, many medical applications for polymers require controlled degradation.

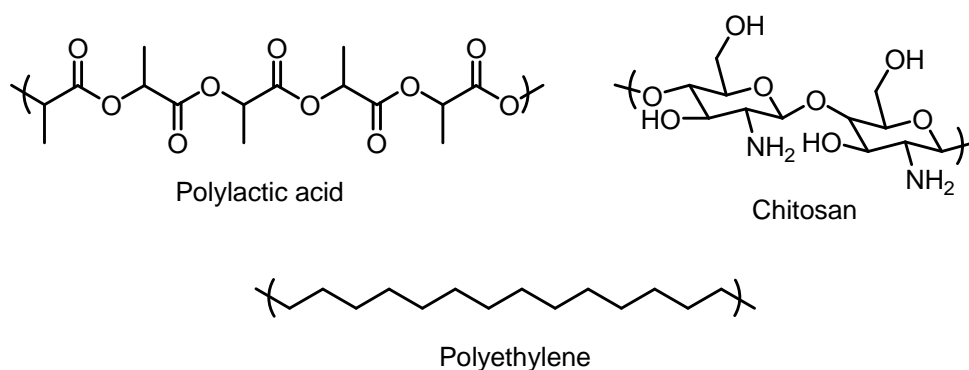


Figure 2 Biodegradable and non-biodegradable polymers used in medicine.

Synthetic, biodegradable polymers have been used in medicine for decades, beginning with the introduction of biodegradable poly(glycolic acid) surgical sutures in 1967. Further examples include biodegradable implants that do not require surgery to remove and have been adopted for use as orthopedic fixation devices,² anastomosis rings,³ and stents.⁴ In addition to being used as fully biodegradable stents, the coating of

metal stents with biodegradable polymers has become the standard treatment for coronary artery disease⁵ (Figure 3). The coatings contain drugs and release them over time to prevent arterial fibrosis.

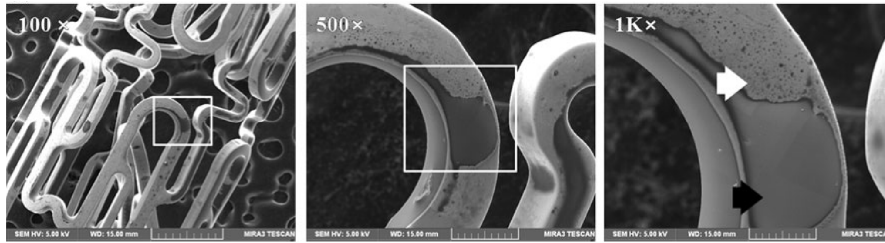


Figure 3 Dopamine-mediated heparin coating on a vascular stent. White and black arrows indicate coated and non-coated areas respectively.⁶

In the field of tissue engineering, biodegradable polymers are used to construct scaffolds which support the growth of cells into functional tissue.⁷ The scaffold decomposes as the cells proliferate, arranging them into functional tissue while providing physical support. At the end of the growth process, the scaffold is completely absorbed, leaving only tissue. Scaffolds can be used to grow tissue both *in vivo*, as seen in Figure 4, and *in vitro*. Biodegradable polymers show promise in the creation of bone,⁸ nerve,⁹ vascular,¹⁰ skin,¹¹ ligament,¹² and genitourinary tissues.¹³

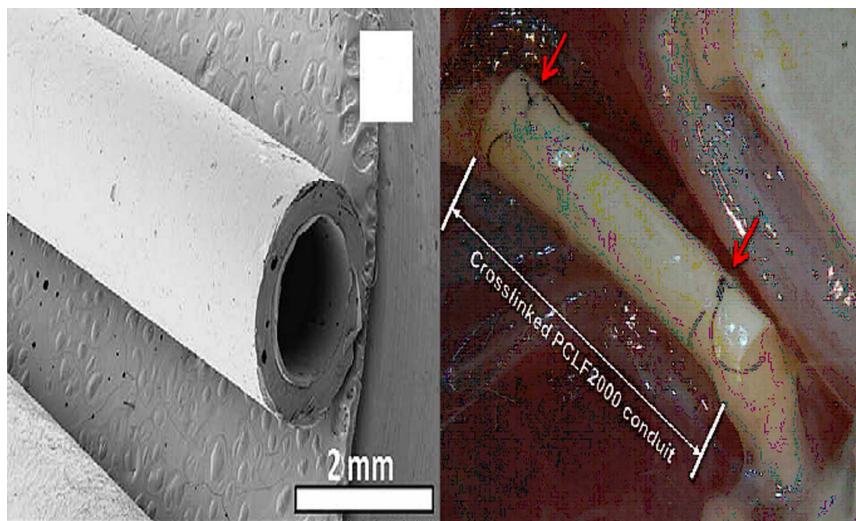


Figure 4 Poly(ϵ -caprolactone fumarate) conduit used for nerve regeneration.¹⁴

Drug delivery

The field of drug delivery is increasingly important to modern medicine, and it will be the focus of the remainder of this introduction. Biodegradable polymers are crucial to this field, as the combination of drugs and polymers allows the release rate of the drug to be controlled. The release rate can be set so that the concentration of a drug is at the therapeutic level for a desired amount of time. The controlled release of a drug reduces side effects compared to the use of unbound drug which must be administered at initial concentrations far above the therapeutic level. Polymer-bound drugs can also target specific sites in the body by using functional groups which degrade only under specific conditions, by targeting groups on the polymer, or by the size of the polymer. Targeting allows the use of very high localized concentrations of drugs without the side effects that exposing the entire body to those concentrations would cause. Polymer-based

drug delivery is accomplished by using polymer-drug conjugates, micelles, and nanoparticles.

Polymer-drug conjugates

Polymer-drug conjugates, also called polymeric prodrugs, consist of polymers covalently bonded to drug molecules. Although research into this method of improving the efficiency of drugs began in the 1950's, it was in 1975 that the definitive model for pharmacologically-active polymers was proposed by H. Ringsdorf.¹⁵ The Ringsdorf model (Figure 5) consists of drugs attached to a polymer backbone through a spacer group. Groups intended for targeting can also be attached to the backbone.

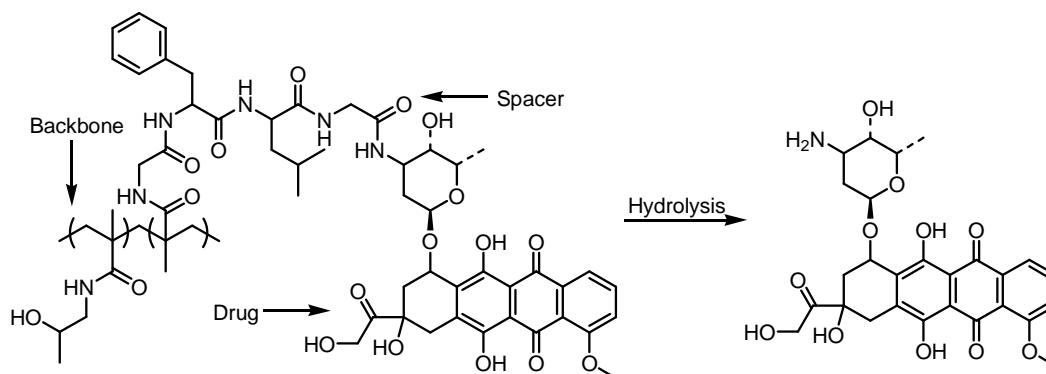


Figure 5 Poly(*N*-(2-hydroxypropyl)methacrylamide) copolymer functionalized with adriamycin via the peptidyl spacer PK1.¹⁶

The size of the polymeric prodrug interferes in its clearance from the body, resulting in slower renal excretion, longer blood circulation, and greater endocytotic uptake compared to unbound drugs.¹⁷ A passive targeting effect called the 'enhanced permeability and retention' (EPR) effect also results from the size of the prodrug.¹⁸ This

effect causes solid tumors to accumulate macromolecules in preference to normal tissue. The basis for this effect is the combination of the discontinuous vascular endothelium and the poor lymphatic drainage present in tumors.

The spacer affects the rate of drug release at specific locations in the body. The focus has been on the development of spacers sensitive to either pH or enzymes. Spacers sensitive to pH can be used to release drug preferentially in the acidic lysosome.¹⁹ Enzyme-sensitive oligopeptide spacers will degrade preferentially in the lysosome of cancerous cells.²⁰

Polymeric prodrugs can be functionalized with antibodies, sugars, or peptides which bind to specific target cells expressing the corresponding receptors. Drugs are then released in the vicinity of the targeted cells. Cancer,²¹ hepatic,²² and endothelial²³ cells have been targeted by polymeric prodrugs using this technique.

Micelles

Polymeric micelles are self-assembled aggregates of amphiphilic block copolymers.²⁴ These copolymers are composed of hydrophobic and hydrophilic sections linked together at one end (Figure 6). Under aqueous conditions, the polymers assemble into spheres, with the hydrophilic blocks on the exterior interacting with water and the hydrophobic blocks grouped together in the interior. Drugs are bonded to the hydrophobic block through a degradable spacer group, where both are protected in the core of the micelle during blood circulation.

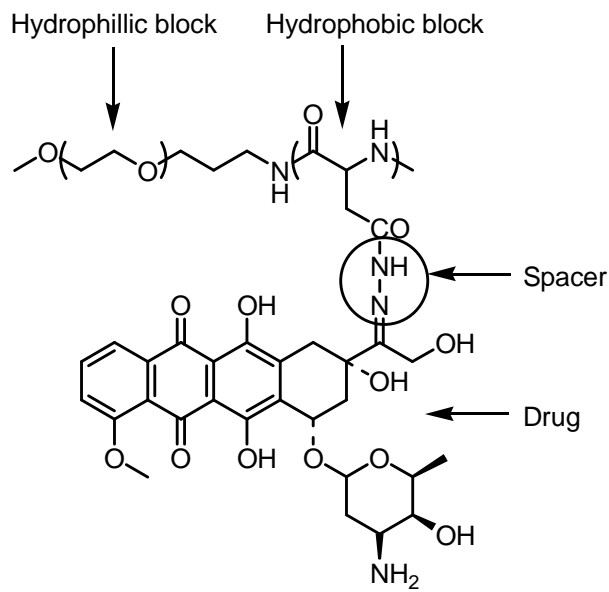


Figure 6 PEG-p(Asp-Hyd-ADR) block copolymer functionalized with adriamycin via a Schiff base spacer.²⁴

Because micelles have diameters of approximately 100 nanometers, their size provides passive targeting of tumors by the EPR effect. Research in polymer micelles has focused on the development of ‘smart’ micelles, capable of stimuli-responsive drug release.^{25,26} Stimuli-responsive micelles undergo a rapid conformational transition in the presence of their stimulus. This transition disrupts the structure of the micelle and exposes the bound drug to the environment resulting in a very fast release of the drug. Release of drugs can be readily controlled by exposure to the appropriate stimulus upon arrival at the target site. Temperature, pH, glucose, and glutathione have been used to affect controlled release using micelles. An acidic pH is an especially useful stimulus due to the increased acidity found in tumors and inflamed tissues.

Polymeric nanoparticles

Polymeric nanoparticles are colloidal particles in which a therapeutic agent can be stored by either encapsulation within the polymer matrix or adsorption to the surface. As the polymer degrades, the therapeutic agents are released. The release rate can be controlled by the choice of polymer and the particle preparation method. Surface modification allows for targeted delivery to, for example, the brain, arteries, lungs, tumors, liver, or spleen.²⁷ Nanoparticles can also be used for long-term, systemic circulation in the body.

Preparation of nanoparticles

Polymeric nanoparticles are commonly formed by emulsification of polymers rather than by emulsion polymerization of monomers. In the emulsification-solvent evaporation method²⁸ shown in Figure 7, the polymer and drug are dissolved in a water-insoluble organic solvent. An aqueous solution containing an emulsifying agent is added to the polymer solution with vigorous stirring, forming an oil-in-water emulsion. Evaporation of the solvent after stabilization of the emulsion yields nanoparticles. The emulsifier, polymer concentration, and stirring rate all influence the size of the nanoparticles formed. Alternate methods of nanoparticle formation include the solvent diffusion method,²⁹ nanoprecipitation,³⁰ and salting out.³¹

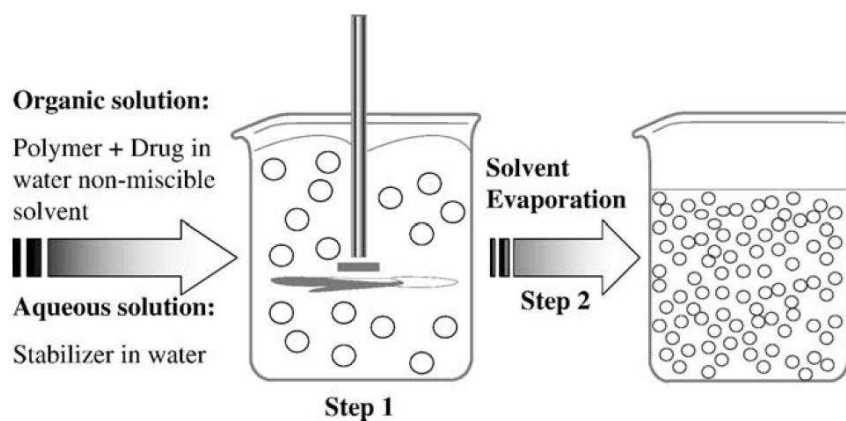


Figure 7 Schematic of the emulsification- evaporation technique for the synthesis of polymeric nanoparticles.²⁷

Surface modification

A problem associated with the use of polymeric nanoparticles in the body is that they are removed from circulation by macrophages. Macrophages are part of the mononuclear phagocytic system, which filters and removes any foreign particulate matter from the bloodstream. Surface modification (Figure 8) allows nanoparticles to avoid recognition and clearance by the phagocytes and increases the probability of the nanoparticles reaching their target. Surface modification of nanoparticles has proven to be critical for their successful applications *in vivo*.³²

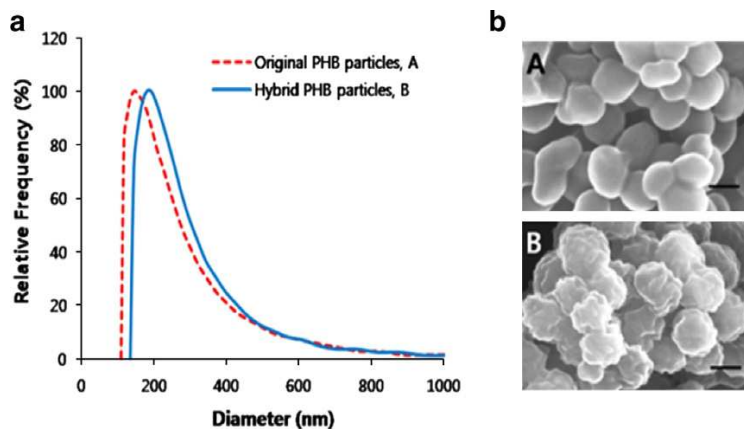


Figure 8 Surface modification of polymeric nanoparticles.

a) Size increase of polyhydroxybutyrate nanoparticles after surface modification with targeting peptide RGD4C. b) SEM micrographs of the nanoparticles before (top) and after modification (bottom).³³

The grafting or adsorption of poly(ethylene glycol) (PEG) onto the surface of a nanoparticle is a common method to modify polymeric nanoparticles. PEG coating of nanoparticles plays an important role in drug delivery by increasing residence time in the body, reducing enzymatic degradation, and reducing protein immunogenicity.³⁴ PEG addition to nanoparticles is hypothesized to interfere sterically with the coating of the surface by serum proteins.^{35,36} These proteins act as both recognition targets and binding enhancers in the process of phagocytosis, and preventing their attachment allows nanoparticles to avoid phagocytes. In addition to PEG, poloxamers, polysorbates, and polysaccharides have been used to coat nanoparticle surfaces.^{37,38}

Drug loading and release

High drug-loading capacity is a very important characteristic of nanoparticles used in medicine, since even biodegradable polymers can exhibit toxicity if their

concentrations are high enough. Drugs are either incorporated into the nanoparticle during its formation or added by soaking preformed nanoparticles in a drug-containing solution.³⁹ Drugs can be encapsulated in the core of nanoparticles, evenly dispersed in the polymer matrix, adsorbed on the surface, or chemically bonded to the polymer chains.

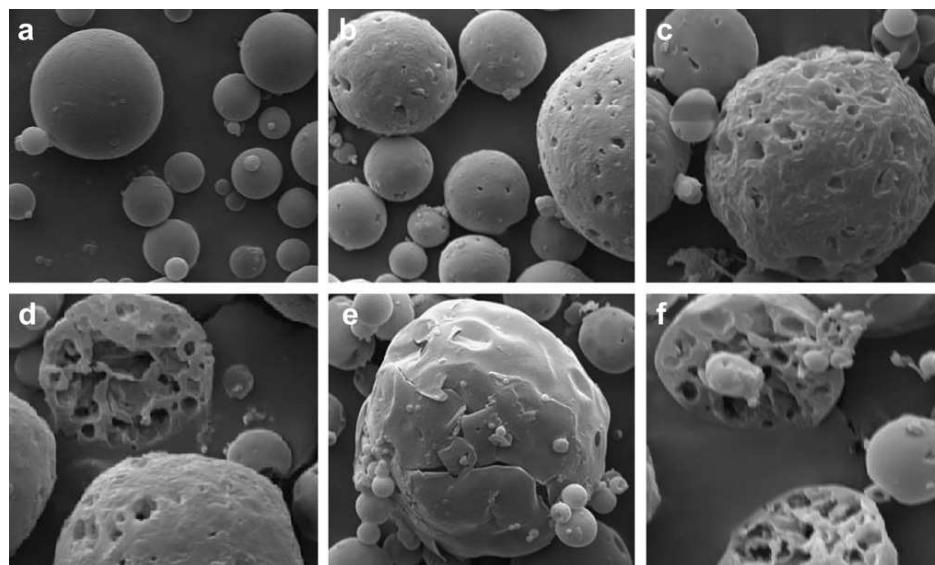


Figure 9 SEM micrographs of poly(lactic acid-glycolic acid) nanoparticle degradation. Condition at pH 7.4 after: a) 0 days, b) 1 week, c) 2 weeks, d) 3 weeks, e) 4 weeks, f) 5 weeks.⁴⁰

The drug release profile of a nanoparticle is a critically important parameter for drug delivery. Release profiles have two stages, an initial burst release and a much slower sustained release. The burst consists of drug adsorbed at or near the nanoparticle surface and typically becomes larger with increased drug loading. Sustained release rate is determined by the combination of drug diffusion through the polymer matrix and the bulk erosion of the nanoparticle (Figure 9).⁴¹ Control of these factors allows the tuning

of the release profile for specific applications. A small nanoparticle or high drug loading favors a large burst release, whereas diffusion and erosion predominate if the drug is distributed throughout the polymer.

Biodegradable polymer functional groups

Commonly used functional groups used to synthesize biodegradable polymers are esters, anhydrides, and orthoesters. Polymers containing these functional groups exhibit useful properties for biomedical applications, especially their degradation by hydrolysis. Less frequently used functional groups such as carbonates, phosphoesters, and amides will not be discussed here.

Polyesters

Polyesters are the most widely used biodegradable polymers in medical applications due to their biodegradability and biocompatibility.⁴² Poly(lactic acid), poly(glycolic acid), and poly(caprolactone) (shown in Figure 10) are especially widely used because the FDA has approved their use in humans. Metal-catalyzed ring-opening polymerization of cyclic esters is the standard method used to synthesize polyesters.⁴³ Condensation polymerization of alcohols and carboxylic acids generates low molecular weight, polydisperse polymers and requires the removal of water from the reaction mixture. With the use of ring-opening polymerization, polymers of narrow polydispersity and controllable molecular weight can be synthesized.

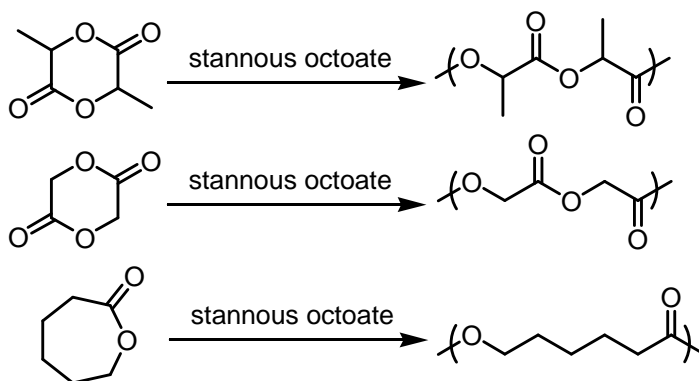


Figure 10 Common cyclic esters used to form polyesters by ring-opening polymerization.⁴³

Recent research has focused on the development of polyesters with variable pendant groups, allowing for tunable properties including hydrophobicity, rate of degradation, and cellular adhesion. Reactive pendant groups could serve as attachment points for drugs or targeting groups. These functionalized polyesters are prepared by the polymerization of cyclic esters bearing a protected functional group followed by deprotection. Polyesters containing carboxyl,⁴⁴ alcohol,⁴⁵ amine,⁴⁶ ketal,⁴⁷ alkene,⁴⁸ and halogen⁴⁹ functionalities have been prepared by this method.

Polyanhydrides

Polyanhydrides are similar to polyesters in that they degrade by hydrolysis to give physiologically-benign products.⁵⁰ Unlike polyesters, polyanhydrides are commonly synthesized from diacids in a high-temperature, solvent-free melt polymerization shown in Figure 11. No purification of the product polymer is needed, as the water produced by the condensation of the acids is evaporated by the high temperature of the reaction. The

use of a mixture of aliphatic and aromatic diacid monomers allows control over the degradation rate of the resulting copolymer by altering the ratio of the monomers. The rapid degradation of the anhydride functional group is the main advantage of polyanhydrides over polyesters, but also results in instability during storage. Because of this, storage of polyanhydrides requires flash freezing with liquid nitrogen and subsequent freeze drying. Despite this limitation, polyanhydrides have found applications in drug delivery to organs including the brain,⁵¹ bones,⁵² blood vessels,⁵³ and eyes.⁵⁴

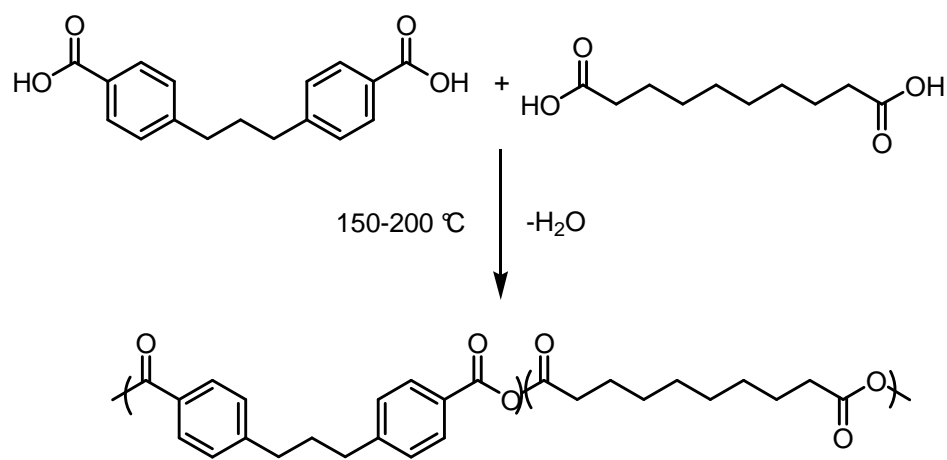


Figure 11 Polyanhydrides are synthesized from diacids using a high-temperature, solvent-free melt condensation polymerization.⁵⁵

Polyorthoesters

Polyorthoesters have been investigated for use in medicine for over 40 years, but have only recently improved sufficiently to be competitive with other biodegradable polymers.⁵⁶ They are synthesized by an acid-catalyzed condensation between a diol and

diketene, as seen in Figure 12.⁵⁷ Atypically, the condensation reaction produces no small molecule byproducts. This allows polyorthoesters to pack tightly in the solid state and to form dense, crosslinked matrices by using polyalcohols of functionality greater than two. Among biodegradable polymers, only polyorthoesters can form such dense structures. As a result of their dense structure, the erosion of bulk polyorthoester is limited to the surface layers. This allows very controlled drug release profile compared to other biodegradable polymers which fracture as they decompose. Taking advantage of these unique properties, polyorthoesters are being investigated for the treatment of periodontal disease⁵⁸ and in the management of post-operative pain.⁵⁹

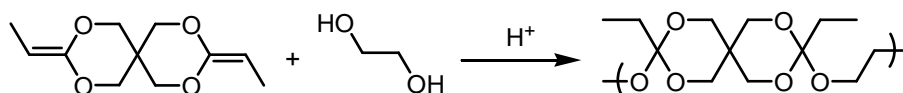


Figure 12 Acid-catalyzed condensation of diols and diketenes yields polyorthoesters.⁵⁷

Polysulfenamides

Polysulfenamides⁶⁰ are a recent development in the field of synthetic biodegradable polymers. These polymers contain a nitrogen-sulfur bond, which was previously unknown in polymer chemistry. Their synthesis involves a condensation reaction between amines and thiosuccinimides, as seen in Figure 13. Polysulfenamides were synthesized with molecular weights up to 6300 g mol^{-1} and conversion of 95-98 % based on the degree of polymerization of the purified polymers.

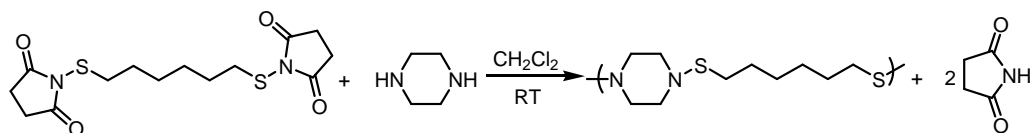


Figure 13 A mild condensation reaction between diamines and dithiosuccinimides yields polysulfenamides.⁶⁰

Polysulfenamides decompose rapidly under acidic, aqueous conditions; making them candidates for drug delivery applications. Microparticles were formed by the solvent evaporation method and placed in solutions of pH 4.0 and 7.4. Figure 14 shows that the weight loss, and thus degradation, of the microparticles is greater at pH 4.0 than pH 7.4. The degradation of the microparticles can be clearly seen in the before and after SEM micrographs.

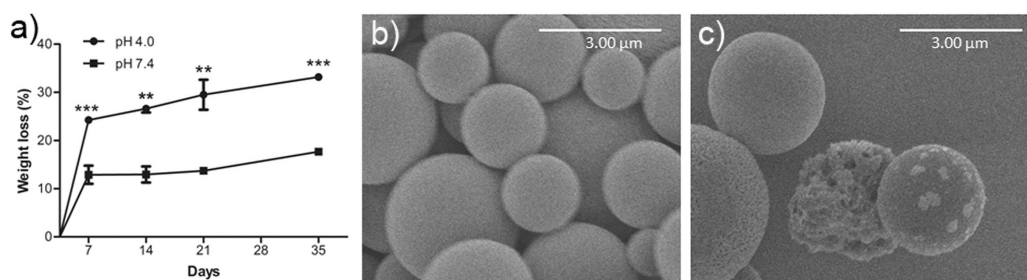


Figure 14 pH-sensitive microparticle degradation.
 a) Microparticle weight loss over time. b) Microparticles before degradation.
 c) Microparticles after 14 days at pH 4.0.⁶⁰

Cellular uptake of the polysulfenamide microparticles was demonstrated by loading the particles with rhodamine B dye. The microparticles were then exposed to

HEK293 and JAWSII cells. Confocal microscopy was used to study the uptake of the microparticles. Figure 15 shows that the microparticles had undergone phagocytosis by both cell types. No cytotoxicity was observed in the cells as a result of the polysulfenamide microparticles, and *in vivo* experiments injecting mice with polysulfenamide microparticles also resulted in no observed toxic effects.

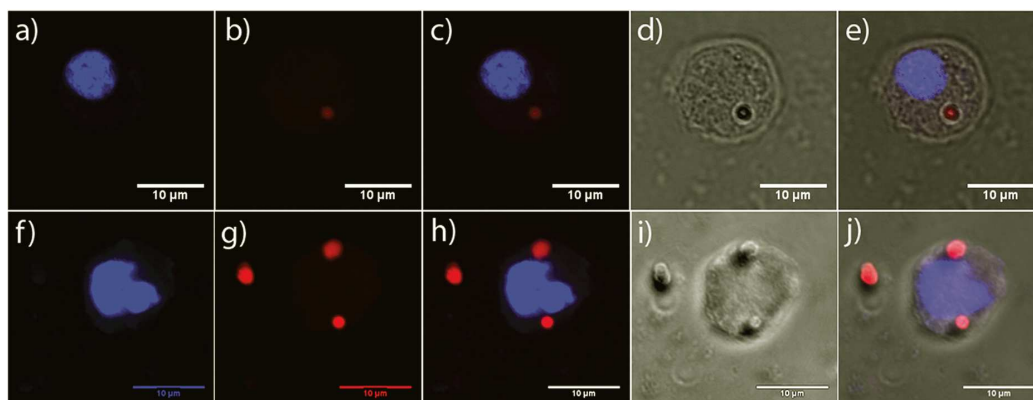


Figure 15 Uptake of polysulfenamide microparticles (red) into JAWSII (top) and HEK293 (bottom) cells.⁶⁰

Polysulfenamides have the right properties to be effective polymers for drug delivery applications. Decomposition under acidic conditions is a property shared by all commonly used synthetic biodegradable polymers. Further, polysulfenamide microparticles have demonstrated both uptake into cells and a lack of observed toxicity both *in vitro* and *in vivo*.

Conclusions

Building on the work done with sulfenamides, both diaminosulfides and disulfidediamines have been investigated. Polymers containing these functional groups have potential applications in drug delivery. Additionally, disulfidediamines show the ability to release the potent signaling molecule hydrogen sulfide.

CHAPTER 2

NEW POLYMERS POSSESSING A DISULFIDE BOND IN A UNIQUE ENVIRONMENT

Introduction

Sulfur has been a critically important atom in polymer chemistry since the beginning of the polymer industry. In the mid 1800's the discovery of the vulcanization of rubber by Charles Goodyear lead to many of the first practical uses of synthetic rubber. Here, sulfur was used to cross-link the polymer, and the physical properties of the material were mostly set by the cross-linked matrix. In more recent work, polymers have been developed that take advantage of the chemical and physical properties that the presence of sulfur adds to the final material. For example, poly(*p*-phenylene sulfide) is sold industrially as Ryton, Fortron, or Sulfar due to its resistance to acids and bases and its stability at high temperatures.⁶¹⁻⁶⁶ Self-healing polymers have been synthesized with either disulfides or trithiocarbonates as the active functional groups that lead to healing after the polymer has been scratched or fractured.⁶⁷⁻⁷³ Monosulfide and disulfide polymers have been studied for their applications in medicine.^{74,75} For instance, polymers with monosulfides have been investigated for their ability to affect the redox cycle inside and outside of cells after an injury has taken place.⁷⁴ Polymers with disulfide bonds have been synthesized as new biodegradable polymers for applications in gene and drug delivery as well as for biodegradable agents in magnetic resonance contrast imaging with Gd(III).^{67,76-81} Polymers with disulfide bonds are biodegradable because of the

presence of disulfide reducing agents, such as glutathione, that degrade polydisulfides into small molecules or oligomers that are readily excreted from the body.⁸²

We were interested in studying the synthesis and properties of polymers containing the disulfidediamine functional group (R_2NSSNR_2) along the backbone. This functional group is very understudied in organic chemistry, and no polymers that contain this functional group are known.⁸³⁻⁹⁰ The most common use of disulfidediamines is as a thermally active cross-linking agent in the rubber industry due to the facile homolytic cleavage of its S-S bond at temperatures below 200 °C.⁹¹⁻⁹³ The cross-linking step yields functional groups that are different from disulfidediamines. This functional group has also found limited applications in the study of insecticides, fungicides, and as corrosion inhibitors in oil.^{94,95} One interesting aspect of the disulfidediamine functional group is that it possesses an S-S bond in a unique environment that leads to a low bond dissociation energy. In a recent report, the stability of the RS-SR bond towards homolytic cleavage (resulting in 2 equivalents of RS·) was studied for a variety of different molecules.^{92,96} Interestingly, $H_2NS-SNH_2$ had the lowest ΔH^0 (43.1 kcal mol⁻¹) for homolytic cleavage for all of the molecules that contained only two sulfur atoms. In contrast, CH_3SSCH_3 ($\Delta H^0 = 63.9$ kcal mol⁻¹) and even $NCS-SCN$ ($\Delta H^0 = 46.6$ kcal mol⁻¹) had significantly higher values for ΔH^0 and higher stabilities. Despite the low bond dissociation energy for the disulfide bond in disulfidediamines, molecules possessing this functional group are stable and readily handled using normal techniques.

Our interest in synthesizing poly(disulfidediamines) was based on their unique structure and the presence of a disulfide bond. Disulfide bonds are common in biology and were recently used in the synthesis of new biodegradable polymers and for self-

healing polymers as previously described. We hypothesized that poly(disulfidediamines) would degrade by two different, complementary routes in the body that would make them attractive targets in medicine. Poly(disulfidediamines) may degrade in a manner similar to that of polydisulfides by the action of glutathione on the interior and exterior of cells.^{67,76-80} Also, poly(disulfidediamines) may be readily cleaved under acidic conditions that is an important degradation pathway for polymers used in drug and gene delivery.⁹⁷⁻¹⁰⁷ Pharmaceutical drugs are often loaded into nanoparticles composed of polyesters that are stable in the bloodstream at pH of 7.4, but rapidly degrade after endocytosis into cells. These nanoparticles are trafficked to the endosome and lysosome within cells where the pH drops to approximately 5.0, which leads to a rapid, acid-catalyzed degradation of polyesters and release of a pharmaceutical drug. Although data in the literature on the acid-catalyzed degradation of disulfidediamines was lacking, we anticipated that they would rapidly degrade under acidic conditions based on analogy to sulfenamides (R_2NSR) and diaminosulfides (R_2NSNR_2). Both of these functional groups degrade within minutes under acidic conditions in water with first-order rate constants of approximately $2 \times 10^{-2} \text{ s}^{-1}$.^{108,109} These rate constants are several orders of magnitude faster than the degradation of ester bonds under similar conditions.¹¹⁰

In related work, we recently reported the synthesis of poly(sulfenamides) and poly(diaminosulfides) that are structurally related to poly(disulfidediamines).^{108,109} These three functional groups possess distinctly different reactivities, structures, and reaction products (Figure 16). One way to understand the differences between these functional groups is to compare them to esters, anhydrides, and acyl peroxides. It is well known that esters, anhydrides, and acyl peroxides belong to the same class of molecules and are

all based on oxygens and carbonyls, but they are well recognized as possessing different reactivities and yield different reaction products. Sulfenamides, diaminosulfides, and disulfidediamines are also members of the same class of molecules and are based on sulfur and nitrogen, but they have very different reactivities and reaction products. Despite the similarities in sulfenamides, diaminosulfides, disulfidediamines, it is the differences that are important and lead to different reactivities and products.

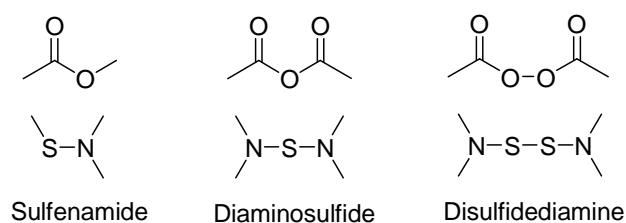


Figure 16 Sulfenamides, diaminosulfides, and disulfidediamines.

Polymers based on esters, anhydrides, and diacyl peroxides belong to one class of polymers, but these polymers have different reactivities and reaction products. Similarly, polymers based on sulfenamides, diaminosulfides, and disulfidediamines belong to the same class of polymers but also have important differences in their reactivities and reaction products.

In this chapter, the first synthesis of poly(disulfidediamines) is reported as well as initial work to demonstrate that the disulfidediamine functional group is stable to various conditions. These polymers were briefly studied for their stability at elevated temperatures as well as their electrical conductivity.

Results and Discussion

Synthesis and Stability of Disulfide Monomers

The synthesis of poly(disulfidediamine)s was proposed to occur by the reaction of secondary diamines with a disulfide monomer as shown in Figure 17. Although sulfur monochloride (S_2Cl_2) was commercially available and known to react with amines to yield disulfidediamines, it was not chosen for the polymerization reaction due to its reactivity with other functional groups such as alcohols and olefins and because HCl would be produced.¹¹¹⁻¹¹³

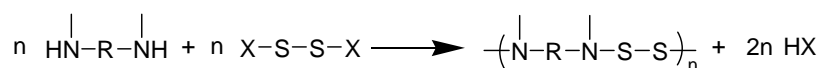


Figure 17 A general reaction scheme for the proposed synthesis of poly(disulfidediamines) is shown.

Disulfide transfer agents based on succinimide and phthalimide were well known in the literature (Figure 18) and were investigated for the synthesis of poly(disulfidediamines).¹¹⁴⁻¹¹⁶ The synthesis of molecule A yielded side products that were challenging to remove from the final product and limited the scale at which this reaction could be completed. Additionally, it was poorly soluble in organic solvents and had an upper limit for solubility of 50 mg mL^{-1} in methylene chloride. Although molecule B was synthesized in good yield and high purity, it possessed lower solubility than molecule A in many organic solvents. It was believed that the low solubility of these molecules would hinder their usefulness in step polymerizations.

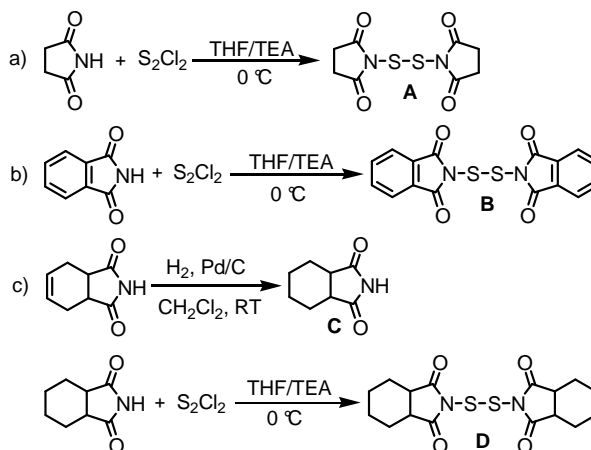


Figure 18 Disulfur transfer reagent syntheses.

a) and b) The synthesis of molecules A and B were based on literature procedures. c) The synthesis of a new disulfide monomer D was developed based on inexpensive, commercially available starting materials.

A modified synthesis of a disulfur monomer was developed as shown in Figure 18c. The first step was the hydrogenation of tetrahydrophthalimide using Pd/C. This reaction yielded a clean product after simple filtration of the Pd/C and did not require any further purification. The product was reacted with S₂Cl₂ in the presence of triethylamine to yield a solid that was readily purified by crystallization. Because neither step in the synthesis required column chromatography, they could be scaled up to >20 g without any limitation.

The stability of molecule A was studied in C₆D₆, CDCl₃, DMSO-*d*₆, and CD₃OD under normal atmospheric conditions to investigate any limitations in the use of this class of molecules. The stability of molecule A rather than molecule D was studied because of the simplicity of its ¹H NMR spectrum made investigating its decomposition clear. No decomposition of molecule A was observed after 61 days in either C₆D₆ or CDCl₃.

Approximately 10% of molecule A decomposed after 50 days in DMSO- d_6 , and 18% of it decomposed in CD₃OD in 5 h.

Synthesis and Stability of Disulfidediamines

The reaction of a disulfide monomer with two molar equivalents of benzylmethylamine was investigated to learn the kinetics of this reaction (Figure 19). This reaction was conducted in both CDCl₃ and C₆D₆ under dilute conditions to slow the reaction so that it could be studied by ¹H NMR spectroscopy.

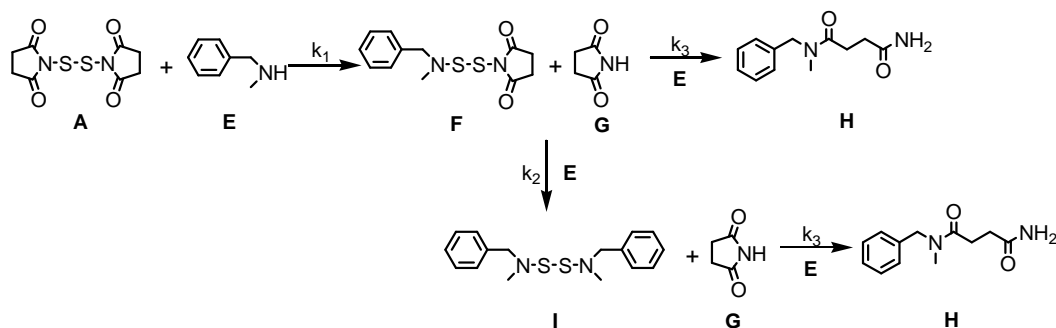


Figure 19 The reaction between molecule A and two molar equivalents of molecule E was investigated according to this reaction scheme.

The reaction kinetics were modeled based on the reactions in Figure 19. The differential equations were solved numerically by a fourth-order Runge-Kutta integration as described in the experimental section, and a fit to the experimental data is shown in Figure 20.¹¹⁷ The values for the rate constants measured in C₆D₆ ($k_1 = 7.8 \times 10^{-4} \text{ M}^{-1} \text{ s}^{-1}$, $k_2 = 1.9 \times 10^{-4} \text{ M}^{-1} \text{ s}^{-1}$, $k_3 = 3.8 \times 10^{-6} \text{ M}^{-1} \text{ s}^{-1}$) were slightly slower than the rate constants measured in CDCl₃ ($k_1 = 1.3 \times 10^{-3} \text{ M}^{-1} \text{ s}^{-1}$, $k_2 = 2.5 \times 10^{-4} \text{ M}^{-1} \text{ s}^{-1}$, $k_3 = 4.4 \times 10^{-6} \text{ M}^{-1} \text{ s}^{-1}$).

Inclusion of the side reaction, with rate constant k_3 , was justified because, when this process was not included, the fits of the time courses were coincident at long reaction times for benzylmethylamine (molecule E) and the monosubstituted product (molecule F). Inclusion of the side reaction accounts for the observation that the concentrations of these two species diverged at long reaction times. It is important to note that the value for k_3 is 50 to 295 times smaller than the values for k_2 and k_1 , so the side reaction is very minor during polymerization.

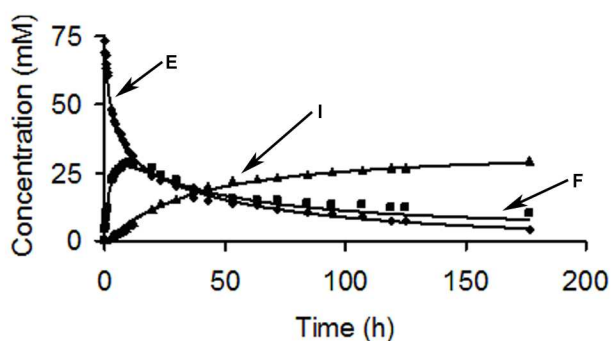


Figure 20 The kinetics of the transamination reaction between molecule A and two molar equivalents of molecule E in C_6D_6 .

Because the disulfidediamine functional group is not well known, the stability of a small molecule with this functional group was investigated in a variety of solvents. The stability of disulfidedi(ethylmethylamine) in different organic solvents was investigated by its addition to NMR tubes with C_6D_6 , $CDCl_3$, $DMSO-d_6$, and CD_3OD followed by sealing the NMR tubes. No evidence of degradation of disulfidedi(ethylmethylamine) was observed in any of these solvents after 61 days at room temperature.

The stability of this molecule was also investigated in 4/1 (v/v) CD₃OD/D₂O under acidic, neutral, and basic conditions to explore its stability in more challenging solvents.¹¹⁸ The decomposition of disulfidedi(ethylmethanamine) with nine molar equivalents of acetic acid was rapid with a rate constant of $1.08 \times 10^{-3} \text{ s}^{-1}$; approximately 95% of it degraded within 42 minutes. The decomposition of disulfidedi(ethylmethanamine) was nearly 10,000 times slower under both neutral and basic conditions. Under neutral conditions the rate constant for decomposition was $2.56 \times 10^{-7} \text{ s}^{-1}$ and only 68% of it degraded after 40 days. Under basic conditions (with nine molar equivalents of KOH) the rate constant was $5.02 \times 10^{-7} \text{ s}^{-1}$ and 75% of it degraded in 20 days.

Synthesis of Poly(disulfidediamines)

In the polymerization reaction shown in Figure 21, secondary amines can react with molecule D to add to a polymer chain, or they can undergo a transamination reaction with a disulfidediamine functional group along the backbone of the polymer. The transamination reaction between a diamine monomer and a disulfidediamine functional group along the polymer backbone will lead to a broadening of the polydispersity of the polymer and affect its final stability if an amine is an end group of the polymer. The kinetics of the transamination reaction shown in Figure 22 were studied in C₆D₆, CDCl₃, DMSO-*d*₆, and CD₃OD. The rate constants for the reaction were found to be approximately 10^4 times slower than the rate constants for the polymerization reactions in C₆D₆ and CDCl₃ (Table 1). Thus, the desired polymerization reaction is heavily favored. In fact, in comparison to similar transamination reactions for diaminosulfides and

sulfenamides, the transamination reactions of disulfidediamines are approximately 10^2 times slower in all solvents measured.

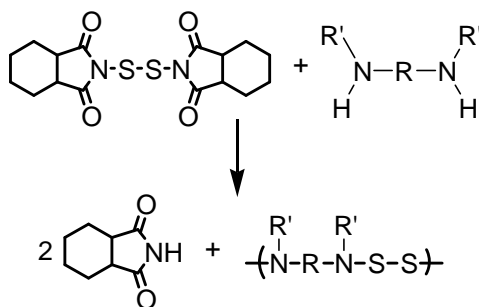


Figure 21 How poly(disulfidediamines) were synthesized using molecule D as the disulfide monomer.

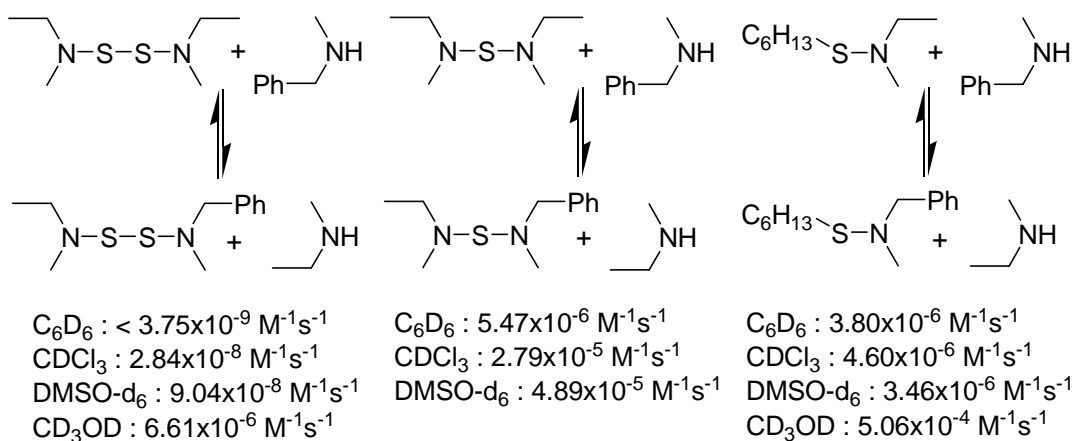


Figure 22 Comparison of transamination rate constants.

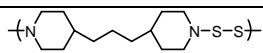
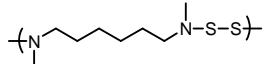
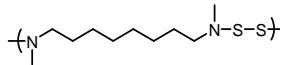
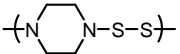
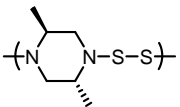
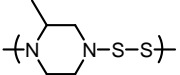
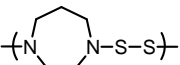
The rate constants for the reactions with the disulfidediamine functional group were measured in this work. The rate constants for the reactions with the diaminosulfide and sulfenamides functional groups were taken from prior work.^{108,109}

Table 1 The rate constants for the reactions shown in Figure 22.

Functional group	Solvent	Rate constant (M ⁻¹ s ⁻¹)	Reference
Disulfidediamine	C ₆ D ₆	<3.75 X 10 ⁻⁹	This chapter
Diaminosulfide	C ₆ D ₆	5.47 x 10 ⁻⁶	49
Sulfenamide	C ₆ D ₆	3.80 x 10 ⁻⁶	48
Disulfidediamine	CDCl ₃	2.84 x 10 ⁻⁸	This chapter
Diaminosulfide	CDCl ₃	2.79 x 10 ⁻⁵	49
Sulfenamide	CDCl ₃	4.60 x 10 ⁻⁶	48
Disulfidediamine	DMSO-d ₆	9.04 x 10 ⁻⁸	This chapter
Diaminosulfide	DMSO-d ₆	4.89 x 10 ⁻⁵	49
Sulfenamide	DMSO-d ₆	3.46 x 10 ⁻⁶	48
Disulfidediamine	CD ₃ OD	6.61 x 10 ⁻⁶	This chapter
Sulfenamide	CD ₃ OD	5.06 x 10 ⁻⁴	48

A series of polymerizations were completed with molecule D as the disulfide monomer and secondary diamines as the other monomer (Table 2). These polymerizations were completed in CH₂Cl₂ at room temperature for 24 h. The solvent was used as purchased without further purification, and the reactions were completed under ambient atmospheric conditions. The polymers were characterized by ¹H and ¹³C NMR spectroscopy and size exclusion chromatography (SEC) using a laser light scattering apparatus (Figure 23). These polymers are the first examples of poly(disulfidediamines) ever reported in the literature.

Table 2 The polymerizations were completed as shown in Figure 21.

Entry	Polymer	Isolated Yield (%)	M_w (g/mol) ^b	DP ^c	Conversion ^c (%)	PDI
1		70	11,400	60	98	1.4
2		73	5,000	37	97	1.3
3		75	4,100	31	97	1.2
4 ^d		71	-	-	-	-
5		65	3,900	37	97	1.2
6		67	5,300	55	98	1.2
7		70	8,700	60	98	1.8

^aAll reactions performed at ambient atmospheric conditions in CH_2Cl_2 . ^bThe measured values for M_w based on the absolute molecular weights calculated from the SEC micrographs and using refractive index and laser light scattering detectors. ^cThe values for the degree of polymerization (DP) and the conversions were calculated from M_n . ^d The solubility of entry 4 was too low to allow for full characterization.

The reactions to yield polymers went to high conversions of 97-98% based on calculations from the values for M_n . Despite the high conversions, the observed molecular weights for the polymers were modest due to the low molecular weights for the monomers. For instance, the disulfide monomer only contributed 64 g mol^{-1} when added to the growing polymer chain. Furthermore, the values for PDIs were lower than expected for step polymerizations for several possible reasons. The polymers may have been fractionated in the isolation steps resulting in a loss of some low molecular weight

polymer. In Table 2 the isolated yields of the polymers are reported to demonstrate that a majority, but not all, of the polymer was isolated. Another possible reason for the lower than expected values for PDI was due to the challenge of accurately measuring the PDI for low molecular weight polymers. For instance, low molecular weight polymers have higher rates of diffusion than high molecular weight polymers which makes separating based on molecular weight and maintaining the separation challenging. Also, although the columns used in the separation were rated to separate polymers with these molecular weights, the choice of columns was not optimized for polymers with these molecular weights. It is important to note that although the PDIs were lower than expected, the molecular weights were found using refractive index and laser light scattering detectors that allowed a determination of the absolute molecular weights. Thus, the molecular weights and conversions found from the isolated polymers are accurate and demonstrate that the polymerizations were successful.

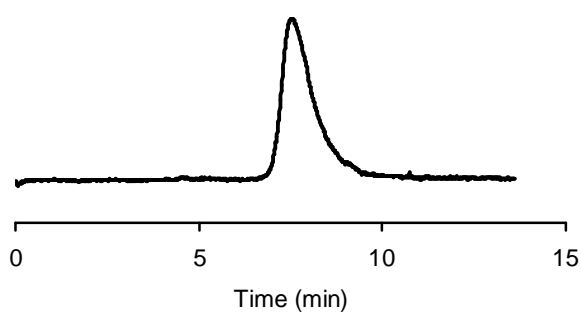


Figure 23 A SEC chromatogram of the polymer from entry 1 of Table 2.

Although small molecule reactions by us and others have shown that the reactions between secondary amines and molecules A, B, or D result in disulfidediamines, the presence of sulfur in the polymers was not directly probed by ^1H or ^{13}C NMR spectroscopy. To provide further evidence for the presence of disulfidediamine functional groups, the polymer shown in entry 1 of Table 2 was studied by elemental analysis. The theoretical mass percentages (C: 57.3%, N: 10.3%, S: 23.5%, and H: 8.8%) for the repeat unit closely matched the values that were measured (C: 55.3%, N: 9.7%, S: 23.1%, and H: 8.5%). The analyzed elements accounted for 97% of the initial mass of the sample.

Thermal Gravimetric Analysis (TGA)

The polymer shown in entry 1 of Table 2 was studied by TGA (Figure 24). The sample was heated at a rate of 1 °C per min under N_2 . The polymer was stable at elevated temperatures but underwent a sudden loss of weight at 175 °C. This sudden loss of mass was expected based on the use of small molecules possessing disulfidediamines as vulcanizing agents in the rubber industry.⁹¹⁻⁹³

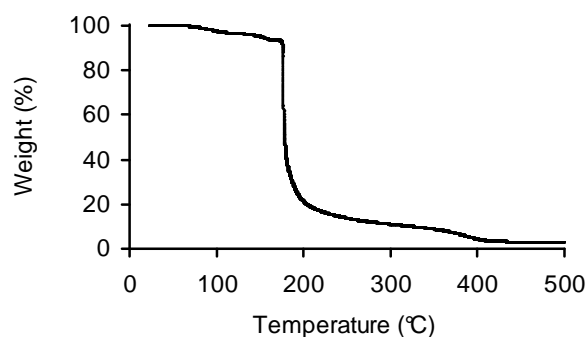


Figure 24 The TGA of the polymer from entry 1 in Table 2.

Electrically Conducting Poly(disulfidediamines)

The first inorganic, electrically conducting polymer was polythiazyl, and it was first synthesized in 1953 (Figure 25).¹¹⁹⁻¹²⁴ In fact, polythiazyl is the only known undoped polymer that is superconducting at low temperatures.^{119,125} Polythiazyl is composed entirely of sulfur and nitrogen arranged in an alternating pattern which does not allow its electrical properties to be readily changed by varying its molecular structure. In contrast, the physical and chemical properties of electrically conducting polymers based on organic functional groups (i.e., polythiophene and polyaniline) can be varied by the addition of functional groups along the polymeric backbone.

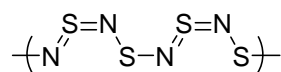


Figure 25 The structure of polythiazyl.

The interesting electrical properties of polythiazyl led us to investigate whether poly(disulfidediamines) were also electrically conducting. The synthesis of the polymer shown in Figure 11 was first attempted using molecule D as the disulfide monomer, but no reaction was observed. Instead, the polymer was synthesized using S_2Cl_2 as the disulfide monomer and triethylamine as a base to remove the HCl by-product. The resulting polymer was characterized by 1H and ^{13}C NMR spectroscopy and SEC using laser light scattering. The value for M_w was $4,300 \text{ g mol}^{-1}$ (PDI = 1.31), which led to a calculated degree of polymerization of 42. This polymer was very interesting because the conjugation was through the inorganic disulfidediamine functional group, but the aromatic ring bonded to the nitrogen would allow the conjugation to be altered by varying the presence of functional groups. Thus, this polymer combined conductivity through inorganic functional groups with the ability to alter the conductivity by the presence of organic functional groups.

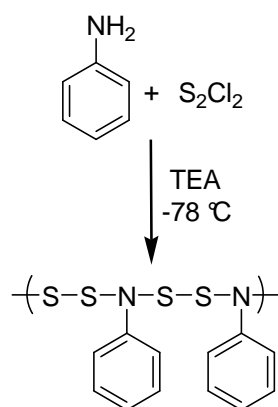


Figure 26 The synthesis of a conjugated poly(disulfidediamine).

This polymer was fabricated into a layered device in order to measure its current-voltage curve in the solid state (Figure 27). The cross-sectional area was $16.9 \times 10^{-3} \text{ mm}^2$ and the thickness of the poly(disulfidediamine) was 40 nm. The data in Figure 27 show that the polymer possessed diode characteristics and was weakly electrically conducting. The conductivity between 9 and 10 V was estimated to be $4.73 \times 10^{-8} \text{ S cm}^{-1}$. Although this value was very low and similar to that of distilled water, it was comparable to values for other undoped polymers. For instance, undoped polythiophene, polyaniline, and polyacetylene have conductivities of approximately 10^{-5} to $10^{-9} \text{ S cm}^{-1}$.¹²⁶⁻¹³⁰ In contrast, insulating polymers such as paraffin wax have conductivities of approximately $10^{-20} \text{ S cm}^{-1}$. Polythiophene, polyaniline, and polyacetylene must be doped in order to reach more desired conductivities of $1-10^3 \text{ S cm}^{-1}$. The effect of dopants was briefly studied by exposing the device to iodine vapor for 5 min and then immediately measuring the conductivity (see Figure 27). The iodine doping enhanced the electrical conductivity, and the measured value was $2.85 \times 10^{-7} \text{ S cm}^{-1}$. In future work we will study how the presence of additives alters the conductivities of poly(disulfidediamines).

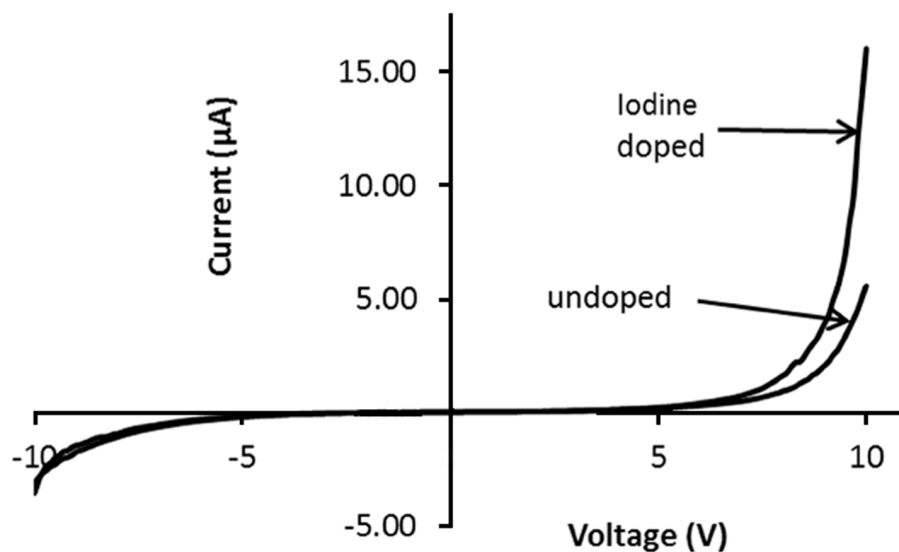


Figure 27 The current-voltage curve for the polymer synthesized as shown in Figure 26.

Conclusions

Poly(disulfidediamines) were unknown prior to this work despite a long-term interest in polymers possessing sulfide and disulfide bonds. To synthesize these polymers, a new disulfide monomer was synthesized in two steps in high yield without the need for chromatography. Despite a low bond dissociation energy for the disulfidediamine functional group, these polymers were very stable in protic and aprotic solvents. Studies with small molecules showed that the disulfidediamine functional group was stable in various solvents, but rapidly decomposed in methanol/water in the presence of a carboxylic acid. These polymers have high stabilities that are desired for many applications, they are easy to handle, and they possess no noticeable odor.

Working with new functional groups offers new opportunities, and two opportunities opened up by the synthesis of poly(disulfidediamines) were explored. In

one application, we showed that these polymers were thermally stable, but underwent a rapid and nearly complete degradation when heated to 175 °C. We believe, but have not shown, that this degradation was due to the homolytic cleavage of the S-S bond in these polymers to yield highly reactive sulfur-based radicals. In a second opportunity, a conducting polymer was synthesized and characterized. This polymer has conjugation through organic and inorganic functional groups and can be considered a “hybrid” polymer. These polymers combine some of the attractive electrical properties of polymers based on SN bonds with the ability to tailor electrical properties by varying the presence of organic functional groups. In future work, the opportunities offered by working with electrically conducting poly(disulfidediamines) will be pursued.

Experimental

Characterization

^1H and ^{13}C NMR spectra were recorded on a Bruker DPX 300 at 300 MHz and 75 MHz, respectively using CDCl_3 as the solvent and were referenced to TMS unless otherwise noted. SEC was performed using chloroform as the mobile phase (1.0 mL min^{-1}) at 35 °C. A Waters 515 HPLC pump and a Waters column (Styragel HR4E) were used. A DAWN EOS 18 angle laser light scattering detector from Wyatt Corp. to measure light scattering and a Wyatt Optilab DSP to measure changes in refractive index were used to measure absolute molecular weights of polymers. Current-voltage (I-V) measurements were performed on a Keithly 2400 source measurement unit. The polymeric film thickness was measured with a Veeco optical profilometer. Thermal gravimetric analysis was performed on a TA Instruments TGA Q5000.

Materials

Phthalimide, *cis*-1,2,3,6-tetrahydrophthalimide, benzylmethylamine, ethylmethylamine, palladium on carbon, acetic acid, potassium hydroxide, and triethylamine were purchased from Aldrich or Acros and used as received. Hydrogen was purchased from PraxAir. Succinimide, 4,4'-trimethylenedipiperidine, piperazine, and *trans*-2,5-dimethylpiperazine were purchased from Aldrich and purified by recrystallization. *N,N'*-Dimethylhexanediamine and *N,N'*-dimethyloctanediamine were purchased from Aldrich and purified by vacuum distillation. Sulfur monochloride and *N,N'*-di-*sec*-butyl-*p*-phenylenediamine were purchased from Aldrich, purified by vacuum distillation, and stored under N₂. HPLC grade chloroform purchased from Acros Organics was used as the GPC solvent after filtration through a glass frit. All other solvents were reagent grade and purchased from Acros Organics.

Synthesis of molecule A

Succinimide (3.0 g, 30.3 mmol) was added to a round bottom flask containing triethylamine (4.5 mL, 32.3 mmol) and THF (75 mL). This mixture was cooled to 0 °C with an ice bath. Sulfur monochloride (1.2 mL, 15.2 mmol) was added dropwise over one min. The solution was immediately filtered by vacuum and washed with additional THF (50 mL). The solvent was removed under vacuum to yield a light yellow solid. This solid was dissolved in a minimal amount of CH₂Cl₂ to which an excess of hexanes was added. The colored impurities precipitated from the solution and the liquid was removed and concentrated under vacuum to yield a white crystalline solid (6.2 g, 46%). ¹H NMR δ 2.86 (s); ¹³C NMR δ 175.7, 29.0. HREIMS calculated for C₈H₈N₂O₄S₂: 259.9926. Found: 259.9931.

Synthesis of molecule B

This molecule was synthesized by modification of a literature procedure.¹¹⁴⁻¹¹⁶ Phthalimide (2.9 g, 19.7 mmol) was dissolved in THF (40 mL) and triethylamine (4 mL). The mixture was cooled in a salt ice bath, and then sulfur monochloride (0.8 mL, 10 mmol) was added dropwise to the cooled mixture. The solution was stirred for one h, and then quenched with 70 mL H₂O. The resulting precipitate was filtered and washed with diethyl ether. Crystallization from 2:1 (v:v) CHCl₃:CH₃OH yielded white crystals (3.5 g, 98%). ¹H NMR δ 7.94-7.98 (m, 4H), 7.81-7.85 (m, 4H); ¹³C NMR δ 167.2, 136.5, 132.5, 125.1.

Synthesis of molecule C

cis-1,2,3,6-Tetrahydrophthalimide (25 g, 165 mmol) was dissolved in CH₂Cl₂ (150 mL) and added to a metal Parr reactor. Palladium (10% wt. on carbon, 500 mg) was added to this solution. The reactor was pressurized with H₂ (1000 psi) and stirred at 25 °C for 24 h. The palladium on carbon was removed by filtration, and the solvent was removed under vacuum to yield a white solid (22 g, 88%). ¹H NMR δ 7.79-8.02 (s, 1H), 2.87-2.95 (m, 2H), 1.75-1.89 (m, 4H), 1.45-1.49 (m, 4H); ¹³C NMR δ 181.0, 41.1, 23.8, 21.9.

Synthesis of molecule D

Molecule C (31.5 g, 209 mmol) was dissolved in 500 mL CH₂Cl₂ and triethylamine (43.5 mL, 312 mmol). The mixture was cooled to -78 °C. Sulfur monochloride (8.5 mL, 104 mmol) was added slowly over 20 min using a pressure-equalizing addition funnel. The solution was stirred for 10 min at -78 °C then washed

with two 500-mL portions of sat. NaCl followed by two 500-mL portions of 0.2 M NaOH. The solution was dried with MgSO₄ and the solvent removed under vacuum. The resulting solid was crystallized from 8:3 (v:v) hexanes:EtOAc yielding a white solid (27.3 g, 71%). ¹H NMR δ 2.99 (m, 4H), 2.05 (m, 8H), 1.5 (m, 8H); ¹³C NMR δ 177.4, 40.6, 25.4, 23.9, 22.1. HREIMS calculated for C₁₆H₂₀N₂O₄S₂: 368.0865. Found: 368.0864.

Procedure for Table 2, entry 1

Molecule D (3.5 g, 9.5 mmol) was combined with 4, 4'-trimethylenedipiperidine (2.0 g, 9.5 mmol) in 50 mL of CH₂Cl₂. The reaction mixture was stirred for 24 h, and then precipitated from CH₃OH to yield a white solid (1.8 g, 70%). ¹H NMR δ 2.96-2.99 (m, 4H), 2.58-2.64 (m, 4H), 1.67-1.70 (m, 4H), 1.19-1.28 (m, 12H); ¹³C NMR δ 57.2, 36.7, 34.5, 33.8, 24.1.

Procedure for Table 2, entry 2

Molecule D (5 g, 13.4 mmol) was combined with *N,N'*-dimethylhexanediamine (1.93 g, 13.4 mmol) in 50 mL of CH₂Cl₂. The reaction mixture was stirred for 48 h, then extracted with three 50 mL portions of 4 M KOH and dried with MgSO₄. Evaporation of the solvent yielded a yellow oil (2.0 g, 72%). ¹H NMR δ 2.62 (m, 5H), 1.45-1.65 (m, 2H), 1.23-1.44 (m, 2H); ¹³C NMR δ 59.5, 46.9, 28.3, 26.9.

Procedure for Table 2, entry 3

Molecule D (2.5 g, 6.86 mmol) was combined with *N,N'*-dimethyloctanediamine (1.18 g, 6.86 mmol) in 50 mL CH₂Cl₂. The reaction mixture was stirred for 48 h, then extracted with three 50 mL portions of 4 M KOH and dried with MgSO₄. Evaporation of

the solvent yielded a yellow oil (1.2 g, 75%). ^1H NMR δ 2.53-2.58 (t, 2H), 2.43 (s, 3H), 1.45-1.49 (m, 2H), 1.30 (m, 4H); ^{13}C NMR δ 59.3, 46.6, 29.5, 28.2, 26.8.

Procedure for Table 2, entry 4

Molecule D (5.36 g, 14.4 mmol) was combined with piperazine (1.24 g, 14.4 mmol) in 50 mL of CH_2Cl_2 . The reaction mixture was stirred for 24 h, and then precipitated from CH_3OH . The white solid was collected by filtration and dried under vacuum (1.55 g, 71%). ^1H NMR δ 2.85-2.97 (s).

Procedure for Table 2, entry 5

Molecule D (4.86 g, 13.2 mmol) was combined with *trans*-2,5-dimethylpiperazine (1.5 g, 13.2 mmol) in 40 mL of CH_2Cl_2 . The reaction mixture was stirred for 24 h, then extracted with six 200-mL portions of 4 M KOH and dried with MgSO_4 . Evaporation of the solvent yielded a white solid (1.5 g, 65%). ^1H NMR δ 2.96 (m, 4H), 2.40-2.70 (m, 2H), 1.17-1.04 (m, 6H); ^{13}C NMR δ 64.1, 57.8, 18.8, 17.9.

Procedure for Table 2, entry 6

Molecule D (10.15 g, 27.6 mmol) was combined with 2-methylpiperazine (2.7 g, 27.6 mmol) in 100 mL of CH_2Cl_2 . The reaction mixture was stirred for 24 h, then extracted with nine 200-mL portions of 4 M KOH and dried with MgSO_4 . Evaporation of the solvent yielded a white solid (2.9 g, 67%). ^1H NMR δ 3.08-2.76 (m, 6H), 2.61-2.46 (m, 1H), 1.20-1.04 (m, 3H); ^{13}C NMR δ 63.9, 56.9, 51.7, 46.8, 18.6, 17.9.

Procedure for Table 2, entry 7

Molecule D (4.2 g, 11.4 mmol) was combined with homopiperazine (1.14 g, 11.4 mmol) in 50 mL of CH₂Cl₂. The reaction mixture was stirred for 24 h, then extracted with four 200-mL portions of 4 M KOH and dried with MgSO₄. Evaporation of the solvent yielded a white solid (1.3 g, 70%). ¹H NMR δ 3.25-3.11 (m, 8H), 1.95-1.87 (m, 2H); ¹³C NMR δ 61.0, 59.2, 30.4.

Stability of disulfidedisuccinimide (molecule A)

Molecule A was dissolved in C₆D₆ at a conc. of 15 mg mL⁻¹, and in CDCl₃, DMSO-d₆, or CD₃OD at a conc. of 30 mg mL⁻¹. Decomposition was monitored by ¹H NMR spectroscopy of the succinimide protons at δ 2.55. Succinimide was the only decomposition product identifiable by ¹H NMR.

Transamination kinetics/Runge-Kutta integration

The reaction of molecule A with two molar equivalents of molecule E was modeled according to the reaction scheme in Figure 28. Reaction progress was monitored by ¹H NMR of the benzyl protons in molecule E (δ 3.76 in CDCl₃, δ 3.52 in C₆D₆), molecule F (δ 4.01 in CDCl₃, δ 3.97 in C₆D₆), and molecule I (δ 3.91 in CDCl₃, δ 3.82 in C₆D₆).

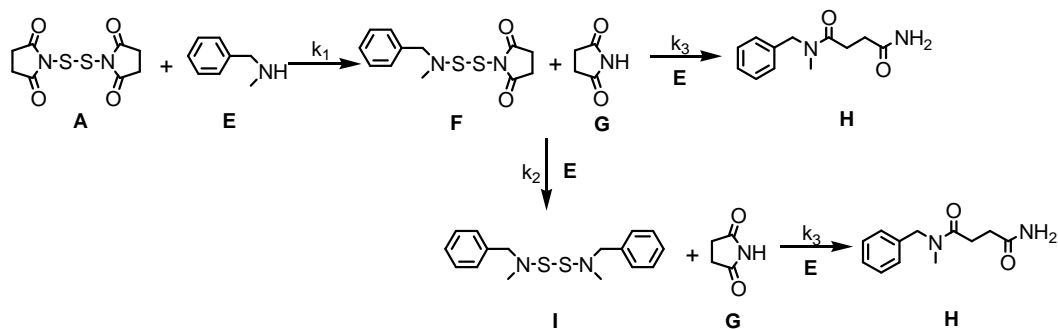


Figure 28 Runge-Kutta intergration.

The corresponding differential rate equations are as follows:

$$d[\mathbf{A}]/dt = -2k_1[\mathbf{A}][\mathbf{E}]$$

$$d[\mathbf{E}]/dt = -2k_1[\mathbf{A}][\mathbf{E}] - k_2[\mathbf{F}][\mathbf{E}] - 2k_3[\mathbf{G}][\mathbf{E}]$$

$$d[\mathbf{F}]/dt = 2k_1[\mathbf{A}][\mathbf{E}] - k_2[\mathbf{F}][\mathbf{E}]$$

$$d[\mathbf{I}]/dt = k_2[\mathbf{F}][\mathbf{E}]$$

$$d[\mathbf{G}]/dt = 2k_1[\mathbf{A}][\mathbf{E}] + k_2[\mathbf{F}][\mathbf{E}] - 2k_3[\mathbf{G}][\mathbf{E}]$$

The factor of two in the differential elements $2k_1[\mathbf{A}][\mathbf{E}]$ and $2k_3[\mathbf{G}][\mathbf{E}]$ are due to a statistical factor that arises from two identical reaction sites in **A** and the fact that the side product **H** is produced by parallel pathways. Figure 29 shows the fits that arise from this analysis for the reaction that was run using CDCl_3 as the solvent. In the main text of the chapter, the data and the fit when the reaction was run in C_6D_6 are shown.

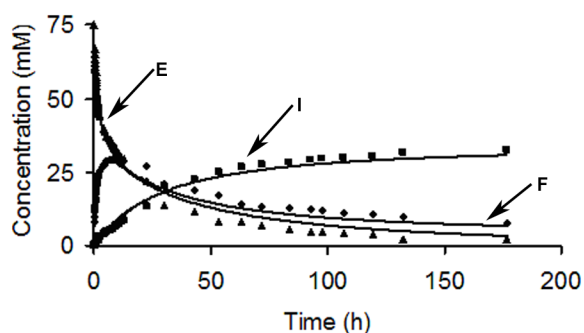


Figure 29 Transamination rates.

The differential rate equations for the reaction were obtained numerically using fourth-order Runge-Kutta integration. For example, the following equations are obtained for the time course for the disappearance of **E**, as measured by the percent integrated intensity of the benzyl protons in the ^1H NMR spectrum:

$$\mathbf{E}_{1j} = \{-2k_1[\mathbf{A}]_{j-1}[\mathbf{E}]_{j-1} - k_2[\mathbf{F}]_{j-1}[\mathbf{E}]_{j-1} - 2k_3[\mathbf{G}]_{j-1}[\mathbf{E}]_{j-1}\} \times \Delta t$$

$$\mathbf{E}_{2j} = \{-2k_1([\mathbf{A}]_{j-1} + \mathbf{A}_{1j}/2)([\mathbf{E}]_{j-1} + \mathbf{E}_{1j}/2) - k_2([\mathbf{F}]_{j-1} + \mathbf{F}_{1j}/2)([\mathbf{E}]_{j-1} + \mathbf{E}_{1j}/2) - 2k_3([\mathbf{G}]_{j-1} + \mathbf{G}_{1j}/2)([\mathbf{E}]_{j-1} + \mathbf{E}_{1j}/2)\} \times \Delta t$$

$$\mathbf{E}_{3j} = \{-2k_1([\mathbf{A}]_{j-1} + \mathbf{A}_{2j}/2)([\mathbf{E}]_{j-1} + \mathbf{E}_{2j}/2) - k_2([\mathbf{F}]_{j-1} + \mathbf{F}_{2j}/2)([\mathbf{E}]_{j-1} + \mathbf{E}_{2j}/2) - 2k_3([\mathbf{G}]_{j-1} + \mathbf{G}_{2j}/2)([\mathbf{E}]_{j-1} + \mathbf{E}_{2j}/2)\} \times \Delta t$$

$$\mathbf{E}_{4j} = \{-2k_1([\mathbf{A}]_{j-1} + \mathbf{A}_{3j})([\mathbf{E}]_{j-1} + \mathbf{E}_{3j}) - k_2([\mathbf{F}]_{j-1} + \mathbf{F}_{3j})([\mathbf{E}]_{j-1} + \mathbf{E}_{3j}) - 2k_3([\mathbf{G}]_{j-1} + \mathbf{G}_{3j})([\mathbf{E}]_{j-1} + \mathbf{E}_{3j})\} \times \Delta t$$

$$[\mathbf{E}]_j = [\mathbf{E}]_{j-1} + (\mathbf{E}_{1j} + 2\mathbf{E}_{2j} + 2\mathbf{E}_{3j} + \mathbf{E}_{4j})/6$$

The first equation is the finite difference analog of the differential equation for **E**, and is used to calculate the concentration increment \mathbf{E}_{1j} from the concentrations of **A**, **E**,

F, and **G** one Δt earlier, i.e. $[\mathbf{A}]_{j-1}$, $[\mathbf{E}]_{j-1}$, $[\mathbf{F}]_{j-1}$ and $[\mathbf{G}]_{j-1}$. A discrete time differential of $\Delta t = 5$ min was used in all calculations. The second through fourth equations calculate concentration increments of **E** that allow for a more accurate extrapolation of the change in $[\mathbf{E}]$ over Δt . The final equation then calculates the concentration of **E** at time j from that at time $j-1$ (one Δt earlier) as a weighted average over the concentration increments \mathbf{E}_{1j} through \mathbf{E}_{4j} . These calculations are repeated over the time domain of the reaction time course. Similar procedures were used to calculate the time courses for the other species **F**, **I**, **G**, and **H**. The first concentration extrapolation in the time course for **E** is from time 0 to 5 min. For this calculation $[\mathbf{E}]_{j-1} = 100$ in % integrated intensity units. Similarly, initial values for **A**, **F**, **I**, **G**, and **H** were 50, 0, 0, 0 and 0, respectively.

A computer program was written to perform the Runge-Kutta integrations, and a component of the input was a set of initial estimates of the rate constants k_1 , k_2 and k_3 . From these estimates the program generated a 11 x 11 x 11 grid of rate constant estimates. The numerical integration was performed for each rate constant set in the grid, and for each set the summed-squared-variance (SSV) was calculated from the following equation:

$$\mathbf{SSV} = \sum_{\mathbf{i}}^{\mathbf{n}} (\%I_{\mathbf{calc},\mathbf{i}} - \%I_{\mathbf{obs},\mathbf{i}})^2$$

For a set of n measured %I values, this equation calculates the sum of the squares of the differences between the calculated and observed values. The rate constant set in the grid that gave the minimum value of SSV was taken as the set of best estimates of rate constants. A coarse initial grid was searched in this way, and the best estimates of the rate constants so calculated were used to seed a second grid search over a narrower

range of rate constants. This process was repeated again – a third grid search – and the rate constants of the final best estimate set are accurate to three significant figures.

Stability of disulfidedi(ethylmethanamine)

Disulfidedi(ethylmethanamine) was dissolved in C_6D_6 , $CDCl_3$, $DMSO-d_6$, or CD_3OD at a conc. of 30 mg mL^{-1} . Decomposition was monitored by 1H NMR spectroscopy of the *N*-methyl protons (δ 2.66 in $CDCl_3$, δ 2.45 in C_6D_6 , δ 2.57 in $DMSO-d_6$, δ 2.63 in CD_3OD) and the *N*-ethyl (δ 2.71 in $CDCl_3$, δ 2.51 in C_6D_6 , δ 2.65 in $DMSO-d_6$, δ 2.71 in CD_3OD).

Stability of disulfidedi(ethylmethanamine) in $CD_3OD:D_2O$

Acidic Conditions. Disulfidedi(ethylmethanamine) (20.6 mg, 0.11 mmol) and acetic acid (60 mg, 1 mmol) were dissolved in a 4:1 (v:v) mixture of $CD_3OD:D_2O$. *tert*-Butanol (11.7 mg, 0.16 mmol) was added as an internal standard.

Neutral Conditions. Disulfidedi(ethylmethanamine) (21.2 mg, 0.12 mmol) was dissolved in a 4:1 (v:v) mixture of $CD_3OD:D_2O$. *tert*-Butanol (12.4 mg, 0.17 mmol) was added as an internal standard.

Basic Conditions. Disulfidedi(ethylmethanamine) (20.7 mg, 0.11 mmol) and potassium hydroxide (56 mg, 1 mmol) were dissolved in a 4:1 (v:v) mixture of $CD_3OD:D_2O$. *tert*-Butanol (10.7 mg, 0.15 mmol) was added as an internal standard.

Decomposition under all three conditions was monitored by 1H NMR spectroscopy of the *N*-methyl signal at δ 2.68 relative to the methyl signal of the *tert*-butanol internal standard at δ 1.22. *N*-ethylmethanamine was the only decomposition

product identifiable by NMR. The decomposition results under neutral and basic conditions are shown in Figure 30.

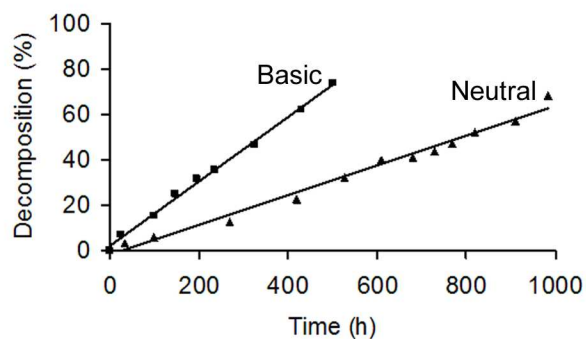


Figure 30 Decomposition of disulfidedi(ethylmethylethylamine).

Transamination kinetics

The reaction between disulfidedi(ethylmethylethylamine) and two molar equivalents of benzylmethylethylamine was studied in four solvents (Figure 31). These reactions were slow, so the kinetics of replacement of one ethylmethylethylamine with one benzylmethylethylamine was studied. Rate constants for all solvents were determined using conversions obtained by ^1H NMR spectroscopy of the benzyl signals in benzylmethylethylamine (δ 3.72 in CDCl_3 , δ 3.43 in C_6D_6 , δ 3.69 in DMSO-d_6 , δ 3.68 in CD_3OD) and the product (δ 3.85 in CDCl_3 , no decomposition in C_6D_6 , δ 3.89 in DMSO-d_6 , δ 3.85 in CD_3OD).

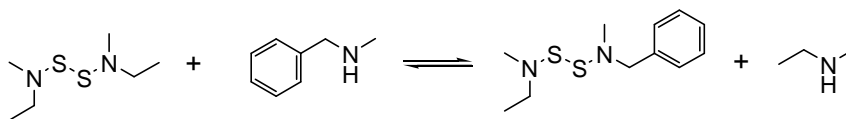


Figure 31 Transamination kinetics

Disulfidedi(ethylmethylamine) (56.3 mg, 0.325 mmol) was combined with methylbenzylamine (75.2 mg, 0.65 mmol) in 1 mL of C_6D_6 .

Disulfidedi(ethylmethylamine) (52.8 mg, 0.30 mmol) was combined with methylbenzylamine (71.0 mg, 0.60 mmol) in 1 mL of $CDCl_3$.

Disulfidedi(ethylmethylamine) (54.0 mg, 0.31 mmol) was combined with methylbenzylamine (72.2 mg, 0.62 mmol) in 1 mL of $DMSO-d_6$.

Disulfidedi(ethylmethylamine) (52.6 mg, 0.29 mmol) was combined with methylbenzylamine (70.4 mg, 0.58 mmol) in 1 mL of CD_3OD .

Thermal gravimetric analysis

The polymer from Table 2, entry 1 (2.97 mg, 3.67×10^{-4} mmol) was added to a platinum balance. The temperature was increased from ambient to 500 °C at a rate of 1 °C per min while under N_2 .

Synthesis of the conjugated poly(disulfidediamine)

Aniline (1.0 mL, 12.5 mmol) and triethylamine (5.2 mL, 37.4 mmol) were combined in 11 mL of freeze-pump-thawed CH_2Cl_2 under N_2 . After the mixture was cooled to -78 °C, sulfur monochloride (1.0 mL, 12.5 mmol) was added dropwise over 10 min. The solution was stirred for 35 min and then poured into 40 mL of cold MeOH to

induce precipitation of the polymer. The resulting precipitate was filtered and washed with an excess of MeOH to yield an orange powder (420 mg, 22%). $^1\text{H NMR}$ (CDCl_3): δ 7.32 (s, 5H).

Diode fabrication

The diode devices fabricated on Si wafers covered with 300 nm of thermal oxide. The wafers were diced into $12.5 \times 9 \text{ mm}^2$ pieces, washed in several solvents, and finally cleaned in an oxygen plasma cleaner. All these steps were performed in a class 1000 clean room. A 2-nm-thick Cr seed layer was deposited by electron-beam evaporation through a shadow mask in high vacuum at a rate of 0.1 nm/s and covered by a 15-nm-thick Au layer, also deposited by e-beam evaporation as the bottom electrode. Then a 60 nm thick layer of the conducting polymer poly(3,4-ethylenedioxythiophene)-poly(styrene-sulfonate) (PEDOT) was spincoated to enhance the hole injection. The polymeric film of the polydisulfidediamine was fabricated by spincoating from chloroform solution (concentration was 5 mg/ml) at 1500 rpm and then transferred into and kept in a high-vacuum chamber for 60 hours to extract any solvent remaining from the spin-coating process. Finally, the top electrode calcium (15 nm), and a capping layer of aluminum (30 nm) layers were deposited by thermal evaporation. Calcium serves as the cathode for the diode devices. The device area was $0.13 \text{ mm} \times 0.13 \text{ mm}$.

Current-voltage (I-V) measurements were performed by Keithley 2400 source measurement unit and the polymeric film thickness was measured by Veeco optical profilometer.

For I-V measurements of iodine doped devices, we exposed the pristine devices to iodine vapor for 5 minutes and the I-V measurements were taken right after the doping process.

^1H NMR Spectra

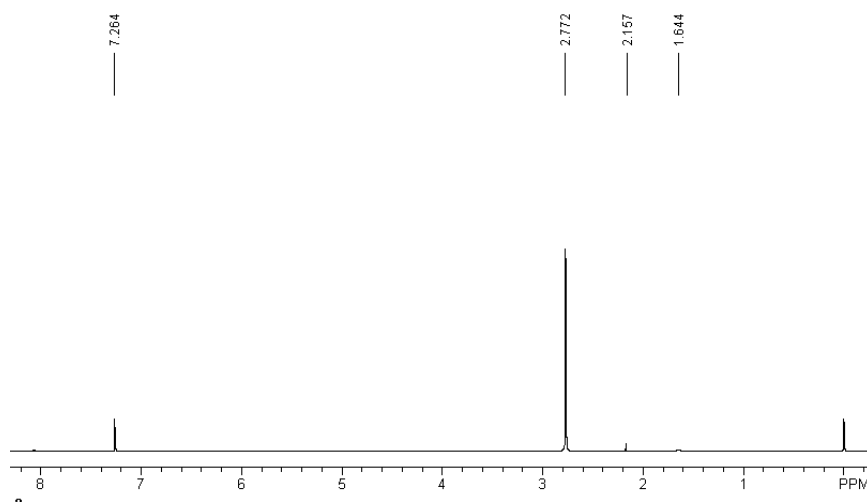


Figure 32 NMR spectra of molecule A.

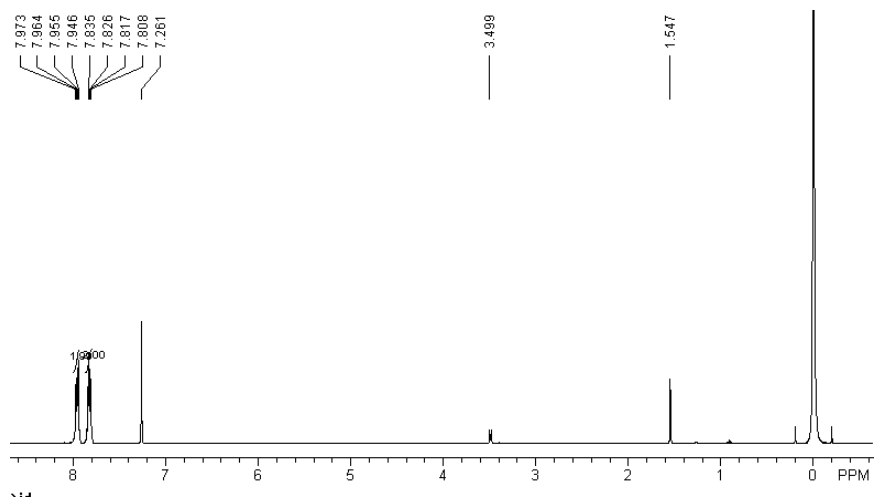


Figure 33 NMR spectra of molecule B.

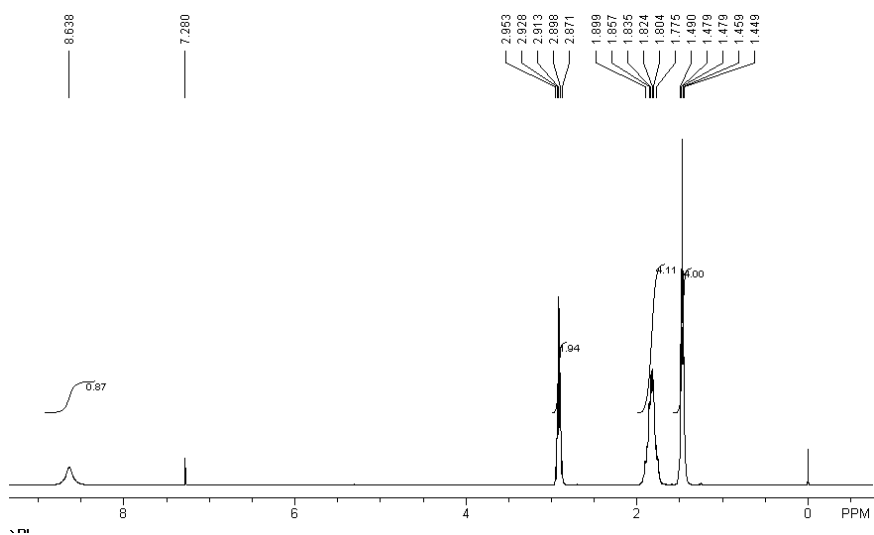


Figure 34 NMR spectra of molecule C.

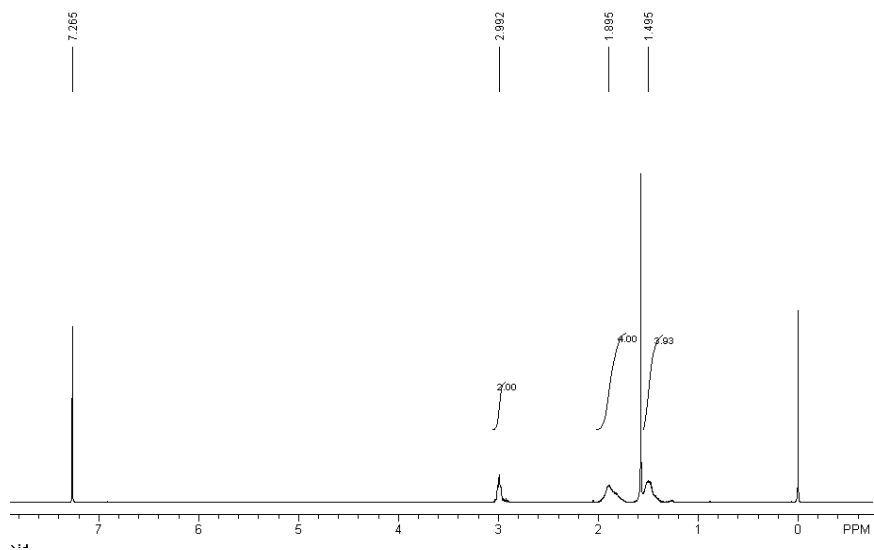


Figure 35 NMR spectra of molecule D.

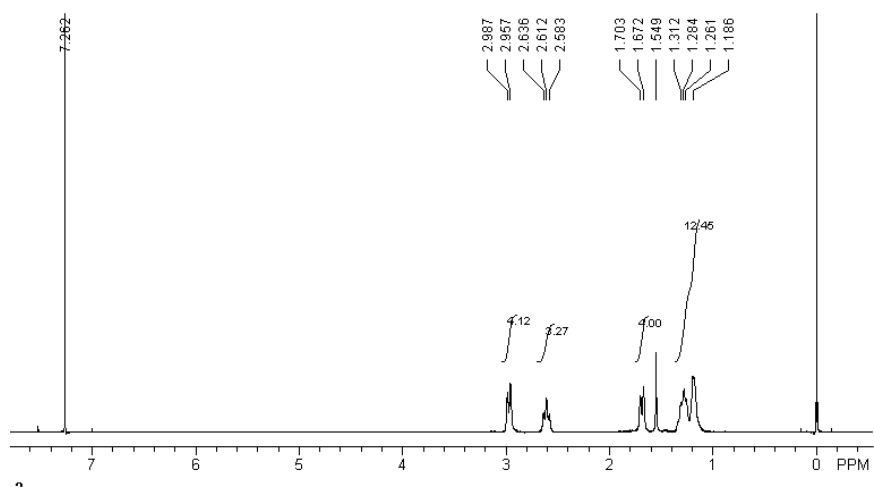


Figure 36 NMR Spectra of Table 2, entry 1.

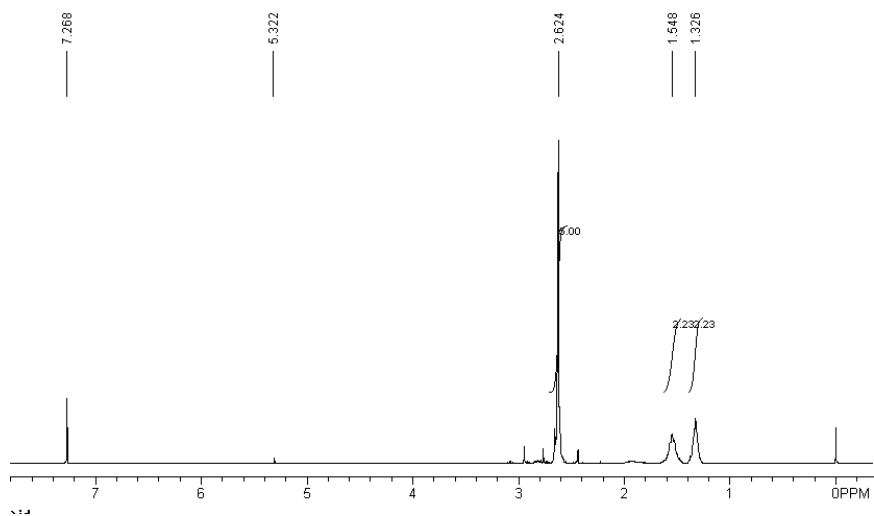


Figure 37 NMR spectra of Table 2, entry 2.

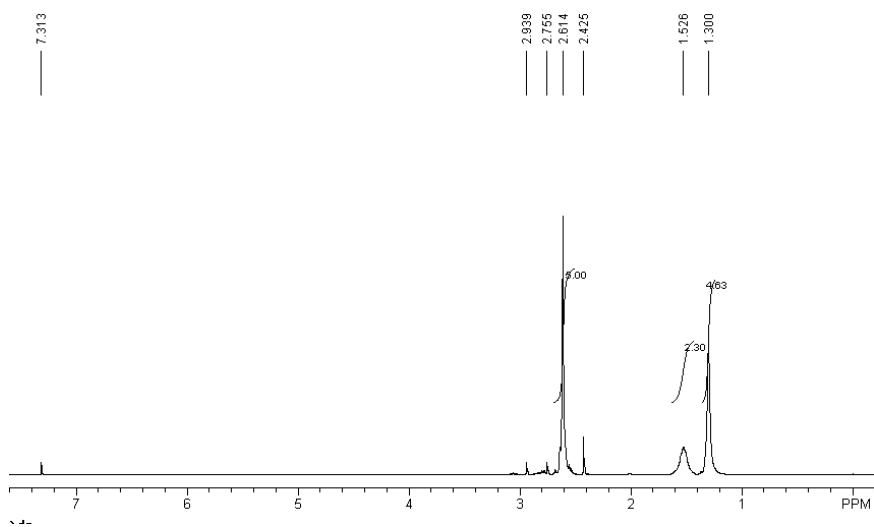


Figure 38 NMR spectra of Table 2, entry 3.

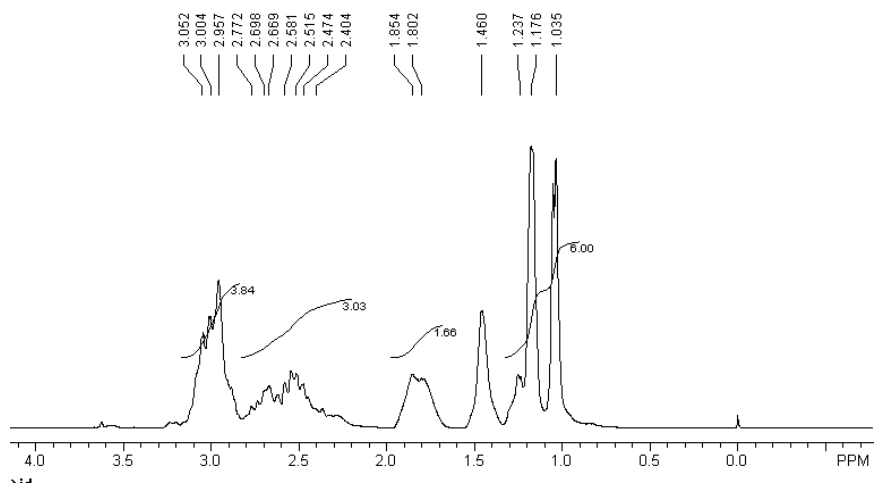


Figure 39 NMR spectra of Table 2, entry 5.

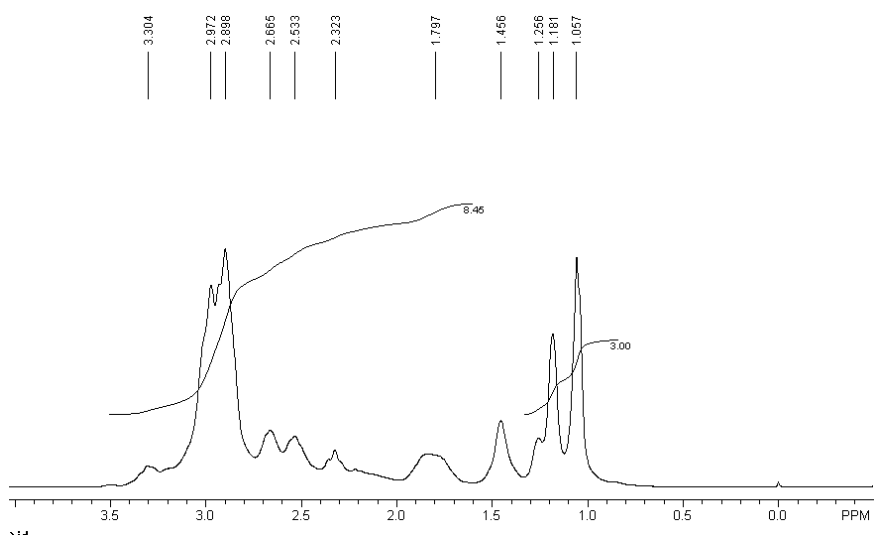


Figure 40 NMR spectra of Table 2, entry 6.

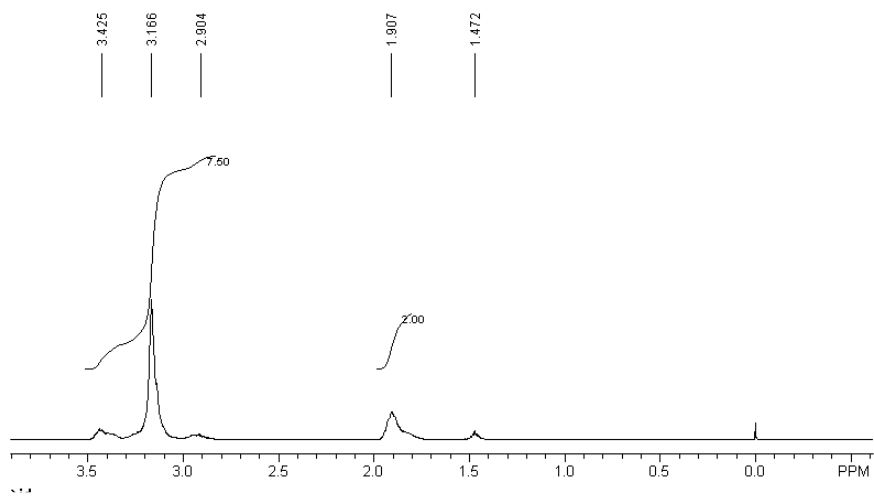


Figure 41 NMR spectra of Table 2, entry 7.

CHAPTER 3

HYDROGEN SULFIDE GENERATION FROM DISULFIDEDIAMINES UNDER AQUEOUS CONDITIONS

Introduction

Hydrogen sulfide (H_2S) has recently been shown to have a prominent role in the physiology of mammals. Along with nitric oxide and carbon monoxide, hydrogen sulfide belongs to the class of molecules called 'gasotransmitters'.¹³¹ These small signaling molecules function by diffusing through cell membranes rather than relying on membrane transport or receptor systems. Gasotransmitters are also generated enzymatically in the body; for instance, H_2S in mammals is mainly produced from cysteine by the enzymes cystathione beta-synthase, cystathione gamma-lyase, and 3-mercaptopyruvate sulfurtransferase.¹³² These enzymes generate H_2S in many tissues, including the vasculature, heart, liver, kidney, brain, nervous system, lung and airway tissues, upper and lower GI tract, reproductive organs, skeletal muscle, pancreas, synovial joints, connective tissues, cochlea, and adipose tissues.¹³³ The correlation between low levels of H_2S and/or H_2S -generating enzymes and disease states including hypertension, diabetes, Alzheimer's, cirrhosis, asthma, and cancer suggests the importance of H_2S to human health.¹³⁴

H_2S has many important effects in the body including antioxidant, anti-apoptotic, and anti-inflammatory effects. It also has metabolic, vasoactive, and cytoprotective effects on normal cells. These properties are being exploited for the treatment of a large number of diseases, as shown in Figure 42. Cancer can also be effectively treated by H_2S

due to the strong prooxidant and apoptotic effects it has upon cancerous cells. H_2S -releasing prodrugs have the potential to be effective against a broad range of cancer types while exhibiting minimal toxic side-effects.

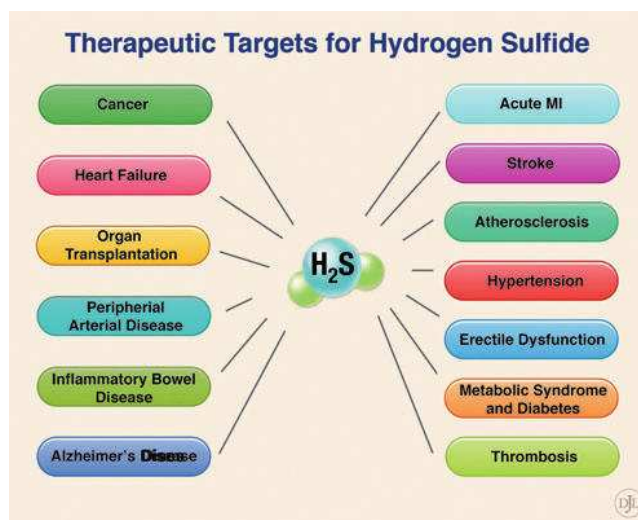


Figure 42 Therapeutic targets for hydrogen sulfide (H_2S).¹³⁵

The use of H_2S in the treatment of disease in animal models has relied heavily on administration of intravenous NaHS or Na_2S solutions or gaseous H_2S .¹³⁵ While sufficient for demonstrating the treatment efficacy of H_2S , the combination of short half-life and inconvenient administration routes ensure that other molecules will need to be used for human patients. Many small organic molecules are used to release H_2S in the body. Two examples of the H_2S precursors, organic polysulfides found in garlic,¹³⁶ are shown in Figure 43. Because they need to undergo enzymatic degradation, organic H_2S precursors release H_2S more slowly than sulfide salts.¹³⁷

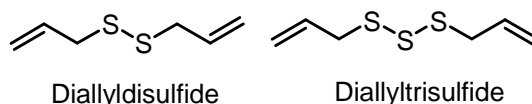


Figure 43 Diallylpolsulfides are endogenous sources of H₂S present in garlic.¹³⁷

Recently, H₂S-releasing moieties have been incorporated into other drugs. L-3,4-Dihydroxyphenylalanine (L-DOPA) is used in the treatment of Parkinson's disease symptoms, but cannot prevent the loss of neurons which underlie the symptoms. However, the inflammation and oxidative stress which cause the neuron loss can be controlled by the prodrugs shown in Figure 44. These molecules are converted to L-DOPA and H₂S *in vivo*, and have shown increased neuroprotective activity compared to L-DOPA alone. Additionally, some of the adverse side-effects of nonsteroidal anti-inflammatory drugs (NSAID) can be ameliorated by releasing H₂S from the drug.¹³⁸ The H₂S-releasing NSAID S-dicloferac (Figure 45) has been shown to cause less gastrointestinal, cardiac, and pulmonary injury and more anti-inflammatory activity compared to diclofenac.

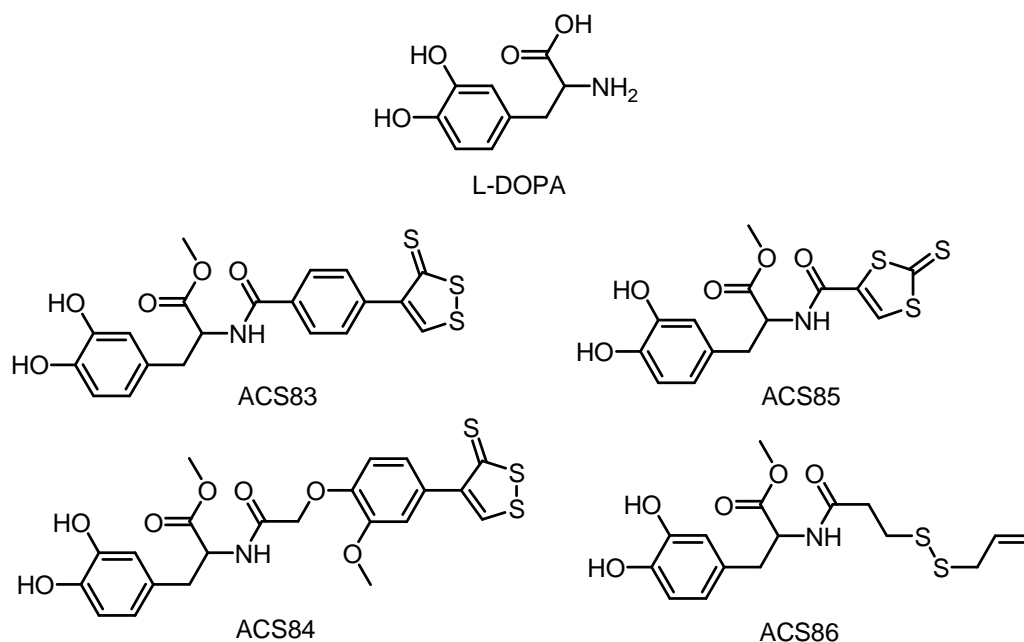


Figure 44 L-DOPA derivatives with various H₂S-releasing functionalities are being investigated for the treatment of Parkinson's.¹³⁴

The most recent work in H₂S delivery is the development of H₂S precursors which are capable of releasing H₂S slowly over time. Slow release is an important objective for the use of H₂S in medicine, as many of the conditions treatable by H₂S are chronic. A 400 μM solution of the H₂S precursor GYY4137 (Figure 45) maintained H₂S at a low concentration of <20 μM over a period of 7 days. In contrast, NaHS release all of its H₂S within 2 hours under the same conditions. In addition to GYY4137, the class of molecules called dithiolethiones has proven to release H₂S in a controlled manner. Members of this class of molecules include S-diclofenac (Figure 44), S-aspirin, S-sildenafil, and ACS67.¹³⁹

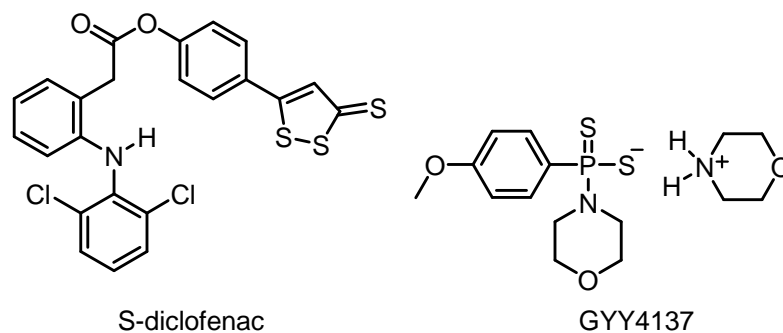


Figure 45 S-diclofenac and GYY4137 were developed for the slow release of H₂S.¹⁴⁰

In this chapter we describe the generation of H₂S from the acid-catalyzed decomposition of molecules containing the disulfidediamine functional group. This is the first report of the use of disulfidediamines as H₂S precursors. Further, this result may lead to H₂S generation from poly(disulfidediamines), which would be the first use of a polymer as a H₂S precursor. We have also studied the products of disulfidediamine decomposition, as well as the effect of acid strength on the composition of those products.

Experimental

Materials

Morpholine, sulfur monochloride, 4-morpholineethanesulfonic acid, acetic acid, hydrochloric acid, sodium sulfide, and solvents were purchased from Aldrich or Acros and used as received. Lead(II) acetate was purchased from Mallinkrodt and purified by filtration of the aqueous solution.

Characterization

^1H NMR spectra were acquired using a Bruker Avance-400 at 400 MHz and were referenced to TMS. X-Ray diffraction measurements were made using a Nonius KappaCCD diffractometer by Dr. Dale Swenson of the University of Iowa.

Synthesis of dimorpholinedisulfide

Morpholine (53.5 mL, 620 mmol) and CH_2Cl_2 (500 mL) were combined in a 1 L round-bottom flask and cooled with an ice bath. Sulfur monochloride (10 mL, 124 mmol) was added slowly to the RBF while stirring the solution. After one hour, the reaction mixture was extracted three times with 300 mL of saturated NaCl solution. Evaporation of the solvent yielded a white/yellow wax. Recrystallization from a mixture of hexanes and ethyl acetate yielded white needles (19.0 g, 65.8 %). ^1H NMR δ 3.75-3.72 (m, 4H), 2.85-2.81(m, 1H).

Release of H_2S from Na_2S

$\text{Pb}(\text{OAc})_2$ (1.5 g, 3.96 mmol) was dissolved in H_2O (10 mL) and degassed by bubbling with N_2 for 10 min in a Schlenk tube. Na_2S (135 mg, 0.56 mmol) was placed in a small vial and added to the Schlenk tube under N_2 . Acetic acid (0.5 mL, 8.75 mmol) was added to the Na_2S via syringe, under N_2 . The reaction was stirred for 24 h. The PbS precipitate in the $\text{Pb}(\text{OAc})_2$ solution was collected by filtration and washed with 200 mL of H_2O . The filter paper was dried for 12 h at 45 °C in an oven. The mass of the PbS was 131.0 mg, accounting for 97 % of the sulfur in the Na_2S .

Release of H₂S from dimorpholinedisulfide with HCl

Pb(OAc)₂ (1.5 g, 3.96 mmol) was dissolved in H₂O (10 mL) and degassed by bubbling with Ar for 10 min in a Schlenk tube. Dimorpholinedisulfide (111 mg, 0.47 mmol) was placed in a small vial, dissolved in 5:3 H₂O:THF (2 mL), and added to the Schlenk tube under Ar. Hydrochloric acid (190 μL, 5.6 mmol) was added to the dimorpholinedisulfide via syringe, under Ar. The reaction was stirred for 24 h. The PbS precipitate in the Pb(OAc)₂ solution was collected by filtration and washed with 200 mL of H₂O. The filter paper was dried for 12 h at 45 °C in an oven. The mass of the PbS was 43.5 mg, accounting for 20 % of the sulfur in the dimorpholinedisulfide.

Release of H₂S from dimorpholinedisulfide with HOAc

Pb(OAc)₂ (1.5 g, 3.96 mmol) was dissolved in H₂O (10 mL) and degassed by bubbling with Ar for 10 min in a Schlenk tube. Dimorpholinedisulfide (135 mg, 0.57 mmol) was placed in a small vial, dissolved in 5:3 H₂O:THF (2 mL), and added to the Schlenk tube under Ar. Acetic acid (300 μL, 8.8 mmol) was added to the dimorpholinedisulfide via syringe, under Ar. The reaction was stirred for 24 h. The PbS precipitate in the Pb(OAc)₂ solution was collected by filtration and washed with 200 mL of H₂O. The filter paper was dried for 12 h at 45 °C in an oven. The mass of the PbS was < 20 mg, accounting for < 7 % of the sulfur in the dimorpholinedisulfide.

Results and discussion

In previous work we smelled the odor of H₂S coming from decompositions of disulfidediamines under acidic conditions and were interested in the potential applications of a H₂S-releasing polymer. Our first objective was to quantify the amount

of H₂S released by the disulfidediamine functional group, since the fraction of sulfur which would be released as H₂S was uncertain. This knowledge would be essential to guide any applications *in vivo*. To make the results of the decomposition experiments relevant to biological applications, dimorpholinedisulfide (Figure 46) was chosen for the decompositions because of its greater water solubility than the disulfidediamines which had been synthesized in previous work.

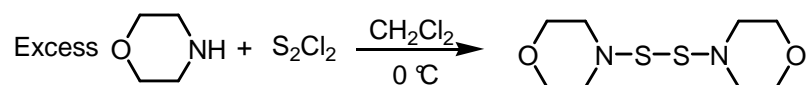


Figure 46 Synthesis of dimorpholinedisulfide.

To detect the H₂S that was released during decomposition, a new detection method was developed based on the formation of PbS from Pb(OAc)₂, a reaction commonly used in H₂S test strips. The apparatus used (Figure 47) consists of a Schlenk tube containing an aqueous, degassed solution of Pb(OAc)₂ and a vial containing a sulfur source. An acid is added to the interior of the vial under inert atmosphere and the Schlenk tube is immediately sealed. The H₂S generated in the vial diffuses into the Pb(OAc)₂ solution where the two compounds react to form water-insoluble PbS. When H₂S generation has stopped, the PbS is collected by filtration, dried, and weighed to determine the amount of H₂S generated.

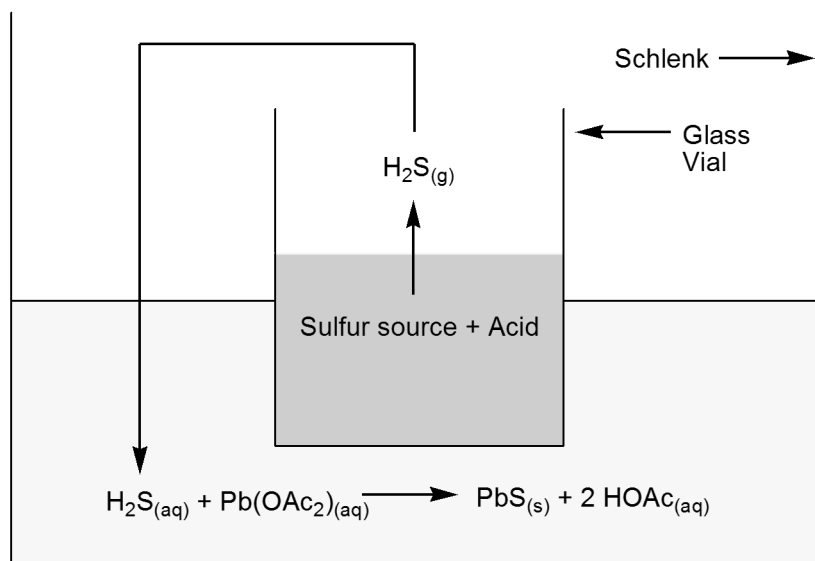


Figure 47 H₂S detection method using Pb(OAc)₂.

In this detection method only H₂S will react with Pb(OAc)₂ to form PbS. Because direct contact between the contents of the vial and the Pb(OAc)₂ solution is prevented, only gaseous sulfur-containing compounds are able to enter the Pb(OAc)₂ solution. Further, only sulfide-containing compounds react with Pb(OAc)₂ to form PbS, compounds containing oxidized sulfur are unreactive. From these considerations we can say with confidence that the sulfur in the PbS comes only from H₂S. With a K_{sp} of 9.04×10^{-29} solid PbS can be easily purified from water-soluble Pb(OAc)₂ and HOAc by washing with water, meaning that the measured weight results from only PbS despite the use of excess Pb(OAc)₂.

Other methods of detecting H₂S have been reported but were unsuitable for this work. Dye-based detection methods require basic conditions to promote sulfide nucleophilicity and are incompatible with acids. The use of H₂S gas sensors requires the

H₂S to remain in the gas phase, but in our decompositions the H₂S would partition between the gas phase and the liquid in the vial. Without knowing the fraction of H₂S in the liquid we cannot trust the concentration readings to be an accurate measure of the total amount of H₂S present in the Schlenk tube. In addition, H₂S is a reactive compound and could undergo oxidation or other side reactions. Our method minimizes the effect of side reactions because the H₂S is quickly converted into unreactive PbS.

The detection method was tested using Na₂S as the source of H₂S, since the reaction of Na₂S with acid is well known and reliable. An average of 92 % of the sulfur added as Na₂S was recovered as PbS over a total of four separate experiments (Table 3, entry 1). When dimorpholinedisulfide was decomposed only a small amount of the total sulfur was recovered as PbS and a yellow precipitate was generated in the vial which we assumed to be elemental sulfur. Initial results indicated that HCl generated more H₂S and generated it faster than HOAc, but these findings may be subject to future change.

Table 3 Recovery of generated H₂S as PbS.

Entry	Sulfur source	Acid	pKa	Reaction time (h)	Sulfur recovered as PbS (%)
1	Na ₂ S	HOAc	4.76	24	92 (avg)
2	dimorpholinedisulfide	HOAc	4.76	24	Trace
3	dimorpholinedisulfide	HCl	-8.00	24	20

^aNot enough PbS collected to measure an accurate weight.

Conclusion

We have developed a reliable method to quantify the amount of H₂S released during the decomposition of disulfidediamines by weighing the resulting solid PbS. The

results of these and future experiments will provide insight into the decomposition mechanism of the disulfidediamine functional group under acidic conditions. This knowledge will be essential for guiding future experiments with applications of disulfidediamines *in vivo*.

CHAPTER 4

EXTENDED LIFETIMES OF GOLD(III) CHLORIDE CATALYSTS USING
COPPER(II) CHLORIDE AND (2,2,6,6-TETRAMETHYL-PIPERIDIN-1-YL)OXYL

Introduction

Previously thought to be catalytically inactive, homogeneous gold catalysts have received increasing attention in recent years due to the discovery of new reactions that they catalyze and successful efforts to yield enantiomerically enriched products.¹⁴¹⁻¹⁵³ These catalysts complete numerous different types of reactions including those requiring Lewis acid activation of alkynes and alkenes, insertion into the C-H bond of alkynes, oxidation of alkenes or alcohols, and reductive silylation of alcohols.¹⁵⁴⁻¹⁷² Asymmetric versions of homogeneous gold catalysts have been reported including recent work with chiral ligands or with chiral counterions that greatly increased the enantioselectivities of gold catalysts.¹⁷³⁻¹⁷⁸ As the reactions and applications of gold catalysts increase, the need to decrease the loadings of gold and increase their turnovers has become an important consideration requiring further development. For instance, both AuCl₃ (\$28,800 per mole at 99% purity from Sigma-Aldrich) and AuCl (\$29,800 per mole at 99.9% purity from Sigma Aldrich) are expensive compounds so efforts to decrease the amounts required for catalysis are important. In this paper, we show unprecedented stabilization of AuCl₃ using a combination of 2,2,6,6-tetramethyl-1-piperidinyloxy (TEMPO) and low levels of CuCl₂ that allowed a Au(III) catalyst to be recycled up to 33 times.

Homogeneous gold catalyzed reactions are typically run at loadings of one to five mole percent catalyst because it is readily reduced to colloidal Au(0) which decreases its

turnovers (Figure 48a).^{166,179-181} Initial strategies to increase the lifetime of Au catalysts involved reduction in the concentration of gold species because the rate of decomposition is proportional to the square of the concentration of the gold species. Unfortunately, this method also slowed the desired reaction and lead to incomplete reactions. In more recent work, bulky ligands were employed to stabilize the catalyst by preventing gold atoms from coming into contact. *N*-Heterocyclic carbene ligands stabilized Au catalysts from decomposition and increased catalytic activity via sterics and significant electron donation by the carbene.¹⁸²⁻¹⁸⁵ In a recent paper by Che *et al.*, a pyridine-based ligand [Au(C^N)Cl₂] bonded to gold salts increased the lifetime of the catalyst in the reaction shown in Figure 48b.¹⁸⁶ When AuCl₃ was used as the catalyst without additional ligand, it decomposed after one cycle and no further activity was observed. In reactions with the ligand shown in Figure 48c, the catalyst was recycled up to ten cycles. The recycling reactions were run for 24 h after which the conversion was checked by ¹H NMR spectroscopy and a new set of substrates were added.¹⁸⁶ Although 812 out of a possible 1,000 turnovers were reached through ten cycles, the reaction did not go to completion after the second cycle and the conversion on the last cycle was only 60%. Catalyst decomposition limited the turnovers and conversions that could be obtained.

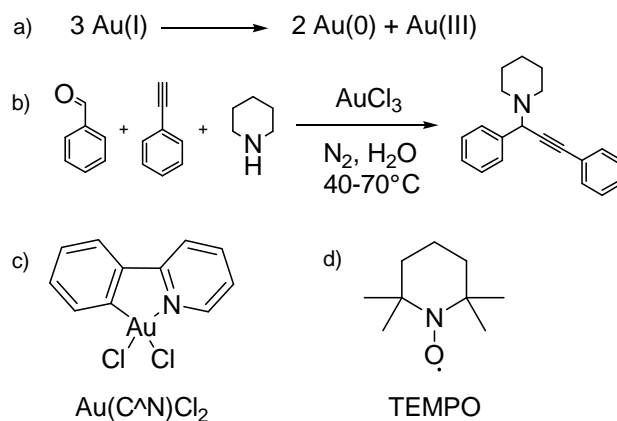


Figure 48 Gold-catalyzed three-component coupling.

a) The decomposition of Au(I) to yield colloidal Au(0). b) The three component reaction that was studied in this article. c) The structure of Au(C^N)Cl₂. d) The structure of TEMPO.

We discovered that although this reaction was successful at loadings of 0.1 to 5 mol% AuCl₃, the catalyst decomposed during the reaction. In a typical reaction, the substrates were allowed to react for 12 h during which a dark solid precipitate was observed to form along the glass walls and in the bottom of the reaction flask. This precipitate was believed to be colloidal Au(0) that is commonly formed in Au catalyzed reactions. When more of the alkyne, aldehyde, and amine were added at the end of the reaction, no further conversion was observed due to the decomposition of the Au catalyst. Although the reactions were completed faster with higher loadings of AuCl₃, the decomposition of the catalyst was also accelerated.

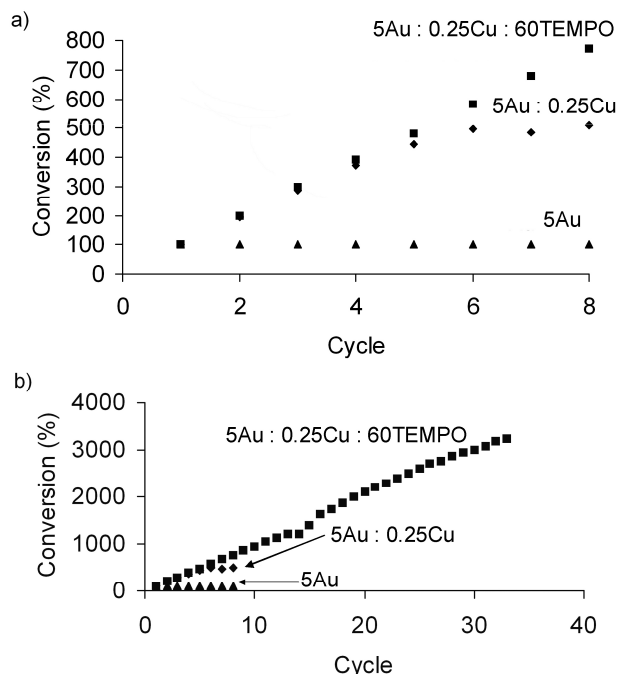


Figure 49 Lifetime extension of AuCl_3 .

- a) Three reactions that were completed at 5 mol% loadings of AuCl_3 , at 5 mol% AuCl_3 and 0.25 mol% CuCl_2 , and at 5 mol% AuCl_3 , 0.25 mol% CuCl_2 , and 60 mol% TEMPO.
- b) This figure shows the same three reactions as in a) but up to 33 cycles for the reaction with AuCl_3 , CuCl_2 , and TEMPO. The dip at the thirteenth cycle corresponds to when the reaction slowed and each cycle time was increased to 24 h at the 15th cycle. At cycle 20 the reaction time was increased to 36 h.

We discovered that when CuCl_2 and TEMPO were added to 5 mol% loadings of AuCl_3 catalyst, the number of cycles where the catalyst was active greatly increased (Figure 49). In these and all subsequent reactions, the catalysts were added at the beginning of the first cycle with the amine, aldehyde, and alkyne and the reaction was heated to 70 °C. After 12 h an aliquot of the organics was removed to check the conversion by ^1H NMR spectroscopy and an additional set of amine, aldehyde, and alkyne were added. The reaction was heated to 70 °C and the conversion was checked by ^1H NMR spectroscopy after 12 h and a new set of amine, aldehyde, and alkyne were

added. Each cycle corresponded to the addition of one set of the amine, aldehyde, and alkyne and 12 h of heating at 70 °C. Thus, the highest conversion after one cycle was 100%, after two cycles it was 200%, and after three cycles it was 300%.

When no TEMPO or CuCl₂ were added with 5 mol% AuCl₃, the reaction went to quantitative conversion after one cycle and then no further turnover was observed upon the addition of more reagents (Figure 49). When 0.25 mol% of CuCl₂ was added (Au:Cu ratio of 20:1) the reaction yielded quantitative turnovers for four cycles and then the catalyst was decomposed by the end of the 7th cycle for a total conversion of 510%. When 60 mol% TEMPO and 0.25 mol% CuCl₂ were added with AuCl₃, the reaction yielded quantitative conversions through 33 cycles. Thus, the number of cycles and turnovers of the AuCl₃ catalyst were increased by a factor of 33 with catalytic amounts of TEMPO and CuCl₂.

Table 4 Effect of CuCl₂ and TEMPO on the lifetimes of AuCl₃.

Entry	AuCl ₃ (mol%)	CuCl ₂ (mol%)	Au:Cu	TEMPO (mol%)	Conversion ^a (%)	Cycles
1	5	0.25	20:1	0	510	8
2	5	0.125	40:1	0	280	4
3	5	0.0625	80:1	0	100	2
4	5	0.125	40:1	60	360	4
5	5	0.0625	80:1	60	370	4
6	5	0.042	120:1	60	290	4
7	5	0.025	200:1	60	100	2
8	5	0.0625	80:1	15	100	4
9	5	0.0625	80:1	5	90	4

^aEach reaction run at 70 °C for 12 h. After 12 h the conversion was checked by ¹H NMR spectroscopy and a new set of substrates were added. The maximum conversion after cycle “n” would be 100 multiplied by n.

A study of the amount of CuCl_2 and TEMPO needed to increase the lifetime of the AuCl_3 catalyst at 5 mol% loadings was undertaken (Table 4). The addition of CuCl_2 with no TEMPO added increased the number of cycles and overall conversions of the AuCl_3 catalyst even at $\text{AuCl}_3:\text{CuCl}_2$ loadings as low as 40:1. When the $\text{AuCl}_3:\text{CuCl}_2$ loading was increased to 80:1, the reaction stopped after the first cycle when no TEMPO was present. In contrast, when 60 mol% TEMPO was added, the catalyst was active over four cycles at $\text{AuCl}_3:\text{CuCl}_2$ loadings as low as 120:1.

Table 5 Control reactions to study how O_2 and different amounts of Au, Cu, and TEMPO affected this reaction.

Entry	AuCl_3 (mol%)	CuCl_2 (mol%)	TEMPO (mol%)	Conversion (%)	Cycles
1 ^a	5	0.25	0	95	2
2	0	0.25	0	0	1
3	0	0	130	0	1
4	0	0.25	60	0	1
5	5	0	60	110	2

^aReaction completed under an atmosphere of O_2 .

A series of control experiments were completed to further study this reaction (Table 5). In entry 1 of Table 5 an experiment to probe whether O_2 could act as the oxidant rather than TEMPO is described. This reaction had Au and Cu loadings identical to Entry 1 of Table 1 that resulted in a conversion of 510% after eight cycles when the reaction was run under an atmosphere of N_2 . When the same reaction was completed under an atmosphere of O_2 the conversion reached 95% after one cycle but no further conversion was observed. An atmosphere of O_2 poisoned the AuCl_3 such that the copper had no noticeable effect on the lifetime of the Au catalyst.

Copper was a poor catalyst for this reaction and at loadings used here no conversion was observed by ^1H NMR spectroscopy in experiments without AuCl_3 but with CuCl_2 , TEMPO, or a combination of TEMPO and CuCl_2 (entries 2-4 in Table 5). In addition, the control experiment with AuCl_3 and TEMPO showed only modest conversion after the first cycle (entry 5 in Table 5), which demonstrated that copper was needed to increase the lifetime of the catalyst. In summary, at 5 mol% of AuCl_3 the addition of CuCl_2 increased the lifetime of the Au catalyst and the addition of both CuCl_2 and TEMPO lead to a greater increase in the lifetime of the catalyst.

It is always desirable to use less of an expensive catalyst such as AuCl_3 , so the three component reaction was studied at 1 and 0.1 mol% loadings of AuCl_3 . Reactions with less than 0.1 mol% of AuCl_3 did not go to completion so they were not studied. Control experiments with only 1 or 0.1 mol% AuCl_3 and no CuCl_2 or TEMPO were carried out for five cycles (entries 1 and 7 in Table 6). These reactions had quantitative conversions after the first cycle, but they only reached 140 - 150% conversion after five cycles. These reactions demonstrated that the Au catalyst decomposed rapidly after the first cycle. A control reaction was completed with a Au:TEMPO ratio of 1:12 and the conversion was 200% after five cycles which demonstrated that TEMPO by itself had little effect on the lifetime of the Au catalyst (entry 2 in Table 6).

Table 6 Reactions at 1 and 0.1 mol% AuCl₃.

Entry ^a	AuCl ₃ (mol%)	CuCl ₂ (mol%)	TEMPO (mol%)	Conversion	Cycles
1	1	0	0	140	5
2	1	0	12	200	5
3	1	0.5	24	930(980) ^b	10
4	1	0.05	12	910(990) ^c	10
5	1	0.5	0	850(980) ^d	10
6	1	0.05	0	840(980) ^d	10
7	0.1	0	0	150	5
8	0.1	0.1	24	400	5
9	0.1	0.02	24	400	5
10	0.1	0.005	24	330	5
11	0.1	0.1	0	820	10
12	0.1	0.02	0	400	5
13	0.1	0.005	0	320	5

^aReactions at 1 mol% AuCl₃ were run for 12 h for each cycle and reactions at 0.1 mol% AuCl₃ were run for 24 h for each cycle. ^bThe number in parenthesis is the conversion after the reaction was allowed to run for 48 h after the end of the tenth cycle. ^cThe number in parenthesis is the conversion after the reaction was allowed to run for 36 h after the end of the tenth cycle. ^dThe number in parenthesis is the conversion after the reaction was allowed to run for 60 h after the end of the tenth cycle.

Reactions completed at one mol% AuCl₃ had high conversions for ten cycles when CuCl₂ was added at mole ratios of Au:Cu of 2:1 and 20:1 (entries 3 to 6 in Table 6). These reactions were not complete after ten cycles, but when the reactions were allowed to proceed for an additional 36 to 60 h after the tenth cycle all of the reactions went to quantitative conversions. The additional time was necessary due to dilution of the reagents and catalysts at later cycles. No organic solvent was used in these reactions so the product acted as a solvent for subsequent cycles and diluted the catalyst and reagents. Interestingly, the presence of TEMPO lead to only a small increase in the conversion at the end of the tenth cycle but no difference in conversion when the reactions were allowed to go to completion after the tenth cycle.

The same result was seen for reactions completed with 0.1 mol% AuCl₃ (entries 8 to 13 in Table 3). In these reactions the presence of 24 mol% TEMPO had no observable effect on the conversions after 5 cycles. Surprisingly, very low concentrations of CuCl₂ had an effect. In the reaction with a CuCl₂ loading of 0.005 mol% the conversions was 330%, but without CuCl₂ the conversion was only 150%. Clearly, small amounts of CuCl₂ had pronounced effects on the turnovers and conversions.

This reaction was complicated to study because Au, Cu, and TEMPO each existed in three oxidation states and the reaction was biphasic with different solubilities for each oxidation state of the molecules in water and the organic phases. In addition, the amines used in the reaction could coordinate to Au and Cu and change their oxidation potentials.^{187,188} Because of these difficulties, it was not possible to completely disentangle the exact mechanism responsible for the long lifetime of the Au catalyst, but a proposed mechanism is outlined in Figure 50.

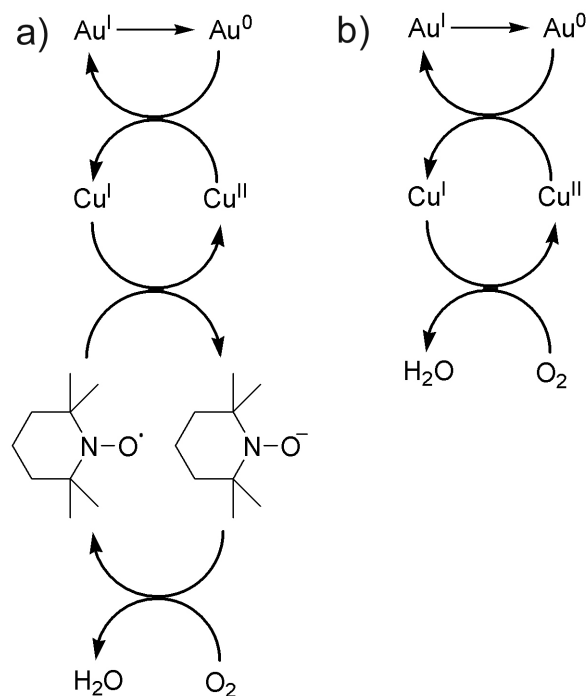


Figure 50 Mechanism for the increased lifetime of AuCl₃.
 a) and b) Two proposed cycles for how Au, Cu, and TEMPO interact to increase the lifetime of the Au catalyst where both TEMPO and O₂ oxidize Cu(I) to Cu(II).

In the original mechanism proposed by Li for this AuCl₃ coupling reaction, the active Au catalyst was Au(I).¹⁸⁹ A limitation of Au(I) catalysis is the well known reduction of Au(I) to colloidal Au(0) by the reaction shown in Figure 48a. We believe that Cu(II) oxidized Au(0) to Au(I) which increased the number of turnovers. The Cu(I) was oxidized back to Cu(II) by O₂ or TEMPO. These reactions were run conditions where most, but not all, of the O₂ was removed from the reaction vessel so low levels of O₂ were present. This mechanism is consistent with the observation that CuCl₂ was necessary to observe an increase in turnover of the AuCl₃ catalyst.

To further investigate this effect, two different sets of three-component coupling reactions were studied (Figure 51). These reactions were completed at loadings of 1 mol% AuCl₃ with and without 1 mol% of CuCl₂. In the control experiments with AuCl₃ and without CuCl₂, the reactions went to conversions of 80% for the reaction with morpholine and 140% for the reaction with *m*-bromobenzaldehyde over three cycles. When AuCl₃ and CuCl₂ were added to the reactions they went to 460 and 470% conversions for five cycles. The increase in conversions by the addition of CuCl₂ was clearly not substrate dependent but successful for three different examples of the three-component coupling reaction.

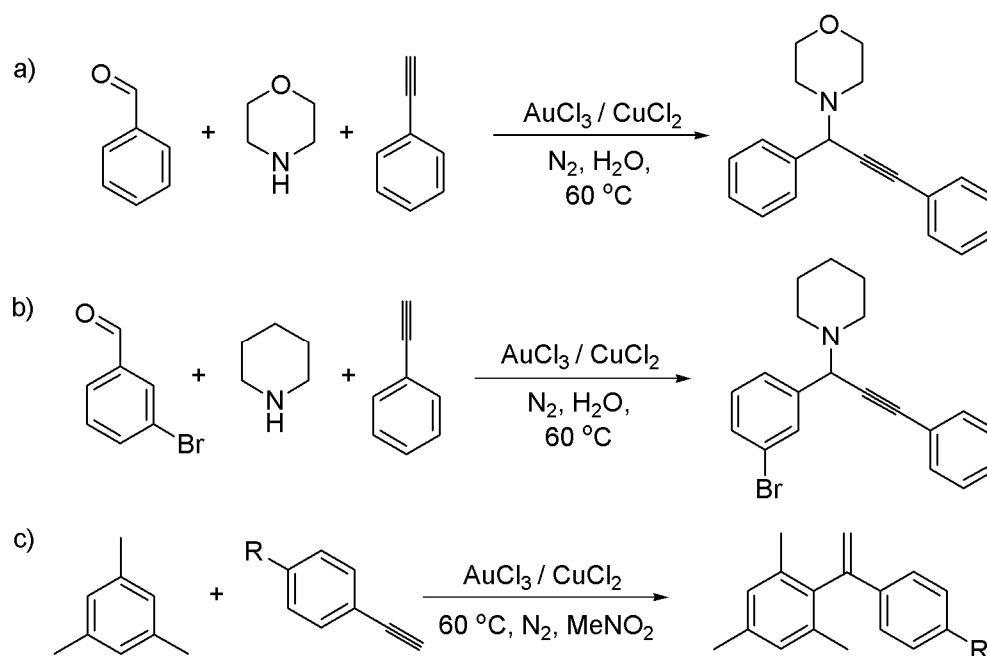


Figure 51 Additional reactions investigated. a) and b) Three-component reactions that were investigated. c) A hydroarylation reaction that was studied for the effect of added CuCl₂.

A second reaction was also studied to investigate whether CuCl_2 would increase the turnovers in a reaction where the Au is proposed to act as a Lewis acid. In the three-component reaction shown in Figure 48b, the Au catalyst was proposed to insert into the C-H bond of the acetylene and then react with the imine formed by the condensation of the aldehyde and amine.¹⁷⁸ In the reaction shown in Figure 51c, the Au is proposed to act as a Lewis acid to activate mesitylene for nucleophilic attack by phenylacetylene.¹⁹⁰ This reaction has been reported by Sommer to proceed with AuCl_3 as the catalyst for a variety of substrates, but our work demonstrated that it does not proceed with CuCl_2 which was only partially soluble in the solvent (Table 4).¹⁹⁰

Multiple reactions with phenylacetylene, mesitylene, and 1 mol% AuCl_3 were completed, and highest conversion was only 20% which was consistent with the report by Sommer. When CuCl_2 was added with AuCl_3 , the highest conversion increased to 36%. More surprising results were found when 4-ethynyltoluene was used as the substrate. The reaction with only AuCl_3 reached 50% conversion but the reaction with AuCl_3 and CuCl_2 reached 79% conversion. Although the effect of the addition of CuCl_2 was much more modest than in the three-component coupling reaction, these experiments demonstrated that CuCl_2 increased the conversions in a second reaction where the Au catalyst has a significantly different role in the catalytic cycle.

Table 7 Effect of AuCl₃ and CuCl₂ on the hydroarylation reactions shown in Figure 51c.

Entry ^a	-R	AuCl ₃ (mol %)	CuCl ₂ (mol %)	Conversion ^b (%)
1	H	1	1	34
2	H	1	0	16
3	H	0	1	0
4	CH ₃	1	1	79
5	CH ₃	1	0	50
6	CH ₃	0	1	0

^aReactions were completed for 24 h and no further turnover was observed for longer reaction times. ^bThe conversions were measured by ¹H NMR spectroscopy at the completion of the reaction.

This work demonstrated a remarkable stabilization of AuCl₃ catalysts using catalytic amounts of CuCl₂. The effect was robust at loadings of AuCl₃ that ranged by 50 fold and allowed up to 33 cycles to be completed. Impressively, the lifetime of the AuCl₃ catalyst at a loading of 5 mol% increased from 12 h to over 792 h when 0.25 mol% CuCl₂ and 60 mol% TEMPO were added. In fact, limitations in determining the conversions rather than catalyst decomposition prevented further study of this reaction.

This research represents one approach to lowering the costs of homogeneous Au catalysts for use in academic or industrial labs. A low loading of AuCl₃ catalyst is desired because of its high cost, but low loadings result in slow reactions or low conversions to product. What is desired is to use a high loading of AuCl₃ so the reactions are rapid, but the AuCl₃ catalysts should be recycled to keep the costs low. Common approaches to solving this problem have been to develop new ligands to accelerate the reaction rate or to find new, cheaper catalysts with higher reactivities. Another solution – the one described in this paper – was to find a method to prevent the Au catalyst from

decomposing such that it could be used in high concentrations and be recycled. In contrast to the high cost of AuCl₃, the cost for CuCl₂ (\$18 per mole for 97% purity from Sigma-Aldrich) and TEMPO (\$1,030 per mole for 98% purity from Sigma-Aldrich) are modest and can be added to increase the conversions and lifetimes of a AuCl₃ catalyst. Because CuCl₂ and TEMPO do not require any ligands on the AuCl₃ to be effective, this method may prove to be applicable to more reactions and will be studied for such activity.

Experimental

Materials and Methods

AuCl₃ was purchased from Sigma-Aldrich at 99% purity. CuCl₂ was purchased from Acros at 99% purity. TEMPO was purchased from Sigma-Adrich and purified by sublimation. Nitromethane was purchased from Acros and dried over sieves. All other reagents were purchased from Sigma-Adrich at their highest purity and used as received. All NMR spectra were recorded on a Bruker Avance 300 (¹H: 300 MHz, ¹³C: 75 MHz) in CDCl₃ and referenced to TMS unless otherwise noted.

¹H NMR analysis of three-component coupling reactions

For the compound synthesized in Table 4, entry 1, the conversion was determined by comparing the integration of the propargyl signal (δ 4.81, 1H, s) for the product to the aldehyde signal (δ 10.02, 1H, s) of the benzaldehyde starting material. The product shown in Figure 49a possessed a chemical shift of δ 4.78 for the propargyl hydrogen. The product shown in Figure 49b possessed a chemical shift of δ 4.81 for the propargyl

hydrogen and the hydrogen on the aldehyde in the starting material possessed a chemical shift of δ 9.94.

Procedure for Table 4, Entry 2

Benzaldehyde (100 μ L, 1.0 mmol), piperidine (110 μ L, 1.1 mmol), and phenylacetylene (160 μ L, 1.5 mmol) were added to a 10 mL Schlenk tube. An aqueous solution of CuCl_2 was made by dissolving 26.1 mg of CuCl_2 in 4.3 mL of H_2O . 28 μ L (0.17 mg, 1.3×10^{-3} mmol) of this solution was added to the organics. AuCl_3 (15 mg, 5.0×10^{-2} mmol) was taken from a glove box and added to the Schlenk tube in 2.0 mL of H_2O under flowing N_2 . The reaction mixture was then heated at 70 $^\circ\text{C}$ and stirred in an oil bath. After 12 h an aliquot of the organic phase was removed to study the conversion by ^1H NMR spectroscopy. Additional benzaldehyde (100 μ L, 1.0 mmol), piperidine (110 μ L, 1.1 mmol), and phenylacetylene (160 μ L, 1.5 mmol) were added at this time. Heating was resumed and the conversion was studied every 12 h. This process was repeated for a total of four cycles. ^1H NMR (300MHz, CDCl_3): δ 7.67-7.62 (m, 2H), 7.55-7.50 (m, 2H), 7.40-7.26 (m, 6H), 4.81 (s, 1H), 2.61-2.50 (m, 4H), 1.70-1.50 (m, 4H), 1.50-1.40 (m, 2H).

Procedure for Table 4, Entry 3

Benzaldehyde (100 μ L, 1.0 mmol), piperidine (110 μ L, 1.1 mmol), and phenylacetylene (160 μ L, 1.5 mmol) were added to a 10 mL Schlenk tube. An aqueous solution of CuCl_2 was made by dissolving 21.4 mg of CuCl_2 in 12.6 mL of H_2O . 50 μ L (8.5×10^{-2} mg, 6.25×10^{-4} mmol) of this solution was added to the organics. AuCl_3 (15 mg, 5.0×10^{-2} mmol) was taken from a glove box and added to the Schlenk tube in 2.0 mL of

H₂O under flowing N₂. The reaction mixture was then heated at 70 °C and stirred in an oil bath. After 12 h an aliquot of the organic phase was removed to study the conversion by ¹H NMR spectroscopy. Additional benzaldehyde (100 μL, 1.0 mmol), piperidine (110 μL, 1.1 mmol), and phenylacetylene (160 μL, 1.5 mmol) were added at this time. Heating was resumed and the conversion studied every 12 h. This process was repeated for two cycles.

Procedure for Table 4, Entry 4

Benzaldehyde (100 μL, 1.0 mmol), piperidine (110 μL, 1.1 mmol), and phenylacetylene (160 μL, 1.5 mmol) were added to a 10.0 mL Schlenk tube. An aqueous solution of CuCl₂ was made by dissolving 21.4 mg of CuCl₂ in 12.6 mL of H₂O. 100 μL (0.17 mg, 1.25x10⁻³ mmol) of this solution was added to the organics. TEMPO (90 mg, 6.0x10⁻¹ mmol) was added to the Schlenk. AuCl₃ (15 mg, 5.0x10⁻² mmol) was taken from a glove box and added to the Schlenk tube in 2.0 mL of H₂O under flowing N₂. The reaction mixture was then heated at 70 °C and stirred in an oil bath. After 12 h an aliquot of the organic phase was removed to study the conversion by ¹H NMR spectroscopy. Additional benzaldehyde (100 μL, 1.0 mmol), piperidine (110 μL, 1.1 mmol), and phenylacetylene (160 μL, 1.5 mmol) were added at this time. Heating was resumed and the conversion studied every 12 h. This process was repeated for a total of four cycles.

Procedure for Table 4, Entry 5

Benzaldehyde (100 μL, 1.0 mmol), piperidine (110 μL, 1.1 mmol), and phenylacetylene (160 μL, 1.5 mmol) were added to a 10 mL Schlenk tube. An aqueous solution of CuCl₂ was made by dissolving 21.4 mg of CuCl₂ in 12.6 mL of H₂O. 50 μL

(0.085 mg, 6.3×10^{-4} mmol) of this solution was added to the organics. TEMPO (90 mg, 6.0×10^{-1} mmol) was added to the Schlenk. AuCl_3 (15 mg, 5.0×10^{-2} mmol) was taken from a glove box and added to the Schlenk tube in 2.0 mL of H_2O under flowing N_2 . The reaction mixture was then heated at 70 °C and stirred in an oil bath. After 12 h an aliquot of the organic phase was removed to study the conversion by ^1H NMR spectroscopy. Additional benzaldehyde (100 μL , 1.0 mmol), piperidine (110 μL , 1.1 mmol), and phenylacetylene (160 μL , 1.5 mmol) were added at this time. Heating was resumed and the conversion studied every 12 h. This process was repeated for a total of four cycles.

Procedure for Table 4, Entry 6

Benzaldehyde (100 μL , 1.0 mmol), piperidine (110 μL , 1.1 mmol), and phenylacetylene (160 μL , 1.5 mmol) were added to a 10 mL Schlenk tube. An aqueous solution of CuCl_2 was made by dissolving 26.1 mg of CuCl_2 in 4.4 mL of H_2O . 10 μL (0.060 mg, 4.2×10^{-4} mmol) of this solution was added to the organics. TEMPO (90 mg, 0.60 mmol) was added to the Schlenk. AuCl_3 (15 mg, 5.0×10^{-2} mmol) was taken from a glove box and added to the Schlenk tube in 2.0 mL of H_2O under flowing N_2 . The reaction mixture was then heated at 70 °C and stirred in an oil bath. After 12 h an aliquot of the organic phase was removed to study the conversion by ^1H NMR spectroscopy. Additional benzaldehyde (100 μL , 1.0 mmol), piperidine (110 μL , 1.1 mmol), and phenylacetylene (160 μL , 1.5 mmol) were added at this time. Heating was resumed and the conversion studied every 12 h. This process was repeated for a total of four cycles.

Procedure for Table 4, Entry 7

Benzaldehyde (100 μL , 1.0 mmol), piperidine (110 μL , 1.1 mmol), and phenylacetylene (160 μL , 1.5 mmol) were added to a 10 mL Schlenk tube. An aqueous solution of CuCl_2 was made by dissolving 24.7 mg of CuCl_2 in 7.3 mL of H_2O . 100 μL (0.034 mg, 2.5×10^{-4} mmol) of this solution was added to the organics. TEMPO (90 mg, 0.60 mmol) was added to the Schlenk. AuCl_3 (15 mg, 5.0×10^{-2} mmol) was taken from a glove box and added to the Schlenk tube in 2.0 mL of H_2O under flowing N_2 . The reaction mixture was then heated at 70 $^\circ\text{C}$ and stirred in an oil bath. After 12 h an aliquot of the organic phase was removed to study the conversion by ^1H NMR spectroscopy. Additional benzaldehyde (100 μL , 1.0 mmol), piperidine (110 μL , 1.1 mmol), and phenylacetylene (160 μL , 1.5 mmol) were added at this time. Heating was resumed and the conversion studied every 12 h. This process was repeated for a total of two cycles.

Procedure for Table 4, Entry 8

Benzaldehyde (100 μL , 1.0 mmol), piperidine (110 μL , 1.1 mmol), and phenylacetylene (160 μL , 1.5 mmol) were added to a 10 mL Schlenk tube. An aqueous solution of CuCl_2 was made by dissolving 22.7 mg of CuCl_2 in 14.0 mL of H_2O . 50 μL (0.085 mg, 6.3×10^{-4}) of this solution was added to the organics. TEMPO (23.4 mg, 0.150 mmol) was added to the Schlenk by dissolving 24.0 mg in 490 μL of phenylacetylene and adding 160 μL of the acetylene. AuCl_3 (15 mg, 5.0×10^{-2} mmol) was taken from a glove box and added to the Schlenk tube in 2.0 mL of H_2O under flowing N_2 . The reaction mixture was then heated at 70 $^\circ\text{C}$ and stirred in an oil bath. After 12 h an aliquot of the organic phase was removed to study the conversion by ^1H NMR spectroscopy. Additional benzaldehyde (100 μL , 1.0 mmol), piperidine (110 μL , 1.1 mmol), and

phenylacetylene (160 μL , 1.5 mmol) were added at this time. Heating was resumed and the conversion studied every 12 h. This process was repeated for a total of four cycles.

Procedure for Table 4, Entry 9

Benzaldehyde (100 μL , 1.0 mmol), piperidine (110 μL , 1.1 mmol), and phenylacetylene (160 μL , 1.5 mmol) were added to a 10 mL Schlenk tube. An aqueous solution of CuCl_2 was made by dissolving 22.7 mg of CuCl_2 in 14.0 mL of H_2O . 50 μL (0.085 mg, 6.3×10^{-4}) of this solution was added to the organics. TEMPO (8 mg, 0.05 mmol) was added to the Schlenk. AuCl_3 (15 mg, 5.0×10^{-2} mmol) was taken from a glove box and added to the Schlenk tube in 2.0 mL of H_2O under flowing N_2 . The reaction mixture was then heated at 70 $^\circ\text{C}$ and stirred in an oil bath. After 12 h an aliquot of the organic phase was removed to study the conversion by ^1H NMR spectroscopy.

Additional benzaldehyde (100 μL , 1.0 mmol), piperidine (110 μL , 1.1 mmol), and phenylacetylene (160 μL , 1.5 mmol) were added at this time. Heating was resumed and the conversion studied every 12 h. This process was repeated for a total of four cycles.

Procedure for Table 5, Entry 1

Benzaldehyde (100 μL , 1.0 mmol), piperidine (110 μL , 1.1 mmol), and phenylacetylene (160 μL , 1.5 mmol) were added to a 10 mL Schlenk tube. An aqueous solution of CuCl_2 was made by dissolving 26.2 mg of CuCl_2 in 7.7 mL of H_2O . 100 μL (0.34 mg, 2.5×10^{-3} mmol) of this solution was added to the organics. AuCl_3 (15 mg, 5.0×10^{-2} mmol) was taken from a glove box and added to the Schlenk tube in 2.0 mL of H_2O . The Schlenk was fitted with a reflux condenser topped with a balloon filled with O_2 . The reaction mixture was then heated at 70 $^\circ\text{C}$ and stirred in an oil bath. After 12 h

an aliquot of the organic phase was removed to study the conversion by ^1H NMR spectroscopy. Additional benzaldehyde (100 μL , 1.0 mmol), piperidine (110 μL , 1.1 mmol), and phenylacetylene (160 μL , 1.5 mmol) were added at this time. Heating was resumed and the conversion studied every 12 h. This process was repeated for two cycles.

Procedure for Table 5, Entry 2

Benzaldehyde (100 μL , 1.0 mmol), piperidine (110 μL , 1.1 mmol), and phenylacetylene (160 μL , 1.5 mmol) were added to a 10 mL Schlenk tube. An aqueous solution of CuCl_2 was made by dissolving 25.2 mg of CuCl_2 in 7.4 mL of H_2O . 100 μL (0.34 mg, 2.5×10^{-3} mmol) of this solution was added to the organics. The reaction mixture was then heated at 70 $^\circ\text{C}$ and stirred in an oil bath. After 12 h an aliquot of the organic phase was removed to study the conversion by ^1H NMR spectroscopy.

Procedure for Table 5, Entry 3

Benzaldehyde (100 μL , 1.0 mmol), piperidine (110 μL , 1.1 mmol), and phenylacetylene (160 μL , 1.5 mmol) were added to a 10 mL Schlenk tube. TEMPO (200 mg, 1.3 mmol) was added to the Schlenk. The reaction mixture was then heated at 70 $^\circ\text{C}$ and stirred in an oil bath. After 12 h an aliquot of the organic phase was removed to study the conversion by ^1H NMR spectroscopy.

Procedure for Table 5, Entry 4

Benzaldehyde (100 μL , 1.0 mmol), piperidine (110 μL , 1.1 mmol), and phenylacetylene (160 μL , 1.5 mmol) were added to a 10 mL Schlenk tube. An aqueous solution of CuCl_2 was made by dissolving 25.2 mg of CuCl_2 in 7.4 mL of H_2O . 100 μL

(0.34 mg, 2.5×10^{-3} mmol) of this solution was added to the organics. TEMPO (90 mg, 0.60 mmol) was added to the Schlenk. The reaction mixture was then heated at 70 °C and stirred in an oil bath. After 12 h an aliquot of the organic phase was removed to study the conversion by ^1H NMR spectroscopy.

Procedure for Table 5, Entry 5

Benzaldehyde (100 μL , 1.0 mmol), piperidine (110 μL , 1.1 mmol), and phenylacetylene (160 μL , 1.5 mmol) were added to a 10 mL Schlenk tube. TEMPO (90 mg, 0.60 mmol) was added to the Schlenk. AuCl_3 (15 mg, 5.0×10^{-2} mmol) was taken from a glove box and added to the Schlenk tube in 2.0 mL of H_2O under flowing N_2 . The reaction mixture was then heated at 70 °C and stirred in an oil bath. After 12 h an aliquot of the organic phase was removed to study the conversion by ^1H NMR spectroscopy. Additional benzaldehyde (100 μL , 1.0 mmol), piperidine (110 μL , 1.1 mmol), and phenylacetylene (160 μL , 1.5 mmol) were added at this time. Heating was resumed and the conversion studied every 12 h. This process was repeated for a total of two cycles.

Procedure for Table 6, Entry 1

Benzaldehyde (130 μL , 1.3 mmol), piperidine (140 μL , 1.4 mmol), and phenylacetylene (220 μL , 2.0 mmol) were added to a 10 mL Schlenk tube. AuCl_3 (5.0 mg, 0.013 mmol) was taken from a glove box and added to the Schlenk tube in 2.0 mL of H_2O under flowing N_2 . The reaction mixture was then heated at 70 °C and stirred in an oil bath. After 12 h an aliquot of the organic phase was removed to study the conversion by ^1H NMR spectroscopy. Additional benzaldehyde (130 μL , 1.3 mmol), piperidine (140 μL , 1.4 mmol), and phenylacetylene (220 μL , 2.0 mmol) were added at this time.

Heating was resumed and the conversion studied every 12 h. This process was repeated for a total of five cycles.

Procedure for Table 6, Entry 2

Benzaldehyde (100 μ L, 1.0 mmol), piperidine (110 μ L, 1.1 mmol), and phenylacetylene (160 μ L, 1.5 mmol) were added to a 10 mL Schlenk tube. 1.6 mL of H₂O was added to the Schlenk. TEMPO (20 mg, 0.12 mmol) was added to the Schlenk. An aqueous solution of AuCl₃ was made by dissolving 35.2 mg of AuCl₃ in 4.7 mL of H₂O. 400 μ L (3.0 mg, 0.010 mmol) was added to the Schlenk tube under flowing N₂. The reaction mixture was then heated at 70 °C and stirred in an oil bath. After 12 h an aliquot of the organic phase was removed to study the conversion by ¹H NMR spectroscopy. Additional benzaldehyde (100 μ L, 1.0 mmol), piperidine (110 μ L, 1.1 mmol), and phenylacetylene (160 μ L, 1.5 mmol) were added at this time. Heating was resumed and the conversion studied every 12 h. This process was repeated for a total of five cycles.

Procedure for Table 6, Entry 3

Benzaldehyde (100 μ L, 1.0 mmol), piperidine (110 μ L, 1.1 mmol), and phenylacetylene (160 μ L, 1.5 mmol) were added to a 10 mL Schlenk tube. An aqueous solution of CuCl₂ was made by dissolving 26.2 mg of CuCl₂ in 7.7 mL of H₂O. 200 μ L (0.70 mg, 5.0×10^{-3} mmol) of this solution was added to the organics. TEMPO (40 mg, 0.24 mmol) was added to the Schlenk. An aqueous solution of AuCl₃ was made by dissolving 150 mg of AuCl₃ in 10 mL of H₂O. 200 μ L (3.0 mg, 0.010 mmol) was added to the Schlenk tube under flowing N₂. The reaction mixture was then heated at 70 °C and

stirred in an oil bath. After 12 h an aliquot of the organic phase was removed to study the conversion by ^1H NMR spectroscopy. Additional benzaldehyde (100 μL , 1.0 mmol), piperidine (110 μL , 1.1 mmol), and phenylacetylene (160 μL , 1.5 mmol) were added at this time. Heating was resumed and the conversion studied every 12 h. This process was repeated for a total of ten cycles. Heating was continued for 48 h, with a ^1H NMR spectrum taken every 12 h.

Procedure for Table 6, Entry 4

Benzaldehyde (100 μL , 1.0 mmol), piperidine (110 μL , 1.1 mmol), and phenylacetylene (160 μL , 1.5 mmol) were added to a 10 mL Schlenk tube. 1.9 mL of H_2O was added to the Schlenk. An aqueous solution of CuCl_2 was made by dissolving 22.1 mg of CuCl_2 in 13.0 mL of H_2O . 40 μL (0.068 mg, 5.0×10^{-4} mmol) of this solution was added to the organics. TEMPO (20 mg, 0.12 mmol) was added to the Schlenk. An aqueous solution of AuCl_3 was made by dissolving 99.8 mg of AuCl_3 in 13.2 mL of H_2O . 40 μL (3.0 mg, 0.010 mmol) was added to the Schlenk tube under flowing N_2 . The reaction mixture was then heated at 70 $^\circ\text{C}$ and stirred in an oil bath. After 12 h an aliquot of the organic phase was removed to study the conversion by ^1H NMR spectroscopy. Additional benzaldehyde (100 μL , 1.0 mmol), piperidine (110 μL , 1.1 mmol), and phenylacetylene (160 μL , 1.5 mmol) were added at this time. Heating was resumed and the conversion studied every 12 h. This process was repeated for a total of ten cycles. Heating was continued for an additional 36 h, with a ^1H NMR spectrum taken every 12 h.

Procedure for Table 6, Entry 5

Benzaldehyde (100 μL , 1.0 mmol), piperidine (110 μL , 1.1 mmol), and phenylacetylene (160 μL , 1.5 mmol) were added to a 10 mL Schlenk tube. 0.5 mL of H_2O added to Schlenk. An aqueous solution of CuCl_2 was made by dissolving 26.1 mg of CuCl_2 in 20.0 mL of H_2O . 500 μL (0.68 mg, 5.0×10^{-3} mmol) of this solution was added to the organics. An aqueous solution of AuCl_3 was made by dissolving 54.1 mg of AuCl_3 in 18.0 mL of H_2O . 1 mL (3.0 mg, 0.010 mmol) was added to the Schlenk tube under flowing N_2 . The reaction mixture was then heated at 70 $^\circ\text{C}$ and stirred in an oil bath. After 12 h an aliquot of the organic phase was removed to study the conversion by ^1H NMR spectroscopy. Additional benzaldehyde (100 μL , 1.0 mmol), piperidine (110 μL , 1.1 mmol), and phenylacetylene (160 μL , 1.5 mmol) were added at this time. Heating was resumed and the conversion studied every 12 h. This process was repeated for a total of ten cycles. Heating was continued for 36 h, with a ^1H NMR spectrum taken every 12 h.

Procedure for Table 6, Entry 6

Benzaldehyde (100 μL , 1.0 mmol), piperidine (110 μL , 1.1 mmol), and phenylacetylene (160 μL , 1.5 mmol) were added to a 10 mL Schlenk tube. An aqueous solution of CuCl_2 was made by dissolving 26.1 mg of CuCl_2 in 20.0 mL of H_2O . 1.0 mL of this solution was diluted to 19.0 mL with H_2O . 1.0 mL (0.068 mg, 5.0×10^{-4} mmol) of this solution was added to the organics. An aqueous solution of AuCl_3 was made by dissolving 54.1 mg of AuCl_3 in 18.0 mL of H_2O . 1.0 mL (3.0 mg, 0.010 mmol) was added to the Schlenk tube under flowing N_2 . The reaction mixture was then heated at 70 $^\circ\text{C}$ and stirred in an oil bath. After 12 h an aliquot of the organic phase was removed to

study the conversion by ^1H NMR spectroscopy. Additional benzaldehyde (100 μL , 1.0 mmol), piperidine (110 μL , 1.1 mmol), and phenylacetylene (160 μL , 1.5 mmol) were added at this time. Heating was resumed and the conversion studied every 12 h. This process was repeated for a total of ten cycles. Heating was continued for 36 h, with a ^1H NMR spectrum taken every 12 h.

Procedure for Table 6, Entry 7

Benzaldehyde (100 μL , 1.0 mmol), piperidine (110 μL , 1.1 mmol), and phenylacetylene (160 μL , 1.5 mmol) were added to a 10 mL Schlenk tube. 1.9 mL of H_2O was added to the Schlenk. An aqueous solution of AuCl_3 was made by dissolving 68.0 mg of AuCl_3 in 22.6 mL of H_2O . 100 μL (0.30 mg, 1.0×10^{-3} mmol) was added to the Schlenk tube under flowing N_2 . The reaction mixture was then heated at 70 $^\circ\text{C}$ and stirred in an oil bath. After 24 h an aliquot of the organic phase was removed to study the conversion by ^1H NMR spectroscopy. Additional benzaldehyde (100 μL , 1.0 mmol), piperidine (110 μL , 1.1 mmol), and phenylacetylene (160 μL , 1.5 mmol) were added at this time. Heating was resumed and the conversion studied every 24 h. This process was repeated for a total of five cycles.

Procedure for Table 6, Entry 8

Benzaldehyde (100 μL , 1.0 mmol), piperidine (110 μL , 1.1 mmol), and phenylacetylene (160 μL , 1.5 mmol) were added to a 10 mL Schlenk tube. 1.9 mL of H_2O added to Schlenk. An aqueous solution of CuCl_2 was made by dissolving 28.7 mg of CuCl_2 in 2.1 mL of H_2O . 10 μL (0.14 mg, 1.0×10^{-3} mmol) of this solution was added to the organics. TEMPO (40 mg, 0.24 mmol) was added to the Schlenk. An aqueous

solution of AuCl₃ was made by dissolving 68.0 mg of AuCl₃ in 22.6 mL of H₂O. 100 μL (0.30 mg, 1.0x10⁻³ mmol) was added to the Schlenk tube under flowing N₂. The reaction mixture was then heated at 70 °C and stirred in an oil bath. After 24 h an aliquot of the organic phase was removed to study the conversion by ¹H NMR spectroscopy.

Additional benzaldehyde (100 μL, 1.0 mmol), piperidine (110 μL, 1.1 mmol), and phenylacetylene (160 μL, 1.5 mmol) were added at this time. Heating was resumed and the conversion studied every 24 h. This process was repeated for a total of five cycles. Heating was continued for 72 h, with a ¹H NMR spectrum taken every 24 h.

Procedure for Table 6, Entry 9

Benzaldehyde (100 μL, 1.0 mmol), piperidine (110 μL, 1.1 mmol), and phenylacetylene (160 μL, 1.5 mmol) were added to a 10 mL Schlenk tube. 1.8 mL H₂O was added to the Schlenk. An aqueous solution of CuCl₂ was made by dissolving 20.9 mg of CuCl₂ in 10.0 mL of H₂O. 100 μL (0.027 mg, 2.0x10⁻⁴ mmol) of this solution was added to the organics. TEMPO (40 mg, 0.24 mmol) was added to the Schlenk. An aqueous solution of AuCl₃ was made by dissolving 34.5 mg of AuCl₃ in 11.5 mL of H₂O. 200 μL (0.30 mg, 1.0x10⁻³ mmol) was added to the Schlenk tube under flowing N₂. The reaction mixture was then heated at 70 °C and stirred in an oil bath. After 24 h an aliquot of the organic phase was removed to study the conversion by ¹H NMR spectroscopy.

Additional benzaldehyde (100 μL, 1.0 mmol), piperidine (110 μL, 1.1 mmol), and phenylacetylene (160 μL, 1.5 mmol) were added at this time. Heating was resumed and the conversion studied every 24 h. This process was repeated for a total of five cycles. Heating was continued for 72 h, with a ¹H NMR spectrum taken every 24 h.

Procedure for Table 6, Entry 10

Benzaldehyde (100 μL , 1.0 mmol), piperidine (110 μL , 1.1 mmol), and phenylacetylene (160 μL , 1.5 mmol) were added to a 10 mL Schlenk tube. 1.8 mL of H_2O added to the Schlenk. An aqueous solution of CuCl_2 was made by dissolving 20.9 mg of CuCl_2 in 12.3 mL of H_2O . 100 μL (6.8×10^{-3} mg, 5.0×10^{-5} mmol) of this solution was added to the organics. TEMPO (40 mg, 0.24 mmol) was added to the Schlenk. An aqueous solution of AuCl_3 was made by dissolving 34.5 mg of AuCl_3 in 11.5 mL of H_2O . 100 μL (0.30 mg, 1.0×10^{-3} mmol) was added to the Schlenk tube under flowing N_2 . The reaction mixture was then heated at 70 $^\circ\text{C}$ and stirred in an oil bath. After 24 h an aliquot of the organic phase was removed to study the conversion by ^1H NMR spectroscopy. Additional benzaldehyde (100 μL , 1.0 mmol), piperidine (110 μL , 1.1 mmol), and phenylacetylene (160 μL , 1.5 mmol) were added at this time. Heating was resumed and the conversion studied every 24 h. This process was repeated for a total of five cycles. Heating was continued for 72 h, with a ^1H NMR spectrum taken every 24 h.

Procedure for Table 6, Entry 11

Benzaldehyde (100 μL , 1.0 mmol), piperidine (110 μL , 1.1 mmol), and phenylacetylene (160 μL , 1.5 mmol) were added to a 10 mL Schlenk tube. 1.8 mL of H_2O was added to the Schlenk tube. An aqueous solution of CuCl_2 was made by dissolving 21.0 mg of CuCl_2 in 10.0 mL of H_2O . 63 μL (0.14 mg, 1.0×10^{-3} mmol) of this solution was added to the organics. An aqueous solution of AuCl_3 was made by dissolving 31.3 mg of AuCl_3 in 10.4 mL of H_2O . 100 μL (0.30 mg, 1.0×10^{-3} mmol) was added to the Schlenk tube under flowing N_2 . The reaction mixture was then heated at 70 $^\circ\text{C}$ and stirred in an oil bath. After 24 h an aliquot of the organic phase was removed to

study the conversion by ^1H NMR spectroscopy. Additional benzaldehyde (100 μL , 1.0 mmol), piperidine (110 μL , 1.1 mmol), and phenylacetylene (160 μL , 1.5 mmol) were added at this time. Heating was resumed and the conversion studied every 24 h. This process was repeated for a total of ten cycles. Heating was continued for 144 h, with a ^1H NMR spectrum taken every 24 h.

Procedure for Table 6, Entry 12

Benzaldehyde (100 μL , 1.0 mmol), piperidine (110 μL , 1.1 mmol), and phenylacetylene (160 μL , 1.5 mmol) were added to a 10 mL Schlenk tube. 1.9 mL of H_2O was added to the Schlenk. An aqueous solution of CuCl_2 was made by dissolving 21.2 mg of CuCl_2 in 20.0 mL of H_2O . 1.0 mL of this solution was diluted to 4.0 mL with H_2O . 100 μL (0.027 mg, 2.0×10^{-4} mmol) of this solution was added to the organics. An aqueous solution of AuCl_3 was made by dissolving 35.2 mg of AuCl_3 in 4.7 mL of H_2O . 40 μL (0.30 mg, 1.0×10^{-3} mmol) was added to the Schlenk tube under flowing N_2 . The reaction mixture was then heated at 70 $^\circ\text{C}$ and stirred in an oil bath. After 24 h an aliquot of the organic phase was removed to study the conversion by ^1H NMR spectroscopy. Additional benzaldehyde (100 μL , 1.0 mmol), piperidine (110 μL , 1.1 mmol), and phenylacetylene (160 μL , 1.5 mmol) were added at this time. Heating was resumed and the conversion studied every 24 h. This process was repeated for a total of five cycles. Heating was continued for 72 h, with a ^1H NMR spectrum taken every 24 h.

Procedure for Table 6, Entry 13

Benzaldehyde (100 μL , 1.0 mmol), piperidine (110 μL , 1.1 mmol), and phenylacetylene (160 μL , 1.5 mmol) were added to a 10 mL Schlenk tube. 1.9 mL of

H₂O was added to the Schlenk. An aqueous solution of CuCl₂ was made by dissolving 21.2 mg of CuCl₂ in 20.0 mL of H₂O. 1.0 mL of this solution was diluted to 4.0 mL with H₂O. 100 μL (6.8x10⁻³ mg, 5.0x10⁻⁵ mmol) of this solution was added to the organics. An aqueous solution of AuCl₃ was made by dissolving 35.2 mg of AuCl₃ in 4.7 mL of H₂O. 40 μL (0.30 mg, 1.0x10⁻³ mmol) was added to the Schlenk tube under flowing N₂. The reaction mixture was then heated at 70 °C and stirred in an oil bath. After 24 h an aliquot of the organic phase was removed to study the conversion by ¹H NMR spectroscopy. Additional benzaldehyde (100 μL, 1.0 mmol), piperidine (110 μL, 1.1 mmol), and phenylacetylene (160 μL, 1.5 mmol) were added at this time. Heating was resumed and the conversion studied every 24 h. This process was repeated for a total of five cycles. Heating was continued for 72 h, with a ¹H NMR spectrum taken every 24 h.

¹H NMR analysis of the hydroarylation reactions

For the compound synthesized in Table 4 (entries 1-3) the conversion was determined by comparing the integration of the product's vinyl signal (δ 5.95, 1H, d) and (δ 5.09, 1H, d) to the alkyne signal of the phenylacetylene reagent (δ 3.06, 1H, s). For entries 4-6 in Table 4, the vinyl signal (δ 5.91, 1H, d) and (δ 5.03, 1H, d) and the alkyne signal (δ 3.03, 1H, s) were compared to find the conversions.

Procedure for Figure 51a with AuCl₃ and CuCl₂

Benzaldehyde (100 μL, 1.0 mmol), morpholine (95 μL, 1.1 mmol), and phenylacetylene (160 μL, 1.5 mmol) were added to a 10 mL Schlenk tube. 0.9 mL of H₂O was added to the Schlenk. An aqueous solution of CuCl₂ was made by dissolving 22.9 mg of CuCl₂ in 3.0 mL of H₂O. 100 μL (0.75 mg, 5.0x10⁻³ mmol) of this solution

was added to the organics. An aqueous solution of AuCl₃ was made by dissolving 45 mg of AuCl₃ in 15 mL of H₂O. 1.0 mL (3.0 mg, 0.010 mmol) was added to the Schlenk tube under flowing N₂. The reaction mixture was then heated at 70 °C and stirred in an oil bath. After 12 h, an aliquot of the organic phase was removed to study the conversion by ¹H NMR spectroscopy. Additional benzaldehyde (100 μL, 1.0 mmol), morpholine (95 μL, 1.1 mmol), and phenylacetylene (160 μL, 1.5 mmol) were added at this time. Heating was resumed and the conversion studied every 12 h. This process was repeated for a total of five cycles. Heating was continued for an additional 24 h, with a ¹H NMR spectrum taken every 12 h. ¹H NMR spectroscopy: (300 MHz, CDCl₃): δ 7.63 (d, 2H), 7.50 (d, 2H), 7.36–7.31 (m, 6H), 4.78 (s, 1H), 3.71–3.64 (m, 4H), 2.62–2.56 (m, 4H).

Procedure for Figure 51a in the absence of CuCl₂

Benzaldehyde (100 μL, 1.0 mmol), morpholine (95 μL, 1.1 mmol), and phenylacetylene (160 μL, 1.5 mmol) were added to a 10 mL Schlenk tube. 0.9 mL of H₂O was added to the Schlenk. An aqueous solution of AuCl₃ was made by dissolving 45 mg of AuCl₃ in 15 mL of H₂O. 1.0 mL (3.0 mg, 0.010 mmol) of this solution was added to the Schlenk tube under flowing N₂. The reaction mixture was then heated at 70 °C and stirred in an oil bath. After 12 h, an aliquot of the organic phase was removed to study the conversion by ¹H NMR spectroscopy. Additional benzaldehyde (100 μL, 1.0 mmol), morpholine (95 μL, 1.1 mmol), and phenylacetylene (160 μL, 1.5 mmol) were added at this time. Heating was resumed and the conversion studied every 12 h. This process was repeated for a total of three cycles.

Procedure for Figure 51b with AuCl₃ and CuCl₂

3-Bromobenzaldehyde (120 μ L, 1.0 mmol), piperidine (110 μ L, 1.1 mmol), and phenylacetylene (160 μ L, 1.5 mmol) were added to a 10 mL Schlenk tube. 0.9 mL of H₂O was added to the Schlenk. An aqueous solution of CuCl₂ was made by dissolving 23 mg of CuCl₂ in 3.0 mL of H₂O. 100 μ L (0.75 mg, 5.0×10^{-3} mmol) of this solution was added to the organics. An aqueous solution of AuCl₃ was made by dissolving 45 mg of AuCl₃ in 15 mL of H₂O. 1.0 mL (3.0 mg, 0.01 mmol) of this solution was added to the Schlenk tube under flowing N₂. The reaction mixture was then heated at 70 °C and stirred in an oil bath. After 12 h, an aliquot of the organic phase was removed to study the conversion by ¹H NMR spectroscopy. Additional 3-bromobenzaldehyde (120 μ L, 1.0 mmol), piperidine (110 μ L, 1.1 mmol), and phenylacetylene (160 μ L, 1.5 mmol) were added at this time. Heating was resumed and the conversion studied every 12 h. This process was repeated for a total of five cycles. Heating was continued for an additional 24 h, with a ¹H NMR spectrum taken every 12 h. ¹H NMR spectroscopy (300 MHz, CDCl₃) δ 7.89-7.87 (m, 1H), 7.66-7.62 (m, 1H), 7.59-7.55 (m, 2H), 7.48-7.44 (m, 1H), 7.41-7.34 (m, 3H), 7.29-7.23 (m, 1H), , 4.81 (s, 1H), 2.65-2.56 (m, 4H), 1.72-1.58 (m, 4H), 1.58-1.45 (m, 2H).

Procedure for Figure 51b the absence of CuCl₂

3-Bromobenzaldehyde (120 μ L, 1.0 mmol), piperidine (110 μ L, 1.1 mmol), and phenylacetylene (160 μ L, 1.5 mmol) were added to a 10 mL Schlenk tube. 0.9 mL of H₂O was added to the Schlenk. An aqueous solution of AuCl₃ was made by dissolving 45 mg of AuCl₃ in 15 mL of H₂O. 1 mL (3.0 mg, 0.010 mmol) of this solution was added to the Schlenk tube under flowing N₂. The reaction mixture was then heated at 70 °C and

stirred in an oil bath. After 12 h, an aliquot of the organic phase was removed to study the conversion by ^1H NMR spectroscopy. Additional 3-bromobenzaldehyde (120 μL , 1.0 mmol), piperidine (110 μL , 1.1 mmol), and phenylacetylene (160 μL , 1.5 mmol) were added at this time. Heating was resumed and the conversion studied every 12 h. This process was repeated for a total of three cycles.

Procedure for Table 7, Entry 1

Phenylacetylene (150 μL , 1.3 mmol), mesitylene (380 μL , 2.6 mmol), CuCl_2 (10 mg, 6.7×10^{-2} mmol), and 2.6 mL of dry nitromethane were added to a 10 mL Schlenk tube. The Schlenk tube was evacuated by three freeze-pump-thaw cycles. AuCl_3 (20 mg, 6.7×10^{-2} mmol) was taken from a glove box and added to the Schlenk tube under flowing N_2 . The reaction mixture was then heated at 60 $^\circ\text{C}$ and stirred in an oil bath. After 24 h, an aliquot of the organic phase was removed to study the conversion by ^1H NMR spectroscopy. ^1H NMR (300 MHz, CDCl_3): δ 7.28-7.19 (m, 5H), 6.90 (s, 2H), 5.95 (d, 1H), 5.09 (d, 1H), 2.31 (s, 3H), 2.11 (s, 6H).

Procedure for Table 7, Entry 2

Phenylacetylene (150 μL , 1.3 mmol), mesitylene (380 μL , 2.6 mmol), and 2.6 mL of dry nitromethane were added to a 10 mL Schlenk tube. The Schlenk tube was evacuated by three freeze-pump-thaw cycles. AuCl_3 (20 mg, 6.7×10^{-2} mmol) was taken from a glove box and added to the Schlenk tube under flowing N_2 . The reaction mixture was then heated at 60 $^\circ\text{C}$ and stirred in an oil bath. After 24 h, an aliquot of the organic phase was removed to study the conversion by ^1H NMR spectroscopy.

Procedure for Table 7, Entry 3

Phenylacetylene (150 μL , 1.3 mmol), mesitylene (380 μL , 2.6 mmol), CuCl_2 (10 mg, 6.7×10^{-2} mmol), and 2.6 mL of dry nitromethane were added to a 10 mL Schlenk tube. The Schlenk tube was evacuated by three freeze-pump-thaw cycles. The Schlenk tube was flushed with N_2 . The reaction mixture was then heated at 60 $^\circ\text{C}$ and stirred in an oil bath. After 24 h, an aliquot of the organic phase was removed to study the conversion by ^1H NMR spectroscopy.

Procedure for Table 7, Entry 4

4-Methylphenylacetylene (170 μL , 1.3 mmol), mesitylene (380 μL , 2.6 mmol), CuCl_2 (10 mg, 6.7×10^{-2} mmol), and 2.6 mL of dry nitromethane were added to a 10 mL Schlenk tube. The Schlenk tube was evacuated by three freeze-pump-thaw cycles. AuCl_3 (20 mg, 6.7×10^{-2} mmol) was taken from a glove box and added to the Schlenk tube under flowing N_2 . The reaction mixture was then heated at 60 $^\circ\text{C}$ and stirred in an oil bath. After 24 h, an aliquot of the organic phase was removed to study the conversion by ^1H NMR spectroscopy. ^1H NMR (300 MHz, CDCl_3): δ 7.16 (d, 2H), 7.06 (d, 2H), 6.90 (s, 2H), 5.91 (d, 1H), 5.03 (d, 1H), 2.31 (s, 6H), 2.11 (s, 6H).

Procedure for Table 7, Entry 5

4-Methylphenylacetylene (170 μL , 1.3 mmol), mesitylene (380 μL , 2.6 mmol), and 2.6 mL of dry nitromethane were added to a 10 mL Schlenk tube. The Schlenk tube was evacuated by three freeze-pump-thaw cycles. AuCl_3 (20 mg, 6.7×10^{-2} mmol) was taken from a glove box and added to the Schlenk tube under flowing N_2 . The reaction

mixture was then heated at 60 °C and stirred in an oil bath. After 24 h an aliquot of the organic phase was removed to study the conversion by ^1H NMR spectroscopy.

Procedure for Table 7, Entry 6

4-Methylphenylacetylene (170 μL , 1.3 mmol), mesitylene (380 μL , 2.6 mmol), CuCl_2 (10 mg, 6.7×10^{-2} mmol), and 2.6 mL of dry nitromethane were added to a 10 mL Schlenk tube. The Schlenk tube was evacuated by three freeze-pump-thaw cycles. The Schlenk tube was flushed with N_2 . The reaction mixture was then heated at 60 °C and stirred in an oil bath. After 24 h an aliquot of the organic phase was removed to study the conversion by ^1H NMR spectroscopy.

CHAPTER 5

CONCLUSIONS AND RECOMMENDATIONS FOR FUTURE WORK

Conclusions

This thesis describes the synthesis and characterization of a new disulfide transfer reagent, and the synthesis of the first disulfidediamine (R_2NSSNR_2) containing polymers. Polymers with molecular weights up to $11,400 \text{ g mol}^{-1}$ were synthesized at room temperature, in air, and without solvent purification. The polymers were stable, but underwent rapid decomposition under acidic, aqueous conditions or when heated to $175 \text{ }^\circ\text{C}$. Poly(disulfidediamines) are promising agents for sustained H_2S release *in vivo*.

A new disulfide transfer reagent was synthesized in two steps from commercially available starting materials. No purification of the starting materials or solvents was necessary and the reactions were performed without special precautions to exclude oxygen or water. *cis*-1,2,3,6-Tetrahydrophthalamide was hydrogenated in a Parr reactor, followed by reaction with sulfur monochloride. The synthesis was able to be easily scaled up to 50 g, with yields of 70 %. No difficult workup was required, as the hydrogenated product required no purification and the final product was easily purified by recrystallization. The transfer reagent was fully characterized by ^1H NMR and ^{13}C NMR spectroscopy and mass spectrometry.

The disulfide transfer reagent was used as a monomer in the step polymerization of poly(disulfidediamines). The polymerizations were carried out at room temperature under atmospheric conditions for 24-48 h. Polymers with molecular weight up to $11,400 \text{ g mol}^{-1}$ were obtained in isolated yields of 65-75 %. Conversions were in the range of

97-98 %, as determined from the degree of polymerization of the isolated polymers. All the polymers were characterized by ^1H NMR and ^{13}C NMR spectroscopy, and one example was sent for elemental analysis which confirmed the presence of two sulfur atoms per repeat unit.

We also studied the decomposition of disulfidediamine functional groups to release hydrogen sulfide. The rate constant for the decomposition of disulfidediamine functional groups in 4:1 DMSO-d_6 : D_2O under acidic conditions was $1.08 \times 10^{-3} \text{ s}^{-1}$ as measured by ^1H NMR spectroscopy. This was approximately 10,000 times faster than decomposition under neutral or basic conditions in the same solvent. Decomposition of disulfidediamines under acidic conditions resulted in the release of a fraction of the sulfur as hydrogen sulfide. The hydrogen sulfide was detected by reacting it with $\text{Pb}(\text{OAc})_2$ and weighing the PbS that precipitated from the solvent. The fraction of sulfur released as hydrogen sulfide varied from approximately 20 % when hydrochloric acid was used, to a trace amount for acetic acid.

Additionally, we developed a method for increasing the turnovers of a AuCl_3 catalyst by 3,300 % using 2,2,6,6-tetramethylpiperidine-1-oxyl (TEMPO) and CuCl_2 . A three component coupling reaction between piperidine, phenylacetylene, and benzaldehyde yielded a propargylamine in quantitative conversions and isolated yields when AuCl_3 was added in catalytic amounts, but the gold catalyst decomposed and had little to no reactivity when a second set of piperidine, phenylacetylene, and benzaldehyde were added after the reaction was complete. Thus, only one cycle was possible with AuCl_3 . The addition of TEMPO and CuCl_2 to reactions with AuCl_3 maintained the catalytic activity of gold for up to 33 cycles, demonstrating a new way to greatly increase

the turnovers of a AuCl_3 catalyst with the addition of inexpensive, commercially available reagents.

Recommendations for future work

Our first future objective is the full elucidation of the influence of acid strength and conjugate base nucleophilicity on the decomposition products of disulfidediamines; particularly in reference to the amount of H_2S produced. Because of the toxicity of even moderate concentrations of H_2S , it is critical for us to know how much H_2S will be produced before disulfidediamines are used *in vivo*. More H_2S is produced when using acids with a lower pK_a , and we suspect that both the pK_a of the acid and the nucleophilicity of the conjugate base could be important influences. To separate the two influences a series of decompositions can be done using pyridinium chloride, pyridinium tosylate, and pyridinium acetate as the acids. The pK_a of these three acids should be almost identical, but the nucleophilicity of the conjugate bases is not. The variance in the amount of H_2S generated by the decompositions using each acid will reveal how much influence the nucleophilicity of the conjugate bases has on the decomposition products.

The decomposition of poly(disulfidediamines) to release H_2S *in vivo* is the ultimate goal of this project. Both linear polymers and polymeric nanoparticles will be used to deliver H_2S to cell cultures in a sustained manner. Cancer cells would be an especially attractive target, since H_2S is well-known to have strong pro-oxidant and apoptotic effects on several cancer types. The sustained delivery of H_2S by poly(disulfidediamine) polymers would be a major advance in the field of H_2S therapy.

APPENDIX

SYNTHESIS OF THE FIRST POLY(DIAMINOSULFIDE)S AND AN
INVESTIGATION OF THEIR APPLICATIONS AS DRUG DELIVERY VEHICLES

Introduction

The integration of new functional groups into polymer chemistry opens new avenues for research and possible commercial applications. For instance, the development of well-defined carbene catalysts based on Mo, W, and Ru in the 80s and 90s increased the types and complexities of polymers that could be synthesized and the problems in macromolecular science that could be addressed.¹⁹¹⁻²⁰² These catalysts led to the development of living ring-opening metathesis polymerization (ROMP) and acyclic diene metathesis (ADMET) polymerization, which were significant reasons the Nobel Prize was awarded to Schrock, Grubbs, and Chauvin in 2005.²⁰³⁻²¹² The use of “click” chemistry is another example, and its use has increased the complexity of the structure of macromolecules and has found widespread applications in polymer science.²¹³⁻²¹⁵ In a recent example by the Hawker group published in 2010, polymers were synthesized for the first time with a functional group that was a precursor to ketenes and provided a simple route to synthesize cross-linked polyethylene to systematically study its materials properties.^{216,217} From these examples and more, it is clear that when new functional groups are integrated into macromolecules, new applications are developed that take advantage of their unique reactivities.

In this article we report the first examples of polymers that utilize diaminosulfide functional groups along their backbones. The diaminosulfide functional group has the

general structure of $R_2N-S-NR_2$ as shown in Figure A-1. Small molecules with this functional group have been synthesized using sulfur transfer reagents such as those molecules shown in Figure A-1b.²¹⁸⁻²²⁰ The most prominent applications of small molecules with diaminosulfides have been in the chemical industry for the high temperature vulcanization of rubber and in the construction of polymers with benzo[1,2,5]thiadiazoles along the backbone (Figure A-1c).²²¹ Polymers that incorporate benzo[1,2,5]thiadiazoles have found uses as semiconductors, fluorophores, and photoactive components in organic solar cells due to their interesting electro-optical properties.²²²⁻²³⁰ These polymers link the monomers through carbon-carbon bonds as shown in Figure A-1c rather than through the nitrogen or sulfur atoms as in poly(diaminosulfide)s. Surprisingly, no one has used diaminosulfides to bond monomers together as shown in Figure A-1a, and these polymers were the focus of this report.

An important characteristic of the diaminosulfide group is that it is based on inorganic atoms (one sulfur and two nitrogens). Most functional groups that are used to synthesize polymers are based on organic functional groups such as esters, amides, anhydrides, acetals, cyclic olefins, vinyl groups, carbonates, urethanes, and epoxides. Although many monomers are known to possess inorganic functional groups, it is uncommon that an inorganic functional group is transformed in the polymerization reaction and used to link monomers together as shown in Figure A-1a. Most inorganic functional groups found in monomers or polymers are not transformed during the polymerization reaction. Three notable examples of inorganic functional groups that have been polymerized include the polymerization of thiols into poly(disulfides), the polymerization of cyclic phosphazenes into poly(phosphazenes), and the polymerization

of cyclic siloxanes into poly(siloxanes).²³¹ Inorganic functional groups are interesting targets for polymer synthesis because they can be expected to have new reactivities that differ from those of organic functional groups and they have the potential to act as ligands for metals.²³²⁻²³⁵ The use of inorganic functional group transformations in the synthesis of polymers is understudied and represents a potentially rich source of functional group diversity in macromolecular science.

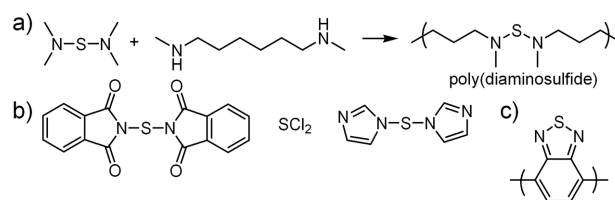


Figure A-1 Diaminosulfide synthesis.

a) A polymerization to yield a poly(diaminosulfide). b) Sulfur transfer reagents that are commonly used in small molecule synthesis. c) A polymer of a benzo[1,2,5]thiadiazole.

One part of our motivation to synthesize polymers through the polymerization of diaminosulfides was based on the chemical properties of this functional group in small molecule synthesis. These polymers are structurally related to polythiazyl $(\text{SN})_x$ which was first synthesized in 1953 from S_2N_2 .²³⁶⁻²⁴⁰ This polymer is electrically conducting at room temperature and superconducting at low temperatures.²³⁶ In prior work by others, molecules with diaminosulfides were stable and readily isolated by traditional methods (distillation or chromatography).²³¹ In addition, some examples of the synthesis of molecules containing diaminosulfides proceeded with isolated yields of 80% or higher. Although promising, these results do not predict immediate success in a step-growth

polymerization. In these polymerizations, the degree of polymerization, X_n , is related to the fractional monomer conversion, P , by the equation $X_n = 1/(1-P)$.²⁴¹ Thus, to synthesize poly(diaminosulfide)s with modest to high molecular weights via a step-growth polymerization, the yield of the coupling reaction must be >95%.

To illustrate a possible application of poly(diaminosulfides), we completed initial experiments to investigate the application of a poly(diaminosulfide)s as a delivery vehicle for drugs. Many drugs suffer from poor bioavailability, poor water solubility, short serum circulation lifetimes, inadequate mechanisms to enter cells, or have serious side effects that limit the amount of drug that can be administered. To overcome these and more limitations, drugs are often condensed with synthetic, biodegradable polymers into nanoparticle delivery vehicles that are administered to patients.²³¹ The polymer protects the drugs from degradation in the bloodstream and allows their delivery to tumors by the enhanced permeation and retention effect where they can be taken into cancer cells. The polymers used in this field degrade slowly in the blood stream but have a rapid rate of degradation when taken into the acidic compartments of cells – the endosome and lysosome – where they release their cargo.²⁴²⁻²⁴⁵ It is critically important that the polymer be biodegradable such that it will not accumulate within the body and cause a toxic response.^{246,247} In this article, some of the characteristics of poly(diaminosulfides) as drug delivery vehicles were investigated including the stabilities of diaminosulfides in water under basic, acidic, and neutral conditions; whether nanoparticles fabricated from these polymers were internalized by cells; and whether any *in vitro* toxicity was observed from the nanoparticles. These studies are meant to illustrate an interesting application of poly(diaminosulfide)s in medicine.

We report the synthesis of a small molecule that is a highly successful sulfur transfer reagent and how this molecule can be used to synthesize the first poly(diaminosulfide)s reported in the literature. Some of the key, initial studies of a diaminosulfide in numerous solvents are reported to demonstrate their stabilities and, by extension, the stabilities of poly(diaminosulfide)s. Finally, one example of a poly(diaminosulfide) was fabricated into microparticles and studied for their ability to be internalized by human embryonic kidney-293 (HEK-293) cells and whether they showed any toxicity towards these cells.

Results and Discussion

Synthesis and reactions of sulfur transfer reagents

We hypothesized that poly(diaminosulfide)s could be synthesized by reacting secondary diamines with a sulfur transfer reagent as shown in Figure A-1a. Many secondary diamines were commercially available or easily synthesized, so the challenge in the polymerization was to develop a useful sulfur transfer reagent. Although SCl_2 is used in the synthesis of small molecules with diaminosulfides, its use has several drawbacks.²⁴⁸⁻²⁵³ This molecule has a low boiling point (59 °C), must be handled under inert atmospheres, is challenging to purify, reacts with multiple functional groups such as alcohols and alkenes, and releases HCl. Because of these limitations, we have not pursued the synthesis or use of SCl_2 .

Two different sulfur transfer reagents were studied (Figure A-2). Molecule B was initially explored as a sulfur transfer reagent based on the rapid reactions of thiosuccinimides with amines.^{254,255} Although the synthesis of B was straightforward and

did not require any chromatography, its purification was challenging because of its poor solubility in many solvents. Molecule B was mostly insoluble in benzene, chloroform, DMSO, and methylene chloride. Molecule B was cleaned by washing the crude product with hexanes and an isolated yield of 69% was obtained. To increase the purity of molecule B, it was recrystallized from methanol. Replacement of *N*-chlorosuccinimide with *N*-chlorophthalimide in the second step yielded a diphthalimide sulfur transfer reagent that also possessed limited solubility in organic solvents.

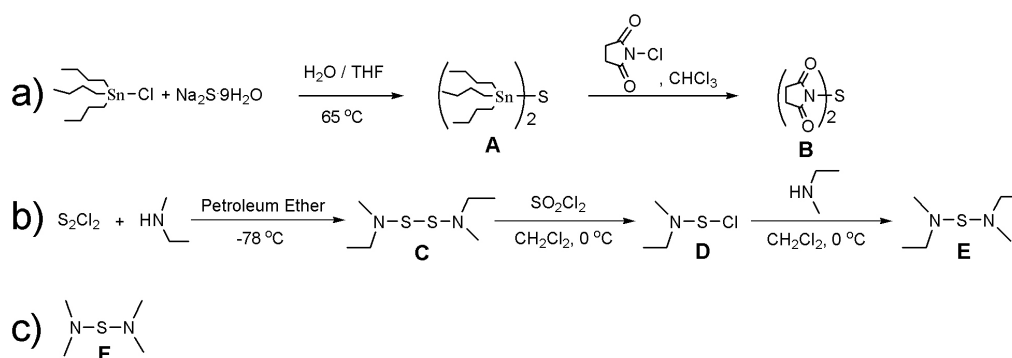


Figure A-2 The synthesis of two sets of sulfur transfer reagents.

a) The synthesis of a dithiosuccinimide. b) The synthesis of a diaminosulfide in two steps. Molecules C and E were purified by distillation. c) Molecule F was synthesized using the same procedure as molecule E.

Although B was partially soluble in DMSO, it was not used to synthesize polymers for several reasons. First, the synthesis of B had poor atom efficiency. The addition of one sulfur (atomic weight: 32 g mol^{-1}) to yield a diaminosulfide functional group along the backbone of a polymer would require the use of two equivalents of tributyltinchloride ($\text{MW}: 326 \text{ g mol}^{-1}$) and two equivalents of *N*-chlorosuccinimide ($\text{MW}:$

134 g mol⁻¹). Thus, significant amounts of waste were produced in the synthesis of molecule B. Second, the poor solubility of molecule B made it challenging to use in solvents that dissolve many polymers. For instance, it decomposed when heated in CDCl₃ and DMSO-d₆.

A second sulfur transfer reagent was synthesized (molecule E in Figure A-2) based on a literature procedure. In the first step, an excess of ethylmethylamine was reacted with sulfur chloride at -78 °C. Reactions run at 0 °C had unidentified side products, but the reaction at -78 °C yielded molecule C in high purity. Molecule C could be carried onto the next step without purification or it could be purified by distillation. In the second step, C reacted with SO₂Cl₂ to yield D that was not isolated. Rather, D was slowly added to ethylmethylamine to yield the sulfur transfer reagent E. This procedure was followed to synthesize F using dimethylamine in both steps. Both E and F were readily purified by distillation and yielded clean products as shown by ¹H and ¹³C NMR spectroscopy and high resolution mass spectrometry. Because no chromatography was necessary for the synthesis of E or F, these reactions could be scaled up to yield large amounts of product in a short period of time.

Kinetics of transamination reactions

To synthesize polymers via transamination reactions between molecule E and secondary diamines, the second-order kinetics of the reaction between molecule E and benzylmethylamine was studied in four solvents (Figure A-3). Benzylmethylamine was chosen for these reactions because of the easily identified benzylic CH₂ group that shifted downfield in the ¹H NMR spectra when proceeding from benzylmethylamine to H to I.

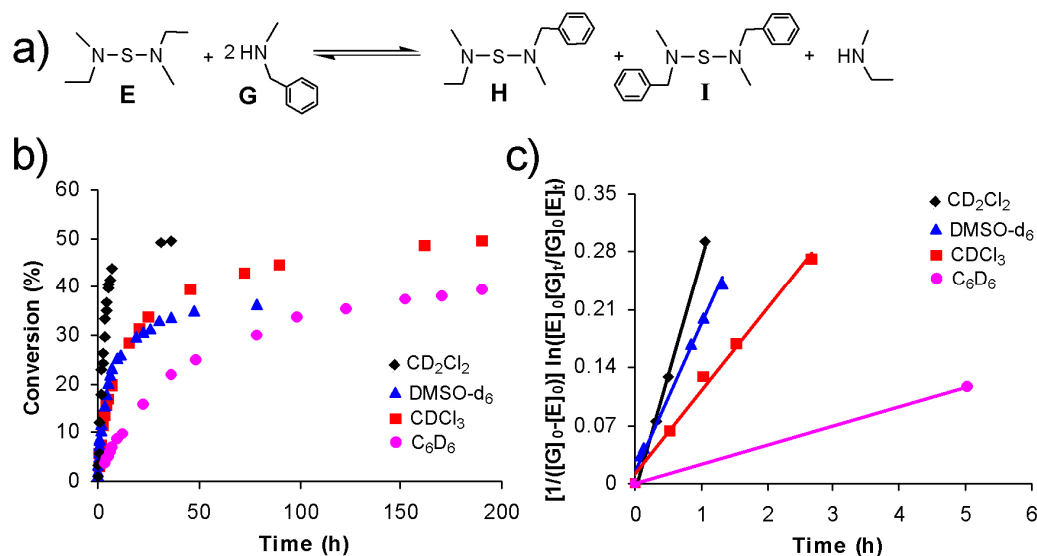


Figure A-3 Kinetics of transamination reactions.

a) The reaction that was studied in a sealed NMR tube. b) The conversion of the transamination reactions as a function of time. The conversion was defined as the sum of the S-N(CH₃)Bn bonds divided by the sum of all of the S-N bonds for molecules E, H, and I. c) The plot of the initial data points used to find the rate constants for the reaction in each solvent. More data points were used to find the rate constant for the experiment in C₆D₆ but they are not shown here.

The reactions between molecule E and two molar equivalents of benzylmethylamine were studied, and the rate constants were measured in CD₂Cl₂ ($7.81 \times 10^{-5} \text{ M}^{-1} \text{ s}^{-1}$), DMSO-d₆ ($4.89 \times 10^{-5} \text{ M}^{-1} \text{ s}^{-1}$), CDCl₃ ($2.79 \times 10^{-5} \text{ M}^{-1} \text{ s}^{-1}$), and C₆D₆ ($5.47 \times 10^{-6} \text{ M}^{-1} \text{ s}^{-1}$). The rate constants were found using the data points for conversions of less than 10% using the assumption that the reaction was irreversible. Although the reaction was reversible, this assumption has been commonly used to find rate constants for reversible reactions at low conversions.²⁵⁶ It is important to note that the ethylmethylamine (boiling point = 36 °C) remained in the sealed NMR tube.

Although the reaction was most rapid in CD_2Cl_2 and reached equilibrium in 14 h, small amounts of unidentified side products were visible. The presence of side products made methylene chloride a poor choice for the polymerization. The reaction in CDCl_3 took 8 days to reach equilibrium and the reaction in C_6D_6 did not reach equilibrium after 8 days. Despite the slow rates for reactions in these solvents, the reactions were clean and no side products were observed. The reaction in DMSO-d_6 also did not show any side products after 3 days, but this reaction reached 37% conversion and did not proceed any further. The final conversion was less than 50% because molecule I had limited solubility in DMSO-d_6 due to the apolar structure of molecule I and the polar structure of DMSO-d_6 . The ^1H NMR spectra of this reaction in DMSO-d_6 showed a lower than expected concentration of molecule I even after three days.

The reaction between molecule E and benzylmethylamine only reached 51% conversion in 17 h when completed at 40 °C in an uncapped NMR tube, despite the low boiling point of ethylmethylamine. Prolonged reaction times resulted in a slow increase in conversion, but this reaction was judged to be too slow. Molecule F was synthesized for the polymerization reactions because of the low boiling point of dimethylamine (boiling point 7 °C) which would make it simple to remove from a reaction.

Reactions between molecule F and benzylmethylamine were studied in CDCl_3 , DMSO-d_6 , and C_6D_6 in vented reaction vessels to allow dimethylamine to boil off (Figure A-4 and Table A-1). Each of the reactions in Table A-1 did not show any impurities by ^1H NMR spectroscopy even when heated to 85 °C for extended periods of time. The conversions for the reactions were high for each solvent for reactions at 50 °C but went to quantitative conversions for reactions in C_6D_6 at 85 °C.

Synthesis of poly(diaminosulfide)s

Poly(diaminosulfide)s were synthesized by reaction of secondary diamines and molecule F at elevated temperatures (Figure A-5 and Table A-2). These polymerizations were run for 24 to 96 h, and the resulting polymers were characterized by GPC against polystyrene standards, ^1H NMR spectroscopy, and ^{13}C NMR spectroscopy.

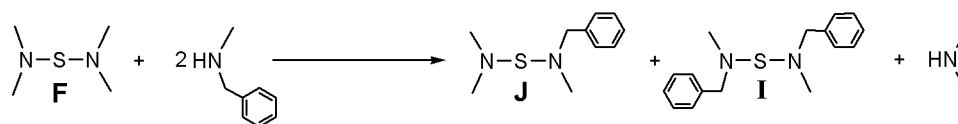


Figure A-4 A transamination reaction with dimethylamine as the leaving group.

Table A-1 Transamination reactions of molecule F and benzylmethylamine.

Entry	Solvent	Temperature (°C)	Reaction time (h)	^a Conversion (%)
1	CDCl ₃	50	24	39
2	CDCl ₃	50	72	93
3	DMSO-d ₆	50	73	84
4	C ₆ D ₆	50	24	41
5	C ₆ D ₆	50	72	84
6	C ₆ D ₆	85	24	>97

^aThe conversion was defined as the sum of the S-N(CH₃)Bn bonds divided by all of the S-N bonds in molecules F, J, and I.

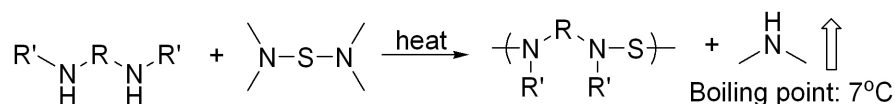
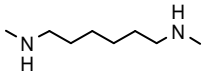
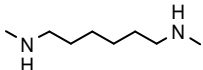
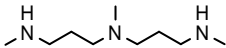
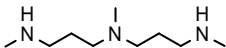
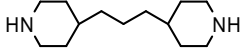
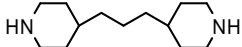
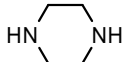


Figure A-5 The polymerization of diamines with the sulfur transfer reagent is shown.

Table A-2 Synthesis of poly(diaminosulfides).

Entry	Diamine	Temperature (°C)	Reaction time (h)	M_n^a (g mol ⁻¹)	PDI ^a	Yield (%)	DP ^b (%)	DP ^c (%)
1		85	24	5,600	3.7	75	98	99
2		85	48	5,200	3.4	97	98	99
3		85	72	810	1.6	97	87	97
4		85	96	1,600	1.6	89	93	98
5		60	72	12,400	6.6	88	99	98
6		60	96	7,200	3.3	95	98	98
^d 7		85						

^aThe M_n and PDI were measured using size exclusion chromatography versus polystyrene standards. ^bThe degree of polymerization were based on the values for M_n measured by GPC. ^cThe degree of polymerization were based on ¹H NMR spectra. ^dThe polymer was insoluble.

The polymers in entries 1, 2, 5, and 6 had high molecular weights and degrees of polymerization. The degrees of polymerization were determined by two methods using the molecular weight measured by GPC and by end group analysis in the ¹H NMR spectra of the polymers. These values for the degree of polymerization agreed with each other and demonstrated that these reactions cleanly proceeded to high conversions. The polymerization with piperazine (entry 7) yielded an insoluble polymer in all solvents.

The polymer synthesized in entries 3 and 4 had limited stability. When this polymer was precipitated into methanol and water, it rapidly degraded as shown by the

presence of numerous, unidentified peaks in the ^1H NMR spectra. To isolate the polymer with minimal degradation, benzene was removed under vacuum after the polymerization was complete, and the polymer was characterized without further purification. The GPC and ^1H NMR spectra were consistent with the indicated polymer. We believe that the internal, tertiary amine reacts with the diaminosulfide through an intramolecular reaction and was the source of the instability of this polymer.

The polymer shown in entry 6 was characterized by elemental analysis to provide further evidence that it possessed the indicated composition. The calculated weight composition of the repeat unit was carbon (64.95%), hydrogen (10.06%), nitrogen (11.65%), and sulfur (13.34%). The measured weight composition of the polymer was carbon (64.70%), hydrogen (9.97%), nitrogen (11.76%), and sulfur (13.44%). The agreement between the calculated and measured elemental compositions provided strong evidence that there was only one sulfur atom bridging between the nitrogens.

Stability of diaminosulfides in organics and water

Numerous small molecules possessing diaminosulfide functional groups have been synthesized, but no reports on their long term stabilities in organic solvents or water have been published. The stability of this functional group was investigated to estimate the stabilities of poly(diaminosulfide)s for future work. Molecule E and an internal standard of diethylene glycol dimethyl ether were added to CDCl_3 , $\text{DMSO-d}_6/\text{D}_2\text{O}$ (10/1 by volume), and C_6D_6 and allowed to sit at room temperature in capped NMR tubes (Figure A-5). Periodic ^1H NMR spectra were collected to determine the percent decomposition by the mole ratio of molecule E to the ether. After 32 days the amount of decomposition ranged from no detectable decomposition in C_6D_6 to 38% decomposition

in DMSO- d_6 /D $_2$ O. Because molecule E was not soluble in methanol, the stability of molecule K was studied in CD $_3$ OD. After 32 days, 15% of molecule K degraded.

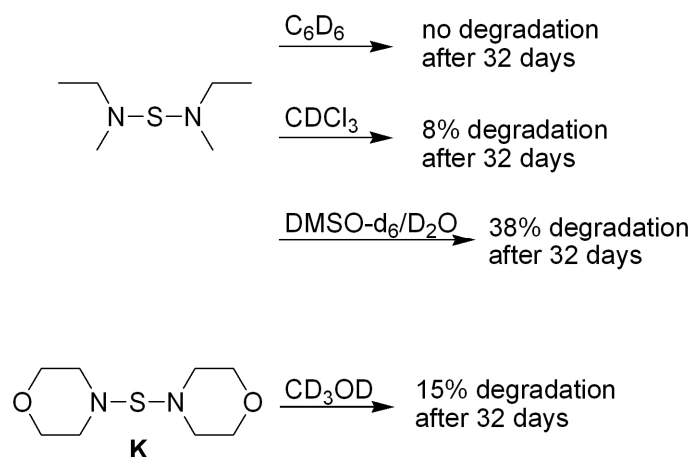


Figure A-6 The stability of two diaminosulfides at room temperature in organic solvents.

These results demonstrated that the diaminosulfide functional group was stable in apolar, aprotic solvents but that it very slowly degraded in polar, protic solvents. The rate of degradation was slow enough that polymers with diaminosulfide functional groups are expected to have reasonable stabilities in these solvents, and this stability was observed for the prepared poly(diaminosulfide)s. The polymers were synthesized in benzene and chloroform at elevated temperatures and isolated by precipitation into methanol. Despite these conditions, the polymers possessed high degrees of polymerization.

To further explore the stability of the diaminosulfide functional group, molecule L was synthesized and studied in water (Figure A-6). Molecule L and an internal standard of *tert*-butanol were added to D $_2$ O with 9 molar equivalents of acetic acid (acidic conditions), 9 molar equivalents of KOH (basic conditions), or no additional acid or base

(neutral conditions). The rate constants for the decomposition of this molecule were $1.29 \times 10^{-4} \text{ s}^{-1}$ under neutral pH conditions and $9.88 \times 10^{-5} \text{ s}^{-1}$ under basic conditions. Under acidic conditions, molecule L completely degraded by the time the first ^1H NMR spectrum was obtained so only a lower limit of the rate constant was calculated ($1.70 \times 10^{-2} \text{ s}^{-1}$).

The only product of degradation determined by ^1H NMR spectroscopy was the secondary diamine used in the synthesis of molecule L. From prior work by others, it was known that diaminosulfides react in water to form sulfur monoxide, which possessed a half-life of seconds and decomposed to release SO_2 and elemental sulfur.^{257,258}

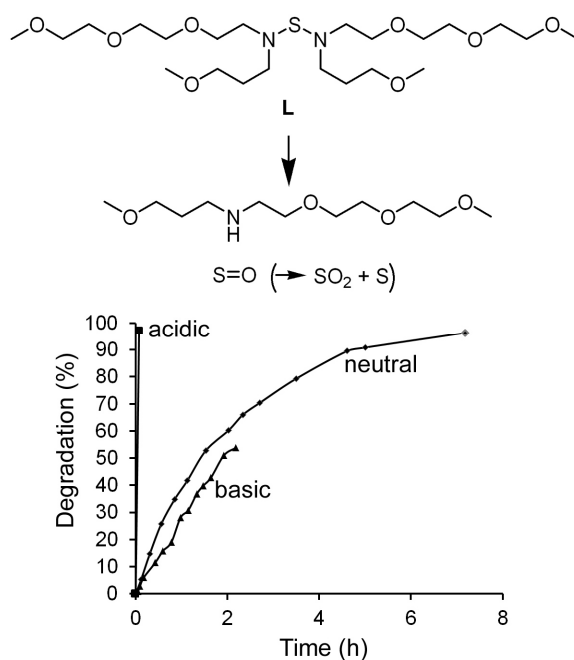


Figure A-7 The degradation of molecule L under acidic, neutral, and basic conditions.

Fabrication and uptake of poly(diaminosulfide) particles

Synthetic polymers are widely used in drug delivery. In this field a polymer and drug are fabricated into nano- to micrometer sized particles and delivered to the body. Most of the polymers used in this field are based on polyesters – although other polymers are under investigation – because of the need to have the polymer degrade *in vivo* before it accumulates in the body and provokes a toxic response. Polyesters are widely used because they degrade in the body under neutral or acidic conditions without the need for enzymes. This observation of the role of polyesters in drug delivery and the degradation of diaminosulfides in water led us to speculate that poly(diaminosulfide)s may be useful as drug delivery vehicles. The diaminosulfide functional group degrades several orders of magnitude faster than ester bonds under acidic conditions, and they possess reasonable stabilities in water under neutral conditions.²⁵⁹ Some of the first key experiments to demonstrate the ability of poly(diaminosulfide)s to function as drug delivery vehicles are described here and more results will be published in subsequent articles.

A polymer with the structure of entry 6 in Table A-2 was used to fabricate microparticles that were studied as potential drug delivery vehicles (Figure A-7). The microparticles were prepared according to a water/oil/water double emulsion-solvent evaporation method using poly(vinyl alcohol) as a surfactant. Since, the poly(diaminosulfide) was insoluble in water, it was added to dichloromethane with a dye (FITC-dextran). A surfactant solution of water with 1% (by weight) poly(vinyl alcohol) was added to the dichloromethane and sonicated to produce the particles. This solution was diluted with more water and poly(vinyl alcohol) and further sonicated. After removal of the dichloromethane by evaporation, the microparticles were filtered and

isolated. The particles were spherical in shape and possessed a smooth, nonporous surface. The z-average particle size determined by dynamic light scattering was 660 nm and consistent with the SEM micrograph shown in Figure A-7. The surface charge was determined to be -11.6 ± 0.8 mV.

Microparticles were fabricated and loaded with fluorescein isothiolate-dextran (FITC-dextran) to appear green under optical microscopy. These microparticles were incubated with HEK-293 cells at 37 °C for 24 h to study if they were internalized into the cells. After 24 h, the cells were washed with PBS buffer twice to remove any microparticles not internalized into cells. The cells were then fixed with paraformaldehyde and stained with 4',6-diamidino-2-phenylindole (DAPI) and phalloidin as described in the experimental section. The results in Figure 8 clearly demonstrated that the microparticles were internalized into the HEK-293 cells. In this image, the microparticles were green, the nucleus was blue (due to the DAPI stain), and the cytoplasm/cell membrane was red (due to the phalloidin stain). In control experiments with cells not exposed to the microparticles and not treated with phalloidin or DAPI, the cells did not fluoresce green. Thus, it is clear that there was no autofluorescence from the cells and that the observed green fluorescence within the cells was due to the uptake of the fluorescently labeled dextran loaded particles. This result demonstrates that these microparticles have potential as new drug delivery vehicles.

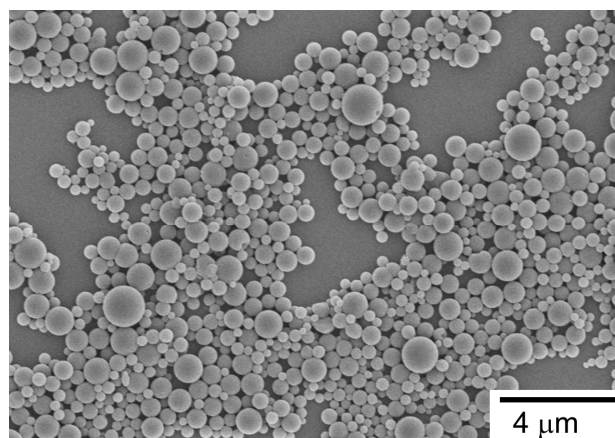


Figure A-8 SEM micrographs of microparticles fabricated from the polymer shown in entry 6 of Table A-2.

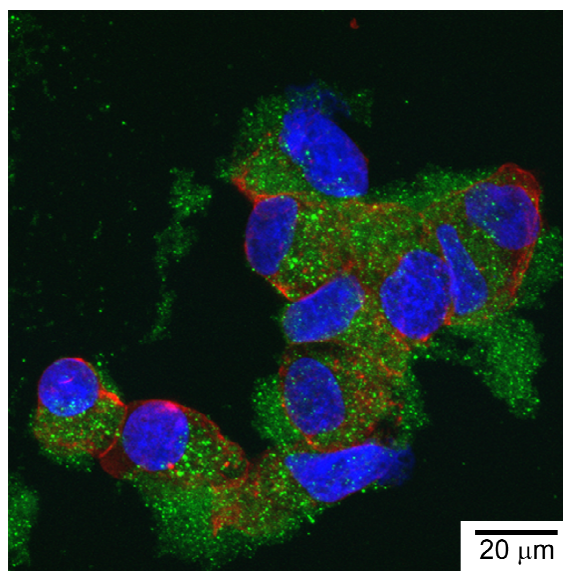


Figure A-9 A laser scanning microscopic image of cellular uptake of microparticles. HEK-293 cells were exposed to microparticles loaded with FITC-dextran (green) for 24 h and then washed to remove microparticles that were not internalized into the cells. The nuclei of the cells were stained blue by DAPI and the cytoplasm/cell membranes were stained red by phalloidin. This image clearly shows that the microparticles were internalized into the cells.

The cell viability of HEK-293 cells was investigated to determine whether the microparticles derived from poly(diaminosulfide)s were toxic. The toxicity of microparticles fabricated from the polymer with the structure shown in entry 6 of Table A-2 were studied via a MTS assay that is widely accepted as one method to determine cell viability in the presence of foreign molecules.^{260,261} Briefly, the MTS assay measures the mitochondrial activity of the cells and is used as an indication of the cell growth and viability. In living cells the MTS reagent (a yellow, water-soluble tetrazolium salt) is cleaved by the mitochondrial enzyme dehydrogenase (NADH-dependent reduction of the tetrazolium ring in MTS) to generate a water-soluble purple product called formazan. The concentration of formazan can be measured and, in this way, the relationship between the cell number and the amount of formazan generated is established since the absorbance is directly proportional to the number of viable cells. Damaged or dead cells exhibit a reduced or diminished enzyme activity and therefore less or no formazan production. Here, the incubation period of 24 h ensured the exposure of the cells to the different treatments in their exponential growth phase. Figure A-9 shows the cell viability as a function of the concentration of microparticles and demonstrates excellent biocompatibility of these novel polymeric microparticles in HEK-293 cells. Microparticles in the concentration range of 1-1000 $\mu\text{g/ml}$ had no adverse effect on cell viability. Even high concentrations of the microparticles did not reduce cell viability with cell survival rates greater than 85% for all the concentrations tested.

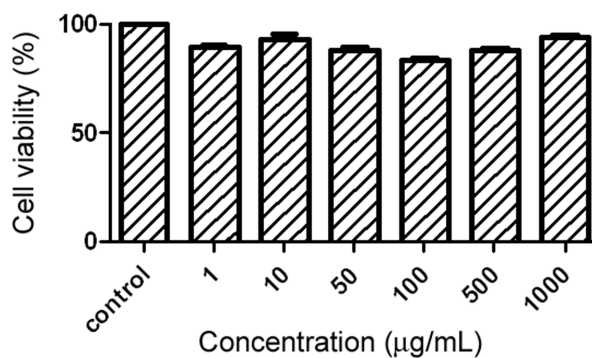


Figure A-10 The cell viabilities of HEK-293 cells incubated with poly(diaminosulfide) microparticles.

Conclusions

This paper described the first synthesis of poly(diaminosulfide)s from two simple starting materials. The sulfur transfer reagent used in the synthesis was readily synthesized in two steps, and, because it was purified by distillation rather than column chromatography, large quantities could be synthesized in only a few days. These polymers have many of the right properties to be used as synthetic polymers for different applications. For instance, we investigated the stabilities of diaminosulfides in different solvents so that future applications of poly(diaminosulfide)s could be envisioned. This functional group was very stable in organic solvents and not prone to oxidation; in fact, no evidence of oxidation of the sulfur was observed in any sample. One exciting application of these polymers as drug delivery vehicles was explored, and the results were very promising. A poly(diaminosulfide) was readily fabricated into nanoparticles that were absorbed into cells. These nanoparticles were also nontoxic towards HEK-293 cells. These results were promising, but more work is needed to investigate the

advantages poly(diaminosulfide)s may possess over polymers used in drug delivery. We propose a general label of poly(NSN) for any poly(diaminosulfide) to emphasize the functional group used in their synthesis and found in their backbones. Poly(NSN) can be used to describe a general family of polymers in the same way that the terms polystyrenes and polyacrylates are used.

One significant characteristic of diaminosulfides is that they are based on an inorganic functional group. Their structures differentiate them from the numerous organic functional groups used in the synthesis of most polymers. We believe that by working with inorganic functional groups with reactivities that differ from those of organic functional groups, new opportunities in macromolecular science will be realized.

Experimental Section

Materials

Sodium sulfide nonahydrate ($\text{Na}_2\text{S}\cdot 9\text{H}_2\text{O}$), tributyltin chloride, *N*-chlorosuccinimide, sulfur monochloride, *N*-ethylmethylaniline, *N*-benzylmethylaniline, *N,N'*-dimethyl-1,6-hexanediamine, *N,N'*-bis[3-(methylamino)propyl]methylaniline, 4,4'-trimethylenedipiperidine, *N,N'*-di-*sec*-butyl-*p*-phenylenediamine, dimethylamine, *p*-toluenesulfonyl chloride, and 3-methoxypropylamine were purchased from Aldrich or Acros Organics at their highest purity and used as received. FITC (fluorescein isothiocyanate)-dextran (Mw 20kDa) and Mowiol (polyvinyl alcohol, PVA, Av Mw~67K, 86.7-88.7% hydrolyzed) was obtained from Sigma-Aldrich™ (Sigma Chemical Co. St. Louis, MO). Deionized distilled water produced by Barnstead Nanopure Diamond™ Water purification Systems (Dubuque, IA) was used throughout.

All other solvents including petroleum ether (39 ~ 56 °C) were reagent grade and purchased from Fisher Scientific. Because dimethylamine is a gas at room temperature, it was condensed inside a graduate cylinder in a -78 °C bath before use. Piperazine (99%) was purchased from Aldrich and was purified by sublimation under vacuum at 130 °C. Genduran silica gel 60 (230-400 mesh) and Basic Alumina Brockman Activity I (60-325 mesh) were purchased from Fisher Scientific and were used for all column chromatography.

Dulbecco's Modified Eagle Medium (DMEM, with high glucose 1X and 4 mM L-glutamine), Trypsin-EDTA (0.25%, 1X solution), and Dulbecco's phosphate buffered saline (PBS) were purchased from Gibco® (Invitrogen™, NY). Fetal bovine serum (FBS) was obtained from Atlanta Biologicals® (Lawrenceville, GA). Gentamycin sulfate (50 mg/ml) was purchased from Mediatech Inc. (Manassas, VA). MTS cell growth assay reagent (Cell Titer 96® Aqueous One Solution cell proliferation assay) was purchased from Promega Corporation, Madison. The HEK-293 cell lines were obtained from the American Type Culture Collection (ATCC®, Manassas, VA).

Characterization

¹H and ¹³C NMR spectra were recorded on a Bruker DPX 300 at 300 MHz and 75 MHz respectively. CDCl₃ was used as the NMR solvent with tetramethylsilane (TMS) as an internal standard. Size-exclusion chromatography (SEC) was performed using tetrahydrofuran as the mobile phase (1.00 mL min⁻¹) at 25 °C. A Shimadzu LC-10AT HPLC pump and one Varian column (PLgel 5 μm MIXED-D) were used in series. A Shimadzu RID-10A refractive index detector and a Shimadzu SCL-10A system controller

were used to measure molecular weights of polymers based on a polystyrene standard calibration curve.

Bis(tributyltin) sulfide

This molecule was prepared according to a literature procedure.²⁶² A solution of sodium sulfide nonahydrate ($\text{Na}_2\text{S}\cdot 9\text{H}_2\text{O}$) (42.0 g, 175 mmol) in deionized water (34.8 ml) was prepared. This solution was added to a solution of tributyltin chloride (28.5 g, 87.4 mmol) in THF (174 mL). Extra deionized water (17.4 mL) was used to transfer the $\text{Na}_2\text{S}\cdot 9\text{H}_2\text{O}$ to the flask. The mixture was reacted at 65 °C for 5 h. After cooling the reaction, the organic layer was evaporated. The residue was extracted with Et_2O . The extract was dried over anhydrous magnesium sulfate and evaporated to give a colorless oil (21.8 g, 81% yield). ^1H NMR (CDCl_3): δ 0.91 (t, 18H, $J = 7.2$ Hz), 1.08 (m, 12H), 1.34 (m, 12H), 1.55 (m, 12H). ^{13}C NMR (CDCl_3): δ 13.66, 15.85, 27.17, 28.68.

Bis(succinimide) sulfide.²⁶²

N-chlorosuccinimide (2.22 g, 16.6 mmol) was slowly added to a solution of molecule A (5.08 g, 8.30 mmol) in CHCl_3 (22 mL) at 0 °C and stirred. After 1.7 h, the ice bath was removed and the reaction was stirred for 8 h. A yellow solid stuck to the walls of the flask. The yellow organic phase was decanted. The yellow solid was washed with hexanes and dried under vacuum to give a crude yellow solid (1.30 g, 69% yield). ^1H NMR (DMSO-d_6): δ 2.57 (s, 8H). ^{13}C NMR (DMSO-d_6): δ 29.55, 179.47.

N,N'-Dithio(bis-ethylmethanamine).²⁶³

A solution of *N*-ethylmethanamine (10.5 g, 178 mmol) in petroleum ether (400 mL) was cooled to -78 °C for 30 min. To this solution, sulfur monochloride (6.00 g,

44.4 mmol) was added dropwise for 10 min. The solution was stirred for 20 min at -78 °C and another 35 min at room temperature. The mixture was washed with a saturated NaCl solution in water. The organic layer was dried over anhydrous magnesium sulfate and evaporated to give a yellow–green oil (7.00 g). The product was isolated by vacuum distillation at 30 ~ 35 °C to yield a colorless oil (6.20 g, 78% yield). ¹H NMR (CDCl₃): δ 1.14 (t, 6H, *J* = 7.2 Hz), 2.64 (s, 6H), 2.69 (q, 4H, *J* = 7.1 Hz). ¹³C NMR (CDCl₃): δ 13.81, 46.28, 53.54. HRMS calcd for C₆H₁₆N₂S₂: 180.0755. Found: 180.0759.

N-Ethylmethylsulfenyl chloride.²⁶⁴

A solution of molecule C (4.81 g, 26.7 mmol) in CH₂Cl₂ (70 mL) was precooled to 0 °C for 40 min under N₂. Sulfuryl chloride (3.96 g, 29.4 mmol) was added dropwise to the solution for 17 min under N₂. The reaction was stirred for 30 min at 0 °C and another 50 min at room temperature to give a crude product (6.70 g, 53.4 mmol), which was used *in situ* for the preparation of molecule E.

Bis(*N*-ethylmethyl)sulfide.²⁶⁴

A solution of molecule D (6.70 g, 53.4 mmol) in CH₂Cl₂ (40 mL) was slowly added to a solution of *N*-ethylmethylamine (7.89 g, 13.3 mmol) in CH₂Cl₂ (60 mL) at 0 °C under N₂ and stirred for 1 h. The reaction was washed with a saturated NaCl solution in water. The organic phase was dried over anhydrous magnesium sulfate and evaporated to give a yellow–green oil (4.22 g). The product was purified by distillation under vacuum at room temperature to yield a colorless oil (2.53 g, 32% yield). ¹H NMR (CDCl₃): δ 1.14 (t, 6H, *J* = 7.2 Hz), 2.95 (s, 6H), 3.11 (q, 4H, *J* = 7.1 Hz). ¹³C NMR (CDCl₃): δ 14.24, 46.29, 54.89. HRMS calcd for C₆H₁₆N₂S: 148.1034. Found: 148.1033.

N,N'-Dithiobis-dimethylamine.²³¹

A solution of dimethylamine (8.01 g, 178 mmol) in anhydrous ether (400 ml) was cooled to -78 °C for 44 min. Sulfur monochloride (6.00 g, 44.4 mmol) was added dropwise to the solution for 14 min. The solution was stirred for 30 min at -78 °C and another 30 min at room temperature. The mixture was washed with a saturated NaCl solution in water. The organic layer was dried over anhydrous magnesium sulfate and evaporated to give a colorless oil (6.66 g, 99% yield), which could be used directly for the preparation of Molecule F without further purification. ¹H NMR (CDCl₃): δ 2.63 (s, 12H). ¹³C NMR (CDCl₃): δ 48.31. HRMS calcd for C₄H₁₂N₂S₂: 152.0442. Found: 152.0444.

N-Dimethylsulfenyl chloride.²³¹

A solution of *N,N'*-dithiobis-dimethylamine (6.03 g, 39.6 mmol) in anhydrous Et₂O (50 mL) was cooled to 0 °C for 1 h under N₂. Sulfuryl chloride (5.88 g, 43.6 mmol) was added dropwise to the solution under N₂. The reaction was stirred for 36 min at 0 °C and another 50 min at room temperature to give a crude product (8.84 g, 79.2 mmol), which was used *in situ* for the preparation of molecule F.

Bis(*N,N'*-dimethyl) sulfide.²⁶⁴

A solution of *N*-dimethylsulfenyl chloride (8.84 g, 79.2 mmol) in anhydrous Et₂O (50 mL) was slowly added to a solution of dimethylamine (17.9 g, 39.6 mmol) in anhydrous Et₂O (75 mL) at -5 °C under N₂ and stirred for 1.2 h. The reaction was washed with saturated aqueous NaCl. The organic phase was dried over anhydrous magnesium sulfate and the solvent was removed after freezing the product at -5 °C to

give yellow-green oil (7.0 g). Further purification was achieved by distillation under vacuum at 30 °C to yield a colorless oil (4.39 g, 46% yield). ^1H NMR (CDCl_3): δ 3.02 (s). ^{13}C NMR (CDCl_3): δ 49.69. HRMS calcd for $\text{C}_4\text{H}_{12}\text{N}_2\text{S}$: 120.0721. Found: 120.0719.

Water-soluble diaminosulfide

In a flask was added *N*-(3-methoxypropyl-(triethylene glycol monomethyl ether)) (2.27 g, 9.64 mmol) and 3.6 mL of benzene. Next, molecule F (0.503 g, 4.18 mmol) was added and the flask was connected to a reflux condenser and heated to 85 °C for 48 h. The benzene was removed under vacuum. The product was cleaned by chromatography on basic alumina oxide using ethyl acetate. The product was a clear oil (1.54 g, 73% yield). ^1H NMR (CDCl_3): δ 1.81 (p, 2H, $J = 6$ Hz), 3.12 (t, 2H, $J = 7.2$ Hz) 3.2-3.4 (m, 10H), 3.5-3.7 (m, 10H). ^{13}C NMR (CDCl_3): δ 29.06, 54.83, 57.53, 58.56, 59.02, 70.13, 70.28, 70.45, 70.56, 70.64, 71.95. HRMS calcd for $\text{C}_{22}\text{H}_{48}\text{N}_2\text{O}_8\text{S}$: 500.3131. Found: 500.3125.

Entry 1, Table A-2

Molecule F (0.942 g, 7.83 mmol) was reacted with *N,N'*-dimethyl-1,6-hexanediamine (1.13 g, 7.83 mmol) in refluxing benzene (11 mL) at 85 °C for 24 h. After evaporating the solvent, the polymer was precipitated into methanol (10 mL). The polymer was dried under vacuum to yield a brown oil (1.02 g, 75 % yield). ^1H NMR (CDCl_3): δ 1.29 (m, 4H), 1.54 (m, 4H), 2.94 (s, 6H), 3.07 (t, 4H, $J = 7.2$ Hz). ^{13}C NMR (CDCl_3): δ 26.88, 28.86, 46.90. 61.05.

Entry 3, Table A-2

Molecule F (0.186 g, 1.55 mmol) was reacted with *N,N'*-bis[3-(methylamino)propyl]methylamine (0.268 g, 1.55 mmol) in refluxing benzene (1.4 mL) at 85 °C for 72 h. The benzene was removed under vacuum. When the polymer was redissolved in 4 mL of CH₃OH and precipitated into 9 mL of water, the polymer decomposed to unknown products and the ¹H NMR spectrum became too complicated to assign the peaks. Therefore, after the polymerization was complete the polymer was dried under vacuum to yield a brown oil (0.310 g, 97 % yield) that was used without further purification. ¹H NMR (CDCl₃): δ 1.71(m, 4H), 2.21 (s, 3H), 2.32 (t, 4H, *J* = 7.5 Hz), 2.95 (s, 6H), 3.12 (t, 4H *J* = 7.1 Hz). ¹³C NMR (CDCl₃): δ 25.59, 42.43, 46.90, 55.38, 59.01.

Entry 5, Table A-2

Molecule F (0.186 g, 1.55 mmol) was reacted with 4,4'-trimethylenedipiperidine (0.326 g, 1.55 mmol) in CHCl₃ (1.6 mL) at 60 °C for 72 h. After evaporating the solvent and redissolving it in CH₂Cl₂ (4 mL), the polymer was precipitated into methanol (8 mL) to give a white-yellow powder (0.330 g, 88 % yield). ¹H NMR (CDCl₃): δ 1.22(m, 12H), 1.59 (m, 4H), 3.08 (t, 4H, *J* = 11.0 Hz), 3.44 (m, 4H). ¹³C NMR (CDCl₃): δ 23.68, 34.02, 34.96, 36.72, 58.57.

Reactions of molecule E and *N*-benzylmethylamine

Molecule E (46.3 mg, 312 μmol) was dissolved in 1.35 mL of CD₂Cl₂ and 1 mL (34.4 mg, 232 μmol) of the solution was transferred to a NMR tube. After the addition of *N*-benzylmethylamine (56.3 mg, 464 μmol) and sealing the NMR tube with a rubber

septum, ^1H NMR spectra were continually recorded for 3 days. The reaction was monitored by conversion of the benzyl hydrogens in *N*-benzylmethylamine at 3.71 ppm to the benzyl hydrogens in molecule H at 4.31 ppm and in molecule I at 4.38 ppm.

The same procedure was also followed for the kinetics in CDCl_3 . The conversion from molecule E to molecules H and I was monitored by comparing the benzyl peak (3.74 ppm) of *N*-benzylmethylamine with the benzyl peak (4.32 ppm) of molecule H and the benzyl peak (4.38 ppm) of molecule I for 10 days.

For the kinetics in DMSO-d_6 , molecule E (51.3 mg, 345 μmol) was dissolved in 1.49 mL of DMSO-d_6 , from which 1 mL (34.4 mg, 232 μmol) was added to an NMR tube. After adding *N*-benzylmethylamine (56.3 mg, 464 μmol) and sealing the NMR tube with a rubber septum, the reaction was monitored by ^1H NMR spectroscopy for 5 days. The conversion was observed by comparing the benzyl hydrogens in *N*-benzylmethylamine at 3.63 ppm with the benzyl hydrogens in molecule H at 4.29 ppm and in molecule I at 4.36 ppm.

For the kinetics in C_6D_6 , molecule E (49.4 mg, 333 μmol) was dissolved in 1.44 mL of C_6D_6 and 1 mL (34.4 mg, 232 μmol) was added to an NMR tube, followed by the addition of *N*-benzylmethylamine (56.3 mg, 464 μmol) and sealing the NMR tube with a rubber septum. The conversion from molecule E to molecules H and I was monitored by comparing the benzyl hydrogens in *N*-benzylmethylamine at 3.62 ppm with the benzyl hydrogens in molecule H at 4.34 ppm and in molecule I at 4.36 ppm.

Transamination of molecule F and *N*-benzylmethylamine

N-benzylmethylamine (153 mg, 1.26 mmol) was added to a solution of molecule F (75.8 mg, 631 μmol) in 1.26 mL of CDCl_3 . After connecting a condenser to the flask,

the mixture was reacted at 50 °C, and the reaction was monitored by ^1H NMR spectroscopy every 24 h showing 9% conversion to J and 88% conversion to I after 72 h.

The same procedure was followed for the reaction of molecule F (88.3 mg, 735 μmol) and *N*-benzylmethylamine (178 mg, 1.47 mmol) in 1.47 mL of DMSO-d_6 showing 13% conversion to J and 77 % conversion to I after 72 h. The reaction of molecule F (82.3 mg, 685 μmol) and *N*-benzylmethylamine (166 mg, 1.37 mmol) in 1.37 mL of C_6D_6 showed 17% conversion to J and 75% conversion to I after 72 h.

Molecule F (89.9 mg, 748 μmol) and *N*-benzylmethylamine (181 mg, 1.50 mmol) were reacted in 1.5 mL of benzene at 85 °C showing 3% conversion to J and 97% conversion to I after 24 h.

Stability of molecule E in organic solvents

The stability of molecule E was studied in CDCl_3 , $\text{DMSO-d}_6/\text{D}_2\text{O}$ (10/1 v/v), and C_6D_6 following the same procedure. Molecule E (34.4 mg, 2.32×10^{-4} mol) was added to an NMR tube with 1 mL of solvent. Next, diethylene glycol dimethyl ether (31.2 mg, 2.32×10^{-4} mol) was added. The NMR tube was capped, and ^1H NMR spectra were periodically collected. The amount of decomposition was determined by the difference in ratio of the peaks due to molecule E and the ether measured on days 1 and 32.

Stability of molecule L in D_2O

Molecule L (31.4 mg, 6.27×10^{-5} mol) was added to an NMR tube. A 1 mL solution in D_2O of *tert*-butanol (5.96 mg, 6.27×10^{-5} mol) and acetic acid (30.3 mg, 5.02×10^{-4} mol) was added to the NMR tube and it was vigorously shaken. The first ^1H NMR

spectrum after 271 s showed no evidence of molecule L and showed the secondary amine as the only degradation product.

The same procedure was followed except that no acetic acid was added (the neutral conditions). The decomposition of molecule L was followed by ^1H NMR spectroscopy. The same procedure was followed except that no acetic acid was added and KOH (9 molar equivalents) was added (the basic conditions). The decomposition of molecule L was followed by ^1H NMR spectroscopy.

Formulation of microparticles

Microparticles were fabricated from the polymer in entry 6 of Table A-2 using a double emulsion-solvent evaporation method that is widely used for the encapsulation of hydrophilic drugs. The surfactant solution (1% (by weight) PVA in water, internal water phase or W_1) was added to the polymer solution (in dichloromethane, oil phase or O) under micro-tip probe sonication for 30 sec (10 watts energy output, Fisher Scientific sonic dismembrator Model 100) to form the first emulsion (W_1/O). This was then immediately added to the second PVA solution (in water, external water phase or W_2) and further sonicated at the same speed for another 30 s to form the second emulsion ($W_1/O/W_2$). These processes were carried out under an ice-bath. The final emulsion was then added to aqueous PVA solution under magnetic agitation and stirred at room temperature and under atmospheric pressure until complete evaporation of dichloromethane. The microparticles were collected by centrifugation at 8500 rpm for 10 min (Fischer Scientific AccuspinTM 400), washed twice with water and freeze-dried for 48 h (FreezeZone 4.5, Labconco®). The FITC-dextran loaded microparticles were

prepared in the same manner by dissolving FITC-dextran in the internal water phase used in making the primary emulsion.

Determination of particle size and size distribution

Particle size and particle size distribution of microparticles were analyzed at a concentration of approximately 1 mg particles/1 mL of deionized water. Appropriate dilution of the particle suspension is necessary in order to avoid multiscattering events. The measurements were carried out on microparticle suspensions using a Zetasizer Nano-ZS (Malvern Instruments). The particle size and size distribution by intensity were measured by dynamic light scattering (He-Ne laser with a fixed wavelength of 633 nm, 173° backscatter at 25°C) in 10 mm diameter cells.

Measurement of surface charge

The zeta potential of microparticles was analyzed by dispersing the microparticles in deionized distilled water at a concentration of 1 mg/mL using folded capillary cells. Sample dilution is often necessary in order to eliminate particle interactions. Zeta potential is an indicator of the charge on the surface of the microparticles. The surface charge measurements of the blank microparticles were performed using the electrophoretic laser scattering method (Laser Doppler Micro-electrophoresis, He-Ne laser 633nm at 25 °C).

Scanning electron microscopy (SEM)

The shape and the surface morphology of the microparticles were studied using a scanning electron microscope. The particles were mounted on silicon wafers which were placed on aluminum specimen stubs using adhesive carbon tape. The mount was then

coated by ion sputtering (K550 Emitech sputter coater, set at 10 mA for 2.5 min) with conductive gold and examined using a Hitachi Model S-4800 SEM, operated at 4 kV accelerating voltage.

Cell culture

The cells were maintained in DMEM supplemented with 10% FBS (by volume) and gentamycin at a concentration 50 µg/ml in a humidified incubator (Sanyo scientific Autoflow, IR Direct Heat CO₂ Incubator) at 37 °C containing 95% air and 5% CO₂. The cells were plated and grown as a monolayer in 75 cm² polystyrene cell culture flasks (Corning Incorporated, NY) and subcultured (subcultivation ratio of 1:4) after 80-90 % confluence was achieved. Cell lines were started from frozen stocks and the medium was changed every 2-3 days. The passages used for the experiment were between 4 and 15.

Investigation of microparticle uptake by HEK-293 cells

To determine the qualitative *in vitro* intracellular uptake of microparticles, cells were plated at a density of 50,000 cells/well in a clear, flat-bottom, 8-chambered glass slide with cover (Lab-Tek, Nunc™, NY) that were previously coated with 0.1% (by weight) poly-*L*-lysine. The cells were allowed to attach overnight and the next day the cell culture medium was removed and the cells were treated with an aliquot of a suspension of FITC-dextran loaded microparticles in medium and further incubated at 37 °C for 24 h. The experiment was terminated by removing the particulate suspension and washing the cell monolayer two times with PBS in order to remove particles not internalized by the cells. The cells were then fixed with 4% (by volume) paraformaldehyde, followed by permeabilization of cells with 0.2% (by weight) Triton®

X-100 (Sigma[®], Sigma-Aldrich, MO). The cells were later treated with phalloidin and finally mounted with Vectashield[®], Hardset[™] mounted medium with DAPI (H-1500, Vector Labs, Inc. CA). The cells were washed with PBS during every step in the process. Cellular uptake of FITC-dextran loaded microparticles and their intracellular distribution was visualized by confocal microscopy (Carl Zeiss LSM 710, 60X oil objective lens) by using DAPI, FITC, and phalloidin filters equipped with Zen 2009 imaging software.

Evaluation of the cytotoxicity of microparticles

The *in vitro* cytotoxicity of blank nanoparticles was examined by a colorimetric MTS assay. A stock suspension of microparticles was prepared by dispersing freeze-dried particles in an appropriate volume of cell culture medium. To obtain different test concentrations (1 – 1000 µg/mL), serial dilutions from the stock microparticle suspension were prepared with the medium. On the first day of the experiment, confluent cells were seeded in clear polystyrene, flat bottom, 96-well plates (Costar[®], Corning Inc, NY) at a density of 10,000 cells/well and allowed to attach overnight in the incubator. Next day, the cells were exposed to the polymer by replacing the culture medium with different dilutions of stock suspensions and further incubating for 24 h. On the last day of the experiment, the treatments were removed and fresh medium was added along with 20 µL of MTS reagent. The plate was incubated at 37 °C in a humidified, 5% CO₂ atmosphere for 4 h. To measure the amount of soluble formazan produced by the reduction of MTS reagent by viable cells, the plate was read by Spectramax 384 Plus (Softmax Pro, Molecular Devices, CA) at a wavelength of 490 nm. The absorbance readings were recorded and quantitated for the colorimetric assay and the cell viability was expressed by the following equation:

Cell viability (%) = (Absorbance intensity of cells treated with MPs x 100) /

Absorbance intensity of cells without any treatment (control)

The cytotoxic effect of different treatments was calculated as a percentage of cell growth with respect to the control. Values are expressed as mean \pm SEM for each microparticle concentration (n=6).

REFERENCES

- (1) Katti, K. S. *Colloids and surfaces. B, Biointerfaces* **2004**, 39, 133.
- (2) Middleton, J. C.; Tipton, A. J. *Biomaterials* **2000**, 21, 2335.
- (3) Joji, S.; Muneshige, H.; Ikuta, Y. *British journal of plastic surgery* **1999**, 52, 559.
- (4) Tammela, T. L.; Talja, M.; Petas, A.; Valimaa, T.; Tormala, P. *Scandinavian journal of urology and nephrology. Supplementum* **1996**, 179, 97.
- (5) Kukreja, N.; Onuma, Y.; Daemen, J.; Serruys, P. W. *Pharmacological research : the official journal of the Italian Pharmacological Society* **2008**, 57, 171.
- (6) Bae, I. H.; Park, I. K.; Park, D. S.; Lee, H.; Jeong, M. H. *Journal of materials science. Materials in medicine* **2012**, 23, 1259.
- (7) Place, E. S.; George, J. H.; Williams, C. K.; Stevens, M. M. *Chemical Society reviews* **2009**, 38, 1139.
- (8) Rezwani, K.; Chen, Q. Z.; Blaker, J. J.; Boccaccini, A. R. *Biomaterials* **2006**, 27, 3413.
- (9) Ciardelli, G.; Chiono, V. *Macromolecular bioscience* **2006**, 6, 13.
- (10) Isenberg, B. C.; Williams, C.; Tranquillo, R. T. *Circulation research* **2006**, 98, 25.
- (11) Venugopal, J.; Ramakrishna, S. *Tissue engineering* **2005**, 11, 847.
- (12) Cooper, J. A.; Lu, H. H.; Ko, F. K.; Freeman, J. W.; Laurencin, C. T. *Biomaterials* **2005**, 26, 1523.
- (13) Atala, A.; Koh, C. *Expert review of medical devices* **2005**, 2, 119.
- (14) Wang, S.; Yaszemski, M. J.; Knight, A. M.; Gruetzmacher, J. A.; Windebank, A. J.; Lu, L. *Acta biomaterialia* **2009**, 5, 1531.
- (15) Ringsdorf, H. *J Polym Sci Polym Symp* **1975**, 135.
- (16) Hoste, K.; De Winne, K.; Schacht, E. *International journal of pharmaceutics* **2004**, 277, 119.
- (17) Maeda, H.; Seymour, L. W.; Miyamoto, Y. *Bioconjug Chem* **1992**, 3, 351.

- (18) Maeda, H. *Advanced drug delivery reviews* **1991**, *6*, 181.
- (19) Kratz, F.; Beyer, U.; Schutte, M. T. *Crit Rev Ther Drug* **1999**, *16*, 245.
- (20) Kopecek, J.; Rejmanova, P.; Chytrý, V. *Makromol Chem* **1981**, *182*, 799.
- (21) Springer, C. J.; Bagshawe, K. D.; Sharma, S. K.; Searle, F.; Boden, J. A.; Antoniow, P.; Burke, P. J.; Rogers, G. T.; Sherwood, R. F.; Melton, R. G. *Eur J Cancer* **1991**, *27*, 1361.
- (22) Pimm, M. V.; Perkins, A. C.; Strohalm, J.; Ulbrich, K.; Duncan, R. *J Drug Target* **1996**, *3*, 385.
- (23) Arap, W.; Pasqualini, R.; Ruoslahti, E. *Science* **1998**, *279*, 377.
- (24) Bae, Y.; Fukushima, S.; Harada, A.; Kataoka, K. *Angewandte Chemie* **2003**, *42*, 4640.
- (25) Kim, G. M.; Bae, Y. H.; Jo, W. H. *Macromolecular bioscience* **2005**, *5*, 1118.
- (26) Chen, W.; Meng, F.; Li, F.; Ji, S. J.; Zhong, Z. *Biomacromolecules* **2009**, *10*, 1727.
- (27) Mahapatro, A.; Singh, D. K. *Journal of nanobiotechnology* **2011**, *9*, 55.
- (28) Scholes, P. D.; Coombes, A. G. A.; Illum, L.; Davis, S. S.; Vert, M.; Davies, M. C. *Journal of Controlled Release* **1993**, *25*, 145.
- (29) Niwa, T.; Takeuchi, H.; Hino, T.; Kunou, N.; Kawashima, Y. *Journal of Controlled Release* **1993**, *25*, 89.
- (30) Govender, T.; Stolnik, S.; Garnett, M. C.; Illum, L.; Davis, S. S. *Journal of Controlled Release* **1999**, *57*, 171.
- (31) Zweers, M. L. T.; Engbers, G. H. M.; Grijpma, D. W.; Feijen, J. *Journal of Controlled Release* **2004**, *100*, 347.
- (32) Veronese, Francesco M.; Pasut, Gianfranco. *Drug Discovery Today* **2005**, *21*, 1451–8.
- (33) Lee, J.; Jung, S. G.; Park, C. S.; Kim, H. Y.; Batt, C. A.; Kim, Y. R. *Bioorganic & medicinal chemistry letters* **2011**, *21*, 2941.
- (34) Veronese, F. M.; Pasut, G. *Drug discovery today* **2005**, *10*, 1451.

- (35) Gref, R.; Luck, M.; Quellec, P.; Marchand, M.; Dellacherie, E.; Harnisch, S.; Blunk, T.; Muller, R. H. *Colloid Surface B* **2000**, *18*, 301.
- (36) Leroux, J. C.; Allemann, E.; DeJaeghere, F.; Doelker, E.; Gurny, R. *Journal of Controlled Release* **1996**, *39*, 339.
- (37) Torchilin, V. P.; Trubetskoy, V. S. *Advanced drug delivery reviews* **1995**, *16*, 141.
- (38) Stolnik, S.; Illum, L.; Davis, S. S. *Advanced drug delivery reviews* **1995**, *16*, 195.
- (39) Soppimath, K. S.; Aminabhavi, T. M.; Kulkarni, A. R.; Rudzinski, W. E. *Journal of Controlled Release* **2001**, *70*, 1.
- (40) Gaurav K. Jain, S. A. P., Sohail Akhter, Niyaz Ahmed, Nilu Jain, Sushma Talegaonkar, Roop K. Khar, Farhan J. Ahmed *Polymer Degradation and Stability* **2010**, *95*, 2360.
- (41) Kumari, A.; Yadav, S. K.; Yadav, S. C. *Colloid Surface B* **2010**, *75*, 1.
- (42) Nair, L. S.; Laurencin, C. T. *Prog Polym Sci* **2007**, *32*, 762.
- (43) Astete, C. E.; Sabliov, C. M. *Journal of biomaterials science. Polymer edition* **2006**, *17*, 247.
- (44) Gerhardt, W. W.; Noga, D. E.; Hardcastle, K. I.; Garcia, A. J.; Collard, D. M.; Weck, M. *Biomacromolecules* **2006**, *7*, 1735.
- (45) Tian D, D. P., Jerome R *Macromolecules* **1997**, *30*, 2575.
- (46) Trollsas M, L. V., Mecerreyes D, Lowenhielm P, Moller M, Miller RD, Hedrick JL *Macromolecules* **2000**, *33*, 4619.
- (47) Tian D, D. P., Grandfils C, Jerome R *Macromolecules* **1997**, *30*, 406.
- (48) Mecerreyes D, H. J., Miller RD, Hedrick JL, Detrembleur C, Lecomte P, Jerome R, San Roman J *Macromol Rapid Commun* **2000**, *21*, 779.
- (49) Liu XQ, L. Z., Du FS, Li FM *Macromol Rapid Commun* **1999**, *20*, 470.
- (50) Kumar, N.; Langer, R. S.; Domb, A. J. *Advanced drug delivery reviews* **2002**, *54*, 889.
- (51) Brem, H.; Walter, K. A.; Langer, R. *Eur J Pharm Biopharm* **1993**, *39*, 2.
- (52) Li, L. C.; Deng, J.; Stephens, D. *Advanced drug delivery reviews* **2002**, *54*, 963.

- (53) Orloff, L. A.; Domb, A. J.; Teomim, D.; Fishbein, I.; Golomb, G. *Advanced drug delivery reviews* **1997**, *24*, 3.
- (54) Albertsson, A. C.; Carlfors, J.; Stureson, C. *J Appl Polym Sci* **1996**, *62*, 695.
- (55) Jain, J. P.; Modi, S.; Domb, A. J.; Kumar, N. *Journal of controlled release : official journal of the Controlled Release Society* **2005**, *103*, 541.
- (56) Heller, J. *Adv Polym Sci* **1993**, *107*, 41.
- (57) Heller, J.; Barr, J.; Ng, S. Y.; Abdellaoui, K. S.; Gurny, R. *Advanced drug delivery reviews* **2002**, *54*, 1015.
- (58) Schwach-Abdellaoui, K.; Loup, P. J.; Vivien-Castioni, N.; Mombelli, A.; Baehni, P.; Barr, J.; Heller, J.; Gurny, R. *Aaps Pharmsci* **2002**, *4*.
- (59) Heller, J.; Barr, J.; Ng, S. Y.; Shen, H. R.; Schwach-Abdellaoui, K.; Gurny, R.; Vivien-Castioni, N.; Loup, P. J.; Baehni, P.; Mombelli, A. *Biomaterials* **2002**, *23*, 4397.
- (60) Yoo, J.; Kuruvilla, D. J.; D'Mello, S. R.; Salem, A. K.; Bowden, N. B. *Macromolecules* **2012**, *45*, 2292.
- (61) Chahma, M.; Hicks, R. G.; Myles, D. J. T. *Macromolecules* **2004**, *37*, 2010.
- (62) Miyatake, K.; Iyotani, H.; Yamamoto, K.; Tsuchida, E. *Macromolecules* **1996**, *29*, 6969.
- (63) Oyama, H. T.; Matsushita, M.; Furuta, M. *Polym. J.* **2011**, *43*, 991.
- (64) Pernstich, K. P.; Schenker, M.; Weibel, F.; Rossi, A.; Caseri, W. R. *ACS Appl. Mater. Interfaces* **2010**, *2*, 639.
- (65) Silvestre, C.; Di, P. E.; Napolitano, R.; Pirozzi, B.; Cesario, G. *J. Polym. Sci., Part B: Polym. Phys.* **2001**, *39*, 415.
- (66) Yamamoto, K.; Shouji, E.; Nishide, H.; Tsuchida, E. *J. Am. Chem. Soc.* **1993**, *115*, 5819.
- (67) Canadell, J.; Goossens, H.; Klumperman, B. *Macromolecules* **2011**, *44*, 2536.
- (68) Burnworth, M.; Tang, L.; Kumpfer, J. R.; Duncan, A. J.; Beyer, F. L.; Fiore, G. L.; Rowan, S. J.; Weder, C. *Nature* **2011**, *472*, 334.
- (69) Shanmuganathan, K.; Capadona, J. R.; Rowan, S. J.; Weder, C. *ACS Appl. Mater. Interfaces* **2010**, *2*, 165.

- (70) Wojtecki, R. J.; Meador, M. A.; Rowan, S. J. *Nat. Mater.* **2011**, *10*, 14.
- (71) Canadell, J.; Goossens, H.; Klumperman, B. *Macromolecules* **2011**, *44*, 2536.
- (72) Kamada, J.; Koynov, K.; Corten, C.; Juhari, A.; Yoon, J. A.; Urban, M. W.; Balazs, A. C.; Matyjaszewski, K. *Macromolecules* **2010**, *43*, 4133.
- (73) Yoon, J. A.; Kamada, J.; Koynov, K.; Mohin, J.; Nicolay, R.; Zhang, Y.; Balazs, A. C.; Kowalewski, T.; Matyjaszewski, K. *Macromolecules* **2012**, *45*, 142.
- (74) Vo, C. D.; Kilcher, G.; Tirelli, N. *Macromol. Rapid Commun.*, *30*, 299.
- (75) Munday, R. *Chem. Res. Toxicol.* **2012**, *25*, 47.
- (76) Braunova, A.; Pechar, M.; Laga, R.; Ulbrich, K. *Macromol. Chem. Phys.* **2007**, *208*, 2642.
- (77) Saito, G.; Swanson, J. A.; Lee, K.-D. *Adv. Drug Delivery Rev.* **2003**, *55*, 199.
- (78) Zhongfan, J.; Jingquan, L.; Cyrille, B.; Davis, T. P.; Boulmus, V. *Biomacromolecules* **2009**, *10*, 3253.
- (79) Kohane, D. S.; Langer, R. *Chem. Sci.* **2010**, *1*, 441.
- (80) Kroeze, R. J.; Helder, M. N.; Govaert, L. E.; Smit, T. H. *Materials* **2009**, *2*, 833.
- (81) Zhang, S.; Zhao, Y. *J. Am. Chem Soc.* **2010**, *132*, 10642.
- (82) Pompella, A. V., A.; Paolicchi, A.; De Tata, V.; Casini, A. F. *Biochem. Pharmacol.* **2003**, *66*, 1499.
- (83) Harp, D. N.; Steliou, K.; Chan, T. H. *J. Am. Chem. Soc.* **1978**, *100*, 1222-1228.
- (84) Arancibia, A.; Diaz, C. *Phosphorus, Sulfur Silicon Relat. Elem.* **1989**, *44*, 1.
- (85) Araki, N.; Ohno, K.; Nakai, M.; Takeyoshi, M.; Iida, M. *Toxicol. in Vitro* **2005**, *19*, 831.
- (86) Diaz, C.; Yutronic, N. *Phosphorus, Sulfur Silicon Relat. Elem.* **1991**, *62*, 219.
- (87) Farahbakhsh, M.; Nekola, H.; Schmidt, H.; Rehder, D. *Chem. Ber.* **1997**, *130*, 1129.
- (88) Matcalf, S. G.; Shreeve, J. M. *Inorg. Chem.* **1972**, *11*, 1631.

- (89) Rahman, M.; Ali, M. A.; Bhattacharjee, P.; Nazimuddin, M. *Polyhedron* **1991**, *10*, 823.
- (90) Sun, R.; Zhang, Y.; Chen, L.; Li, Y.; Li, Q.; Song, H.; Huang, R.; Bi, F.; Wang, Q. *J. Agric. Food Chem.* **2009**, *57*, 3661.
- (91) Das, P. K.; Datta, R. N.; Basu, D. K. *Rubber Chem. Technol.* **1987**, *60*, 803.
- (92) Denk, M. K. *Eur. J. Inorg. Chem.* **2009**, 1358.
- (93) Datta, R. N.; Das, P. K.; Basu, D. K. *J. Appl. Polym. Sci.* **1986**, *32*, 5849.
- (94) Beerheide, W.; Sim, M. M.; Tan, Y.-J.; Bernard, H.-U.; Ting, A. E. *Bioorg. Med. Chem.* **2000**, *8*, 2549.
- (95) Kapanda, C. N.; Muccioli, G. G.; Labar, G.; Poupaert, J. H.; Lambert, D. M. *J. Med. Chem.* **2009**, *52*, 7310.
- (96) Kaur, D.; Sharma, P.; Bharatam, P. V. *J. Mol. Struct.: THEOCHEM* **2007**, *810*, 31.
- (97) Anderson, D. G.; Nurdick, J. A.; Langer, R. *Science* **2004**, *305*, 1923.
- (98) Cao, J.; Langer, R. *Nano Lett.* **2010**, *10*, 3223.
- (99) Thierry, B. *Curr. Drug Delivery* **2009**, *6*, 391.
- (100) Arima, H.; Motoyama, K. *Sensors* **2009**, *9*, 6346.
- (101) Green, J. J.; Langer, R.; Anderson, D. G. *Accts. Chem. Res.* **2008**, *41*, 749.
- (102) Jabbari, E.; Lu, L.; Yaszemski, M. J. *Synthesis and characterization of injectable and biodegradable composites for orthopedic applications*, 2006; Vol. 2.
- (103) Meng, F.; Hiemstra, C.; Engbers, G. H. M.; Feijen, J. *Macromolecules* **2003**, *36*, 3004.
- (104) Mohanad, M.; Dixon, A. S.; Lim, C. S. *Therapeutic Del.* **2010**, *1*, 169.
- (105) Nguyen, D. N.; Green, J. J.; Chan, J. M.; Langer, R.; Anderson, D. G. *Adv. Mater.* **2009**, *21*, 847.
- (106) Peter, S. J.; Miller, M. J.; Yasko, A. W.; Yaszemski, M. J.; Mikos, A. G. *J. Biomed. Mater. Res.* **1998**, *43*, 422.

- (107) Twaites, B.; de las Heras Alarcon, C.; Alexander, C. *J. Mater. Chem.* **2005**, *15*, 441.
- (108) Yoo, J.; Kuruvilla, D. J.; D'Mello, S. R. D.; Salem, A. K.; Bowden, N. B. *Macromolecules* **2012**, *45*, 2292.
- (109) Yoo, J.; D'Mello, S. R. D.; Graf, T. A.; Salem, A. K.; Bowden, N. B. *Macromolecules* **2012**, *45*, 688.
- (110) Wolfenden, R.; Yuan, Y. *J. Am. Chem. Soc.* **2011**, *133*, 13821.
- (111) Vasconceilos da Silva, B. *Synlett* **2008**, 1265.
- (112) Rakitin, O. A. *Targets Heterocycl. Syst.* **2010**, *14*, 103.
- (113) Adelowo, F. E.; Ojo, I. A. O.; Amuda, O. S. *Adv. Biol. Chem.* **2011**, *1*, 122.
- (114) Harpp, D. N.; Steliou, K.; Chan, T. H. *J. Am. Chem. Soc.* **1978**, *100*, 1222.
- (115) Kalnins, M. V. *Can. J. Chem.* **1966**, *44*, 2111.
- (116) Huang, N.; Lakshmikantham, M. V.; Cava, M. P. *J. Org. Chem.* **1987**, *52*, 169.
- (117) Carpenter, B. K. *Determination of Organic Reaction Mechanisms*; John Wiley & Sons: New York, 1984.
- (118) Furukawa, M.; Sato, K.; Okawara, T. *Chem. Lett.* **1982**, 2007.
- (119) Labes, M. M.; Love, P.; Nichols, L. F. *Chem. Rev.* **1979**, *79*, 1.
- (120) Banister, A. J.; Gorrell, I. B. *Adv. Mater.* **1998**, *10*, 1415.
- (121) Gerratt, J.; McNicholas, S. J.; Karadakov, P. B.; Sironi, M.; Raimondi, M.; Cooper, D. L. *J. Am. Chem. Soc.* **1996**, *119*, 6472.
- (122) Haddon, R. C.; Wasserman, S. R.; Wudl, F.; Williams, G. R. J. *J. Am. Chem. Soc.* **1980**, *102*, 6687.
- (123) Mawhinney, R. C.; Goddard, J. D. *Inorg. Chem.* **2003**, *42*, 6323.
- (124) Somasundram, K.; Handy, N. C. *J. Phys. Chem.* **1996**, *100*, 17485.
- (125) Jones, W. H.; Bardo, R. D. *J. Phys. Chem.* **1993**, *97*, 4974.
- (126) Soderholm, L.; Mathis, C.; Francois, B. *Synth. Met.* **1985**, *10*, 261.

- (127) Ozdemir, C.; Can, H. K.; Colak, N.; Guner, A. *J. Appl. Polym. Sci.* **2006**, *99*, 2182.
- (128) Paosawatyanong, B.; Kamphiranon, P.; Bannarakkul, W.; Srithana-anant, Y.; Bhanthumnavin, W. *Surface & Coatings Tech.* **2010**, *204*, 3053.
- (129) Tanaka, K.; Yoshizawa, K.; Takeuchi, T.; Yamabe, T. *Synth. Met.* **1990**, *38*, 107.
- (130) Roviello, A.; Buono, A.; Carella, A.; Roviello, G.; Cassinese, A.; Barra, M.; Biasucci, M. *J. Polym. Sci., Part A: Polym. Chem.* **2007**, *45*, 1758.
- (131) Wang, R. *Faseb J* **2002**, *16*, 1792.
- (132) Hildebrandt, T. M.; Grieshaber, M. K. *Febs J* **2008**, *275*, 3352.
- (133) Li, L.; Rose, P.; Moore, P. K. *Annu Rev Pharmacol* **2011**, *51*, 169.
- (134) Predmore, B. L.; Lefer, D. J.; Gojon, G. *Antioxid Redox Sign* **2012**, *17*, 119.
- (135) Calvert, J. W.; Elston, M.; Nicholson, C. K.; Gundewar, S.; Jha, S.; Elrod, J. W.; Ramachandran, A.; Lefer, D. J. *Circulation* **2010**, *122*, 11.
- (136) Benavides, G. A.; Squadrito, G. L.; Mills, R. W.; Patel, H. D.; Isbell, T. S.; Patel, R. P.; Darley-USmar, V. M.; Doeller, J. E.; Kraus, D. W. *P Natl Acad Sci USA* **2007**, *104*, 17977.
- (137) Benavides, G. A.; Squadrito, G. L.; Huynh, J. J.; Doeller, J. E.; Kraus, D. W. *Free Radical Bio Med* **2007**, *43*, S89.
- (138) Rossoni, G.; Manfredi, B.; Tazzari, V.; Sparatore, A.; Trivulzio, S.; Del Soldato, P.; Berti, F. *Eur J Pharmacol* **2010**, *648*, 139.
- (139) Tang, X. Q.; Chen, R. Q.; Ren, Y. K.; Soldato, P. D.; Sparatore, A.; Zhuang, Y. Y.; Fang, H. R.; Wang, C. Y. *Medical gas research* **2011**, *1*, 20.
- (140) Lee, Z. W.; Zhou, J. B.; Chen, C. S.; Zhao, Y. J.; Tan, C. H.; Li, L.; Moore, P. K.; Deng, L. W. *Plos One* **2011**, *6*.
- (141) Gorin, D. J.; Sherry, B. D.; Toste, F. D. *Chem. Rev.* **2008**, *108*, 3351.
- (142) Hashmi, A. S. K.; Schaefer, S.; Bats, J. W.; Frey, W.; Rominger, F. *Eur. J. Org. Chem.* **2008**, 4891.
- (143) Jimenez-Nunez, E.; Echavarren, A. M. *Chem. Commun.* **2007**, 333.
- (144) Shapiro, N. D.; Toste, F. D. *J. Am. Chem. Soc.* **2007**, *129*, 4160.

- (145) Hashmi, A. S. K. *Chem. Rev.* **2007**, *107*, 3180.
- (146) Hashmi, A. S. K. *Angew. Chem. Int. Ed.* **2008**, *47*, 6754.
- (147) Denes, F.; Perez-Luna, A.; Chemla, F. *Chem. Rev.* **2010**, *110*, 2366.
- (148) Arcadi, A. *Chem. Rev.* **2008**, *108*, 3266.
- (149) Gorin, D. J.; Sherry, B. D.; Toste, F. D. *Chem. Rev.* **2008**, *108*, 3351.
- (150) Jimenez-Nunez, E.; Echavarren, A. M. *Chem. Rev.* **2008**, *108*, 3326.
- (151) Li, Z.; Brouwer, C.; He, C. *Chem. Rev.* **2008**, *108*, 3239.
- (152) Furstner, A. *Chem. Soc. Rev.* **2009**, *38*, 3208.
- (153) Sengupta, S.; Shi, X. *ChemCatChem* **2010**, *2*, 609.
- (154) Alfonsi, M.; Arcadi, A.; Aschi, M.; Bianchi, G.; Marinelli, F. *J. Org. Chem.* **2005**, *70*, 2265.
- (155) Arnanz, A.; Gonzalez-Arellano, C.; Juan, A.; Villaverde, G.; Corma, A.; Iglesias, M.; Sanchez, F. *Chem. Commun.* **2010**, *46*, 3001.
- (156) Bolte, B.; Odabachian, Y.; Gagosz, F. *J. Am. Chem. Soc.* **2010**, 7294.
- (157) Brand, J. P.; Charpentier, J.; Waser, J. *Angew. Chem. Int. Ed.* **2009**, *48*, 9346.
- (158) Breman, A. C.; Dijkink, J.; van Maarseveen, J. H.; Kinderman, S. S.; Hiemstra, H. *J. Org. Chem.* **2009**, *74*, 6327.
- (159) Cui, L.; Peng, Y.; Zhang, L. *J. Am. Chem. Soc.* **2009**, *131*, 8394.
- (160) Enomoto, T.; Girard, A.-L.; Yasui, Y.; Takemoto, Y. *J. Org. Chem.* **2009**, *74*, 9158.
- (161) Georgy, M.; Boucard, V.; Campagne, J.-M. *J. Am. Chem. Soc.* **2005**, *127*, 14180.
- (162) Hashmi, A. S. K.; Hamzic, M.; Rominger, F.; Bats, J. W. *Chem. Eur. J.* **2009**, *15*, 13318.
- (163) Korner, C.; Starkov, P.; Sheppard, T. D. *J. Am. Chem. Soc.* **2010**, *132*, 5968.
- (164) Jou, M. J.; Chen, X.; Swamy, K. M. K.; Na Kim, H.; Kim, H.-J.; Lee, S.-G.; Yoon, J. *Chem. Commun.* **2009**, 7218.

- (165) Mauleon, P.; Zeldin, R. M.; Gonzalez, A. Z.; Toste, F. D. *J. Am. Chem. Soc.* **2009**, *131*, 6348.
- (166) Ramamoorthy, V.; Wu, Z.; Yi, Y.; Sharp, P. R. *J. Am. Chem. Soc.* **1992**, *114*.
- (167) Nieto-Oberhuber, C.; Lopez, S.; Echavarren, A. M. *J. Am. Chem. Soc.* **2005**, *127*, 6178.
- (168) Sherry, B. D.; Toste, F. D. *J. Am. Chem. Soc.* **2004**, *126*, 15978.
- (169) Marion, N.; Nolan, S. *Chem. Soc. Rev.* **2008**, *37*, 1776.
- (170) Lee, E.-S.; Yeom, H.-S.; Hwang, J.-H.; Shin, S. *Eur. J. Org. Chem.* **2007**, 3503.
- (171) Zeng, X.; Kinjo, R.; Donnadieu, B.; Bertrand, G. *Angew. Chem. Int. Ed.* **2010**, *49*, 942.
- (172) Zhang, X.; Corma, A. *Chem. Commun.* **2007**, 3080.
- (173) Hamilton, G. L.; Kang, E. J.; Mba, M.; Toste, F. D. *Science* **2007**, *317*, 496.
- (174) Uemura, M.; Watson, I. D. G.; Katsukawa, M.; Toste, F. D. *J. Am. Chem. Soc.* **2009**, *131*, 3464.
- (175) Munoz, M. P.; Adrio, J.; Carretero, J. C.; Echavarren, A. M. *Organometallics* **2005**, *24*, 1293.
- (176) Gonzalez, A. Z.; Toste, F. D. *Org. Lett.* **2010**, *12*, 200.
- (177) La Londe, R. L.; Wang, Z. J.; Mba, M.; Lackner, A. D.; Toste, F. D. *Angew. Chem. Int. Ed.* **2010**, *49*, 598.
- (178) Liu, Y.; Xu, W.; Wang, X. *Org. Lett.* **2010**, *12*, 1448.
- (179) Bakrania, S. D.; Rathore, G. K.; Wooldridge, M. S. *J. Therm. Anal. Calorim.* **2009**, *95*, 117.
- (180) Schuster, O.; Liao, R.-Y.; Schier, A.; Schmidbaur, H. *Inorg. Chim. Acta* **2005**, *358*, 1429.
- (181) Tossell, J. A. *Chem. Phys. Lett.* **1998**, *286*, 73.
- (182) Correa, A.; Marion, N.; L., F.; Malacria, M.; Nolan, S. P.; Cavallo, L. *Angew. Chem. Int. Ed.* **2008**, *47*, 718.

- (183) Lavallo, V.; Frey, G. D.; Kousar, S.; Donnadieu, B.; Gertrand, G. *Proc. Natl. Acad. Sci. U. S. A.* **2007**, *104*, 13569.
- (184) Wiltham, C. A.; Maulon, P.; Shapiro, N. D.; Sherry, B. D.; Toste, F. D. *J. Am. Chem. Soc.* **2007**, *129*, 5838.
- (185) Bender, C. F.; Widenhoefer, R. A. *Org. Lett.* **2006**, *8*, 5303.
- (186) Lo, V. K.-Y.; Kung, K. K.-Y.; Wong, M.-K.; Che, C.-M. *J. Organomet. Chem.* **2009**, *694*, 583.
- (187) Iwamoto, R. T.; Manahan, S. E. *J. Electroanal. Chem.* **1967**, *13*, 411.
- (188) Williams, R. J. P.; James, B. R. *J. Chem. Soc.* **1961**, 2007.
- (189) Wei, C.; Li, C.-J. *J. Am. Chem. Soc.* **2003**, *125*, 9584.
- (190) Reetz, M. T.; Sommer, K. *Eur. J. Org. Chem.* **2003**, *18*, 3485.
- (191) Chauvin, Y. *Angew. Chem. Int. Ed.* **2006**, *45*, 3741.
- (192) Schrock, R. R. *Angew. Chem. Int. Ed.* **2006**, *45*, 3748.
- (193) Grubbs, R. H. *Angew. Chem. Int. Ed.* **2006**, *45*, 3760.
- (194) Connon, S. J.; Blechert, S. *Angew. Chem., Int. Ed.* **2003**, *42*, 1900.
- (195) Fuerstner, A. *Angew. Chem., Int. Ed.* **2000**, *39*, 3012.
- (196) Garber, S. B.; Kingsbury, J. S.; Gray, B. L.; Hoveyda, A. H. *J. Am. Chem. Soc.* **2000**, *122*, 8168.
- (197) Grubbs, R. H.; Chang, S. *Tetrahedron* **1998**, *54*, 4413.
- (198) Schrock, R. R.; Murdzek, J. S.; Bazan, G. C.; Robbins, J.; DiMare, M.; O'Regan, M. *J. Am. Chem. Soc.* **1990**, *112*, 3875.
- (199) Schwab, P.; France, M. B.; Ziller, J. W.; Grubbs, R. H. *Angew. Chem., Int. Ed.* **1995**, *34*, 2039.
- (200) Schwab, P.; Grubbs, R. H.; Ziller, J. W. *J. Am. Chem. Soc.* **1996**, *118*, 100.
- (201) Trnka, T. M.; Grubbs, R. H. *Acc. Chem. Res.* **2001**, *34*, 18.
- (202) Wilkes, J. S.; Zaworotko, M. J. *J. Chem. Soc., Chem. Commun.* **1992**, 965.

- (203) Bielawski, C. W.; Grubbs, R. H. *Prog. Polym. Sci.* **2007**, *32*, 1.
- (204) Buchmeiser, M. R. *Chem. Rev. (Washington, D. C.)* **2000**, *100*, 1565.
- (205) Lynn, D. M.; Kanaoka, S.; Grubbs, R. H. *J. Am. Chem. Soc.* **1996**, *118*, 784.
- (206) Trnka, T. M.; Morgan, J. P.; Sanford, M. S.; Wilhelm, T. E.; Scholl, M.; Choi, T.-L.; Ding, S.; Day, M. W.; Grubbs, R. H. *J. Am. Chem. Soc.* **2003**, *125*, 2546.
- (207) Weskamp, T.; Kohl, F. J.; Hieringer, W.; Gleich, D.; Herrmann, W. A. *Angew. Chem., Int. Ed.* **1999**, *38*, 2416.
- (208) Weskamp, T.; Schattenmann, W. C.; Spiegler, M.; Herrmann, W. A. *Angew. Chem., Int. Ed.* **1998**, *37*, 2490.
- (209) Baughman, T. W.; Wagener, K. B. *Adv. Polym. Sci.* **2005**, *176*, 1.
- (210) Smith, D. W., Jr.; Wagener, K. B. *Macromolecules* **1993**, *26*, 1633.
- (211) Smith, J. A.; Brzezinska, K. R.; Valenti, D. J.; Wagener, K. B. *Macromolecules* **2000**, *33*, 3781.
- (212) Sworen, J. C.; Smith, J. A.; Berg, J. M.; Wagener, K. B. *J. Am. Chem. Soc.* **2004**, *126*, 11238.
- (213) Ayres, N. *Polym. Rev.* **2011**, *51*, 138.
- (214) Braunecker, W. A.; Matyjaszewski, K. *Prog. Polym. Sci.* **2007**, *32*, 93.
- (215) Matyjaszewski, K.; Xia, J. *Chem. Rev.* **2001**, *101*, 2921.
- (216) Leibfarth, F. A. K.; Minhyuk; Ham, Myungsoo; Kim, Joohee; Campos, Luis M.; Gupta, Nalini; Moon, Bongjin; Hawker, Craig J. *Nature Chem.* **2010**, *2*, 207.
- (217) Leibfarth, F. A. S.; Yanika; Lynd, Nathaniel A.; Schultz, Alison; Moon, Bongjin; Kramer, Edward J.; Bazan, Guillermo C.; Hawker, Craig J. *J. Am. Chem. Soc.* **2010**, *132*, 14706.
- (218) Harpp, D. N.; Gringras, M.; Aida, T.; Chan, T. H. *Synthesis* **1987**, *12*, 1122.
- (219) Huang, N.-Z.; Lakshmikantham, M. V.; Cava, M. P. *J. Org. Chem.* **1987**, *52*, 169.
- (220) Harpp, D. N.; Steliou, K.; Chan, T. H. *J. Am. Chem. Soc.* **1978**, *100*, 1222.
- (221) Losev, Y. P.; Paushkin, Y. M. *J. Appl. Polym. Sci.* **1992**, *45*, 1517.

- (222) Chen, C.-H.; Lin, J. T.; Yeh, M.-C. P. *Org. Lett.* **2006**, *8*, 2233.
- (223) Hou, J.; Park, M.-H.; Zhang, S.; Yao, Y.; Chen, L.-M.; Li, J.-H.; Yang, Y. *Macromolecules (Washington, DC, U. S.)* **2008**, *41*, 6012.
- (224) Mishra, S. P.; Palai, A. K.; Srivastava, R.; Kamalasanan, M. N.; Patri, M. J. *Polym. Sci., Part A: Polym. Chem.* **2009**, *47*, 6514.
- (225) Wang, E.; Wang, M.; Wang, L.; Duan, C.; Zhang, J.; Cai, W.; He, C.; Wu, H.; Cao, Y. *Macromolecules (Washington, DC, U. S.)* **2009**, *42*, 4410.
- (226) Woo, C. H.; Holcombe, T. W.; Unruh, D. A.; Sellinger, A.; Frechet, J. M. J. *Chem. Mater.* **2010**, *22*, 1673.
- (227) Bundgaard, E.; Krebs, F. C. *Macromolecules* **2006**, *39*, 2823.
- (228) Hennrich, G.; Sonnenschein, H.; Resch-Genger, U. *J. Am. Chem. Soc.* **1999**, *121*, 5073.
- (229) Karikomi, M.; Kitamura, C.; Tanaka, S.; Yamashita, Y. *J. Am. Chem. Soc.* **1995**, *117*, 6791.
- (230) Thomas, K. R. J.; Lin, J. T.; Velusamy, M.; Tao, Y.-T.; Chuen, C.-H. *Adv. Funct. Mater.* **2004**, *14*, 83.
- (231) Ayres, N. *Polym. Rev.* **2011**, *51*, 138.
- (232) Gates, D. P. *Annu. Rep. Prog. Chem., Sect. A: Inorg. Chem.* **2005**, *101*, 452.
- (233) Gates, D. P. *Ann. Reports Prog. Chem. Section A: Inorg. Chem.* **2009**, *105*, 397.
- (234) Rivard, E. *Ann. Reports Prog. Chem. Section A: Inorg. Chem.* **2010**, *106*, 391.
- (235) Rivard, E. *Ann. Reports Prog. Chem. Section A: Inorg. Chem.* **2011**, *107*, 319.
- (236) Banister, A. J.; Gorrell, I. B. *Adv. Mater.* **1998**, *10*, 1415.
- (237) Kanazawa, H.; Stejny, J.; Keller, A. *J. Mater. Sci.* **1990**, *25*, 3838.
- (238) Kurmaev, E. Z.; Poteryaev, A. I.; Anisimov, V. I.; Karla, I.; Moewes, A.; Schneider, B.; Neumann, M.; Ederer, D. L.; Lyubovskaya, R. N. *Physica C* **1999**, *321*, 191.
- (239) Larsson, S. *Faraday Discuss.* **2006**, *131*, 69.
- (240) Rawson, J. M.; Longridge, J. J. *Chem. Soc. Rev.* **1997**, *26*, 53.

- (241) Odian, G. G. *Principles of polymerization*; Wiley, 1991.
- (242) Arima, H.; Motoyama, K. *Sensors* **2009**, *9*, 6346.
- (243) Meng, H.; Xue, M.; Xia, T.; Zhao, Y.-L.; Tamaoi, F.; Stoddart, J. F.; Zink, J. I.; Nel, A. E. *J. Am. Chem. Soc.* **2010**, *132*, 12690.
- (244) Mohanad, M.; Dixon, A. S.; Lim, C. S. *Therapeutic Del.* **2010**, *1*, 169.
- (245) Oh, K. T.; Yin, H.; Lee, E. S.; Bae, Y. H. *J. Mater. Chem.* **2007**, *17*, 3987.
- (246) Kohane, D. S.; Langer, R. *Chem. Sci.* **2010**, *1*, 441.
- (247) Kroeze, R. J.; Helder, M. N.; Govaert, L. E.; Smit, T. H. *Materials* **2009**, *2*, 833.
- (248) Banister, A. J.; Bricklebank, N.; Clegg, W.; Elsegood, M. R. J.; Gregory, C. I.; Lavender, I.; Rawson, J. M.; Tanner, B. K. *J. Chem. Soc., Chem. Commun.* **1995**, 679.
- (249) Cooper, D. L.; Cunningham, T. P.; Gerratt, J.; Karadakov, P. B.; Raimondi, M. *J. Am. Chem. Soc.* **1994**, *116*, 4414.
- (250) Derbesy, G.; Harpp, D. N. *Tetrahedron Lett.* **1994**, *35*, 5381.
- (251) Harpp, D. N.; Steliou, K.; Chan, T. H. *J. Am. Chem. Soc.* **1978**, *100*, 1222.
- (252) Kuhn, N.; Bohnen, H.; Fahl, J.; Blaeser, D.; Boese, R. *Chem. Ber.* **1996**, *129*, 1579.
- (253) Weinstock, L. M.; Davis, P.; Handelsman, B.; Tull, R. J. *J. Org. Chem.* **1967**, *32*, 2823.
- (254) Refvik, M. D.; Schwan, A. L. *J. Org. Chem.* **1996**, *61*, 4232.
- (255) Bowman, W. R.; Clark, D. N.; Marmon, R. J. *Tet. Lett.* **1991**, *32*, 6441.
- (256) Anslyn, E. V.; Dougherty, D. A. *Modern physical organic chemistry*; University Science Books: Sausalito, California, 2006.
- (257) Grainger, R. S.; Patel, B.; Kariuki, B. M.; Male, L.; Spencer, N. *J. Am. Chem. Soc.* **2011**, *133*, 5843.
- (258) Schenk, P. W.; Steudel, R. *Inorganic sulfur chemistry*; Elsevier: Amsterdam, 1968.
- (259) Wolfenden, R.; Yuan, Y. *J. Am. Chem. Soc.* **2011**, *133*, 13821.

- (260) Mosmann, T. *J. Immunological Meth.* **1983**, *65*, 55.
- (261) Cory, A. H.; Owen, T. C.; Barltrop, J. A.; Cory, J. G. *Cancer Commun.* **1991**, *3*, 207.
- (262) Harpp, D. N.; Gingras, M.; Aida, T.; Chan, T. H. *Synthesis* **1987**, *12*, 1122.
- (263) Kapanda, C. N.; Muccioli, G. G.; Labar, G.; Poupaert, J. H.; Lambert, D. M. *Journal of Medicinal Chemistry* **2009**, *52*, 7310.
- (264) Sun, R.; Zhang, Y.; Chen, L.; Li, Y.; Li, Q.; Song, H.; Huang, R.; Bi, F.; Wang, Q. *Journal of Agricultural and Food Chemistry* **2009**, *57*, 3661.